Exploring QGP properties through high-$p_\perp$ theory and data

Bojana Ilic (Blagojevic)

Institute of Physics Belgrade, University of Belgrade

In collaboration with: Magdalena Djordjevic (P.I.), Dusan Zigic, Stefan Stojku, Jussi Auvinen, Igor Salom, Marko Djordjevic and Pasi Huovinen

European Research Council
Established by the European Commission

Република Србија
МИНИСТАРСТВО НАУКЕ, ТЕХНОЛОШКОГ РАЗВОЈА И ИНОВАЦИЈА

Outline of the talk

I. Introduction of DREENA framework and testing its ability to adequately reproduce high-$p_\perp$ observables
   1. high-$p_\perp$ parton-medium interactions modeled by dynamical energy loss formalism
   2. QGP medium evolution:
      - Constant (average) temperature DREENA-C
      - 1D Bjorken DREENA-B
      - smooth (3(2)+1)D temperature evolution DREENA-A (Adaptive)
      - event-by-event fluctuating hydro background ebe-DREENA

II. DREENA as a high-$p_\perp$ tomography tool for inferring bulk QGP properties?

III. Specific improvement: The effect of including a finite number of scattering centers on high-$p_\perp$ observables

Motivation (I. and II.)

Traditionally, low-$p_\perp$ probes ($p_\perp \leq 2$ GeV) are used to study bulk medium (99.9% of particles formed in HIC) properties

Some important bulk QGP properties difficult to constrain by low-$p_\perp$ theory/simulations

NJP 13, 075004; PRC 97, 044905; PRC 102,, 044911

Commonly, rare (0.1%) high-$p_\perp$ probes ($p_\perp \geq 5$ GeV) are utilized for studying the nature of jet-medium interaction

A decisive role in the QGP discovery.

NPA 750, 30

High-$p_\perp$ QGP tomography: Constraining bulk QGP parameters jointly, by low- and high-$p_\perp$ approaches.

I. Introduction of DREENA framework and testing its ability to adequately reproduce high-$p_{\perp}$ observables

The basis: the dynamical energy loss formalism

Describes high-$p_\perp$ parton-medium interactions

Features:

- QCD medium of finite size and finite temperature
- The medium consists of dynamical (i.e., moving) partons
- Based on finite T field theory and generalized HTL approach M. Djordjevic, PRC 74, 064907; PRC 80, 064909, M. Djordjevic, U. Heinz, PRL 101, 022302
- The same theoretical framework for both radiative and collisional energy loss
- Applicable to both light and heavy flavor M. Djordjevic and M. Gyulassy, NPA 733, 265
- Finite magnetic mass effects M. Djordjevic and M. Djordjevic, PLB 709, 229
- Running coupling M. Djordjevic and M. Djordjevic, PLB 734, 286
- Relaxed soft-gluon approximation BB, M. Djordjevic, M. Djordjevic, PRC 99, 024901

✓All these ingredients important for adequately addressing the data BB and M.Djordjevic, JPG 42, 075105

✓No fitting parameters

✓Temperature as a natural variable in the model (only input)

Numerical framework

- Comparison with a wide range of high-$p_\perp$ experimental data – ultimate test of dynamical energy loss formalism reliability
- We developed a numerical framework, which includes:
  - Light and heavy flavor production

    PLB 718, 482 (2012); PRC 80, 054902 (2009)
  - Dynamical energy loss

    M. Djordjevic and M. Djordjevic, PLB 734, 286
  - Multi-gluon fluctuations

    PLB 538, 282 (2002)
  - Path-length fluctuations, hard sphere restriction $r < R_A$ introduced in WS nuclear density distribution

    EPJ C33 : 495 (2004); D. Zigic, I. Salom, J. Auvinen, M. Djordjevic and M. Djordjevic, JPG 46, 085101 (2019)
  - Fragmentation for light and heavy flavor

DSS, PRD 75, 114010 (2007); BCFY JHEP 0309 , 006 (2003), PRD 51, 4819; KLP, PLB 78, 615

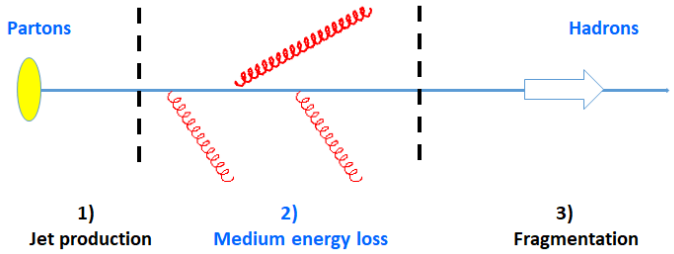

Experimental validation of dynamical energy loss formalism

PLB 734, 286

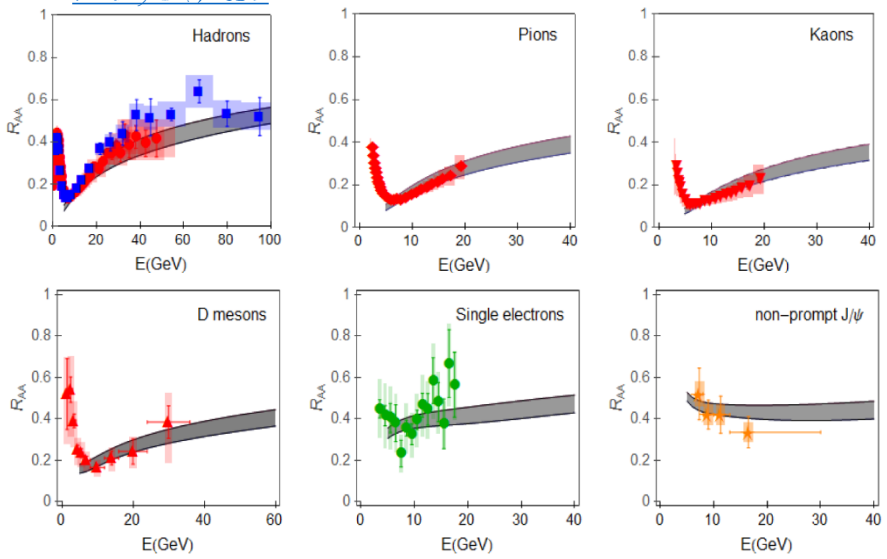

PRC 94, 044908

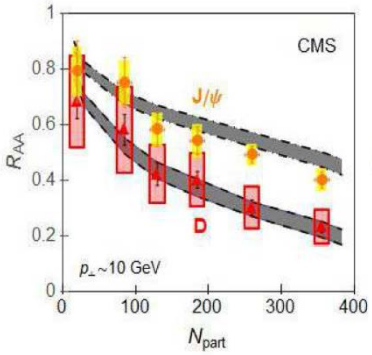

PLB 763, 439

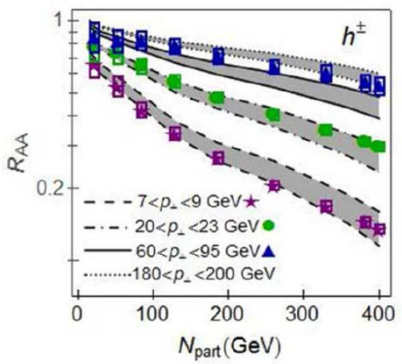

Explains high-$p_\perp$ R_{AA} data for different probes, collision systems (Au+Au, Pb+Pb, Xe+Xe) (experiments), energies and centralities!

PRC 90, 034910

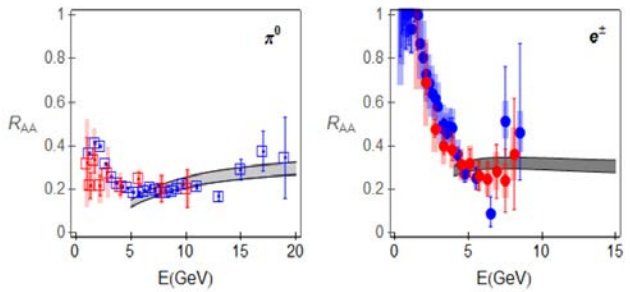

PRL 112, 042302

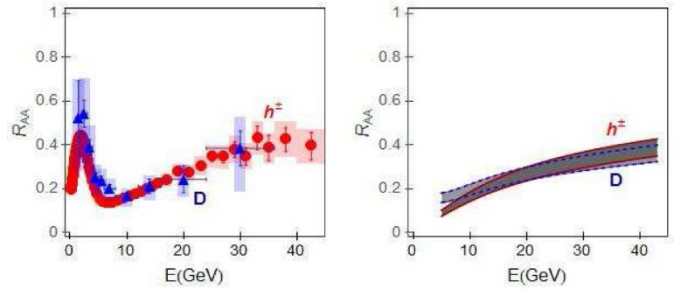

Addresses heavy-flavor puzzle.

PRC 92, 024918

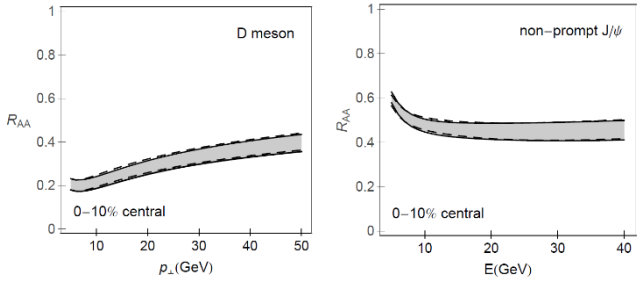

2.76 TeV vs 5.02 TeV

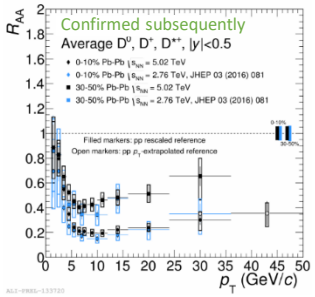

Clear predictive power.

Accurately addresses high-$p_\perp$ parton-medium interactions → Suitable for these studies!

DREENA framework (Dynamical Radiative and Elastic ENergy loss Approach)

✓For using high-p_T theory/data to study the bulk QGP properties:

- Include arbitrary medium evolution (T profile) as the only input (both averaged and ebe)
- Preserve all dynamical energy loss model ingredients
- Develop an efficient (timewise) numerical procedure
- Produce a wide set of light and heavy flavor suppression predictions
- Compare predictions with the data (same numerical procedure and parameter set)
- (Iterate comparison for different combinations of QGP parameters)
- Constrain medium properties consistent with both low- and high-p_T sector

✓Introducing more complex/realistic temperature evolutions:

- DREENA-C: constant temperature medium

D. Zigic, I. Salom, J. Auvinen, M. Djordjevic and M. Djordjevic, J. Phys. G 46, no. 8, 085101 (2019)

- DREENA-B: 1D Bjorken expansion

D. Zigic, I. Salom, J. Auvinen, M. Djordjevic and M. Djordjevic, Phys. Lett. B 791, 236 (2019)

- DREENA-A: smooth (3(2)+1)D temperature evolution

D. Zigic, I. Salom, J. Auvinen, P. Huovinen and M. Djordjevic, Front. in Phys. 10, 957019 (2022).

- ebe-DREENA: event-by-event fluctuating hydro background

D. Zigic, J. Auvinen, I. Salom, P. Huovinen and M. Djordjevic, Phys. Rev. C 106, no.4, 044909 (2022)

$h^{\pm}$ Pb+Pb $\sqrt{s_{NN}}$=5.02 TeV

DREENA-C and DREENA-B overview

DREENA-C: constant temperature medium D. Zigic, I. Salom, J. Auvinen, M. Djordjevic and M. Djordjevic, J. Phys. G 46, no. 8, 085101 (2019)

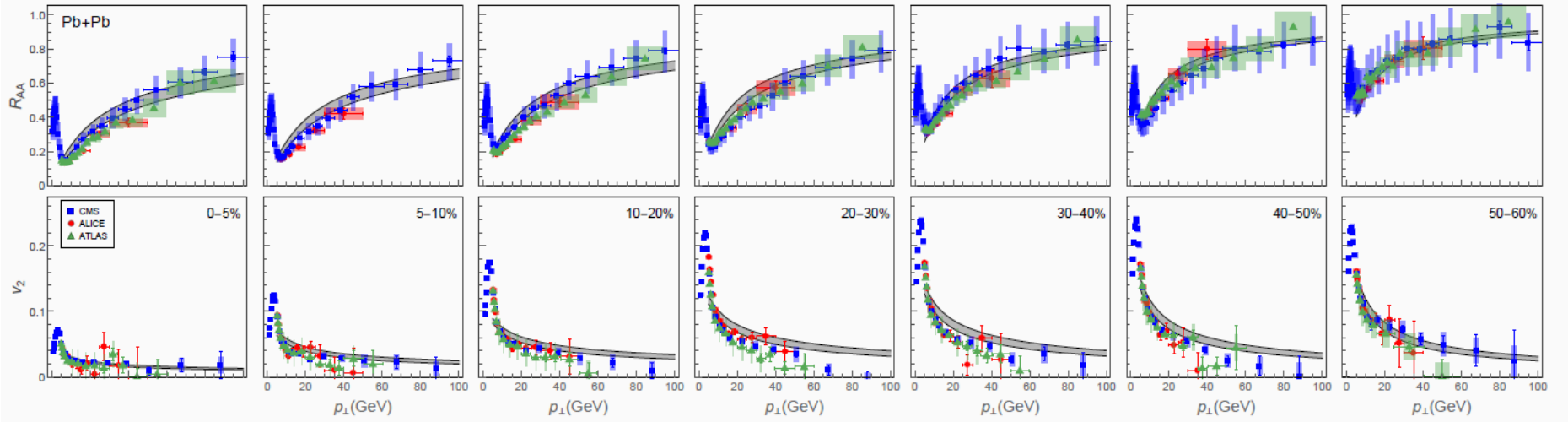

Qualitatively good agreement with high-p_T R_{AA} and v_2 but overestimation of v_2.

DREENA-B: 1D Bjorken expansion D. Zigic, I. Salom, J. Auvinen, M. Djordjevic and M. Djordjevic, Phys. Lett. B 791, 236 (2019)

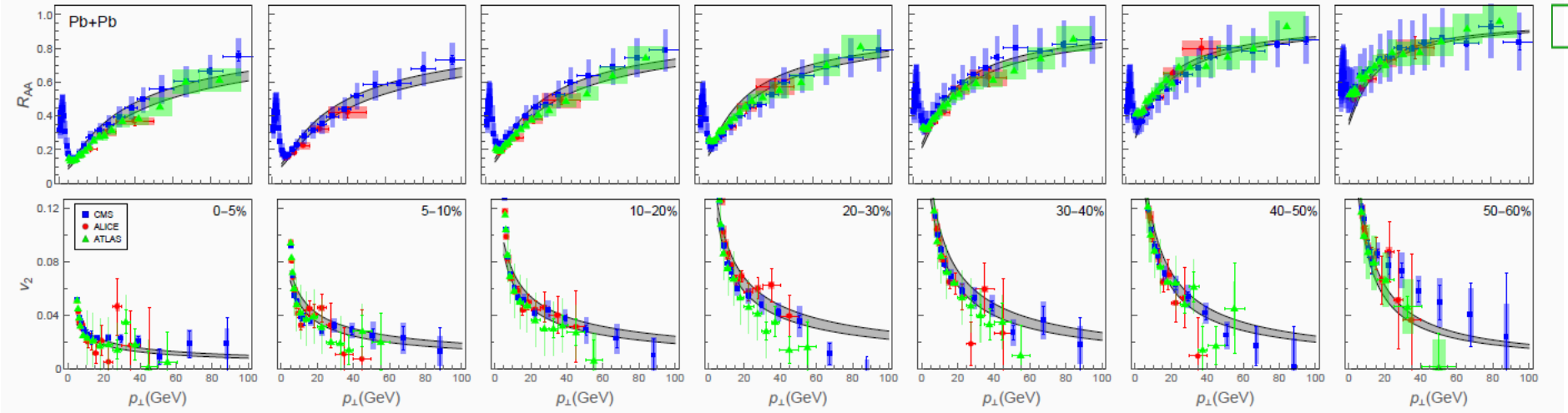

Very good agreement with both R_{AA} and v_2.

Solves v_2 puzzle. R_{AA} remain robust and suitable for calibrating parton-medium interaction model.

PRD 27, 140

PRL 116, no. 25, 252301; JHEP 1410, 043 (2014) ; arXiv:1305.1046 [nucl-th]

DREENA-A:Could high-p_T theory/data provide a constraint on different medium evolution models?

DREENA-A (Adaptive temperature profile)

τ_0=1 fm

τ_0=0.2 fm

τ_0=1.16 fm

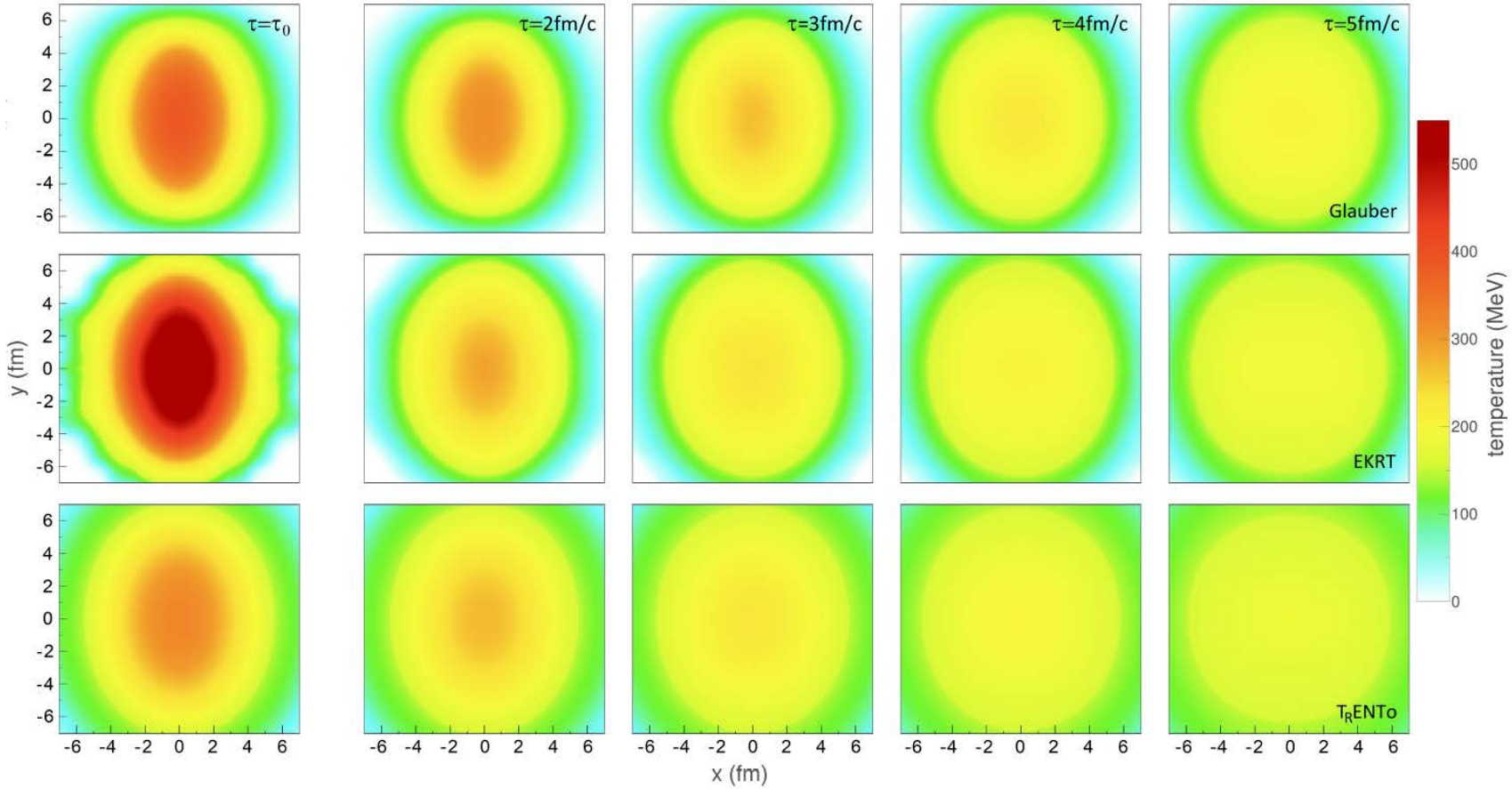

All three evolutions agree with low- p_T data.

Could high-p_T sector additionally constrain these evolutions?

τ_0 = initial time – onset of fluid-dynamical expansion

D. Zigic, I. Salom, J. Auvinen, P. Huovinen and M. Djordjevic, Front. in Phys. 10, 957019 (2022).

Qualitative observations

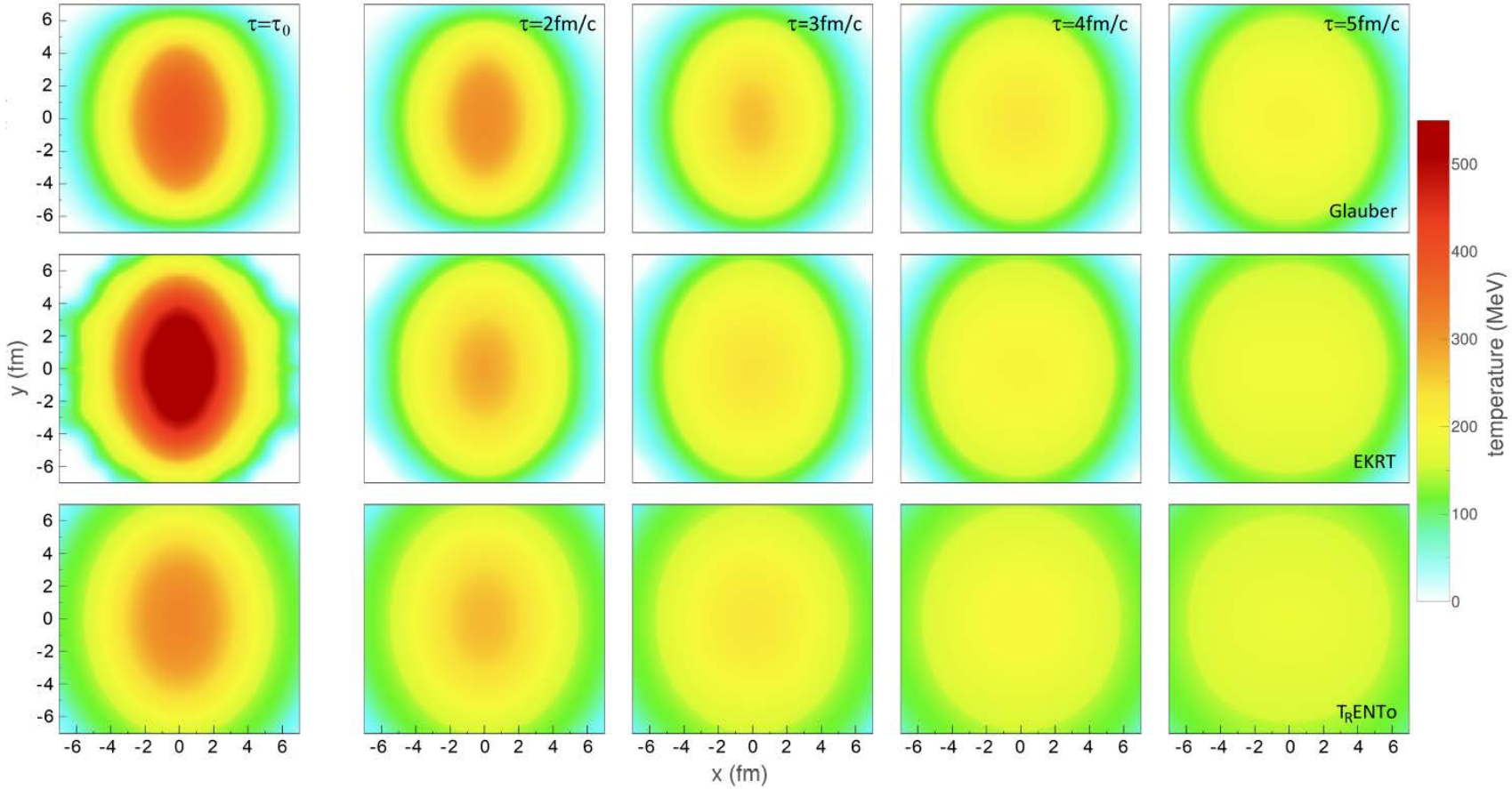

'EKRT' shows the largest T → expected the smallest R_{AA}

Asymmetry: 'Glauber'>'EKRT' >'T_RENTo' → expected v_2(Glauber)> v_2(EKRT)> v_2(T_RENTo)

D. Zigic, I. Salom, J. Auvinen, P. Huovinen and M. Djordjevic, Front. in Phys. 10, 957019 (2022).

Test of DREENA-A predictions (quantitative observations)

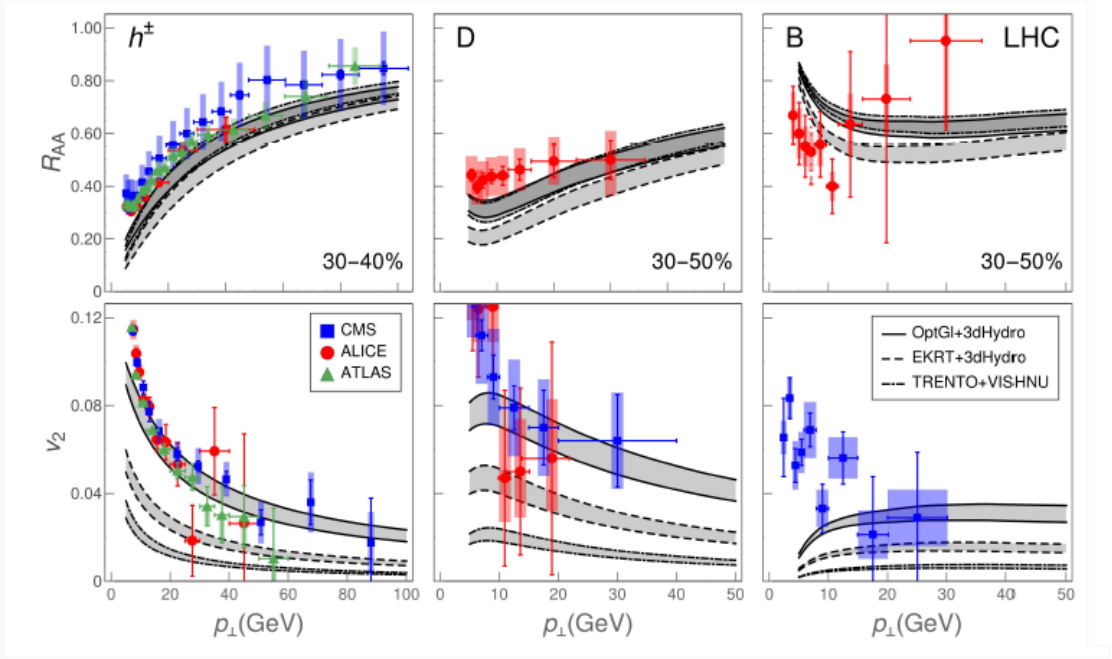

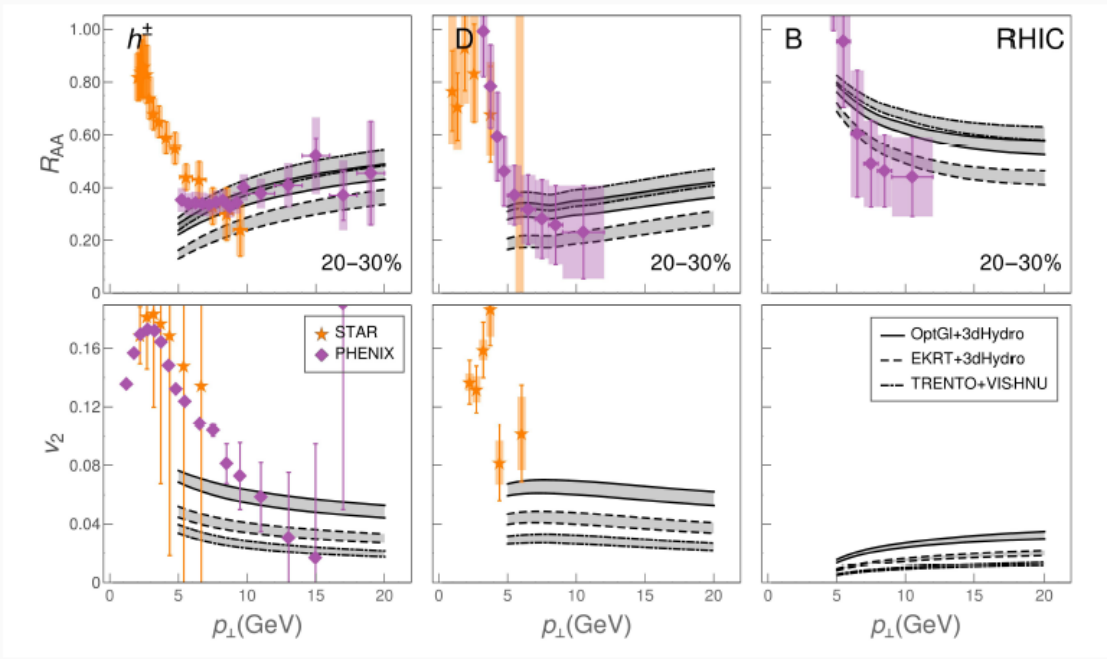

Heavy flavor even more sensitive to different T profiles.

'EKRT' results in the smallest R_{AA}

The same v_2 ordering as the system anisotropy ('Glauber' the largest v_2, 'T$_R$ENTo' the lowest v_2)

Different T profiles: DREENA-A can distinguish between them → complement constraint to low-p_T sector.

D. Zigic, I. Salom, J. Auvinen, P. Huovinen and M. Djordjevic, Front. in Phys. 10, 957019 (2022).

ebe-DREENA: The role of higher harmonics in QGP tomography

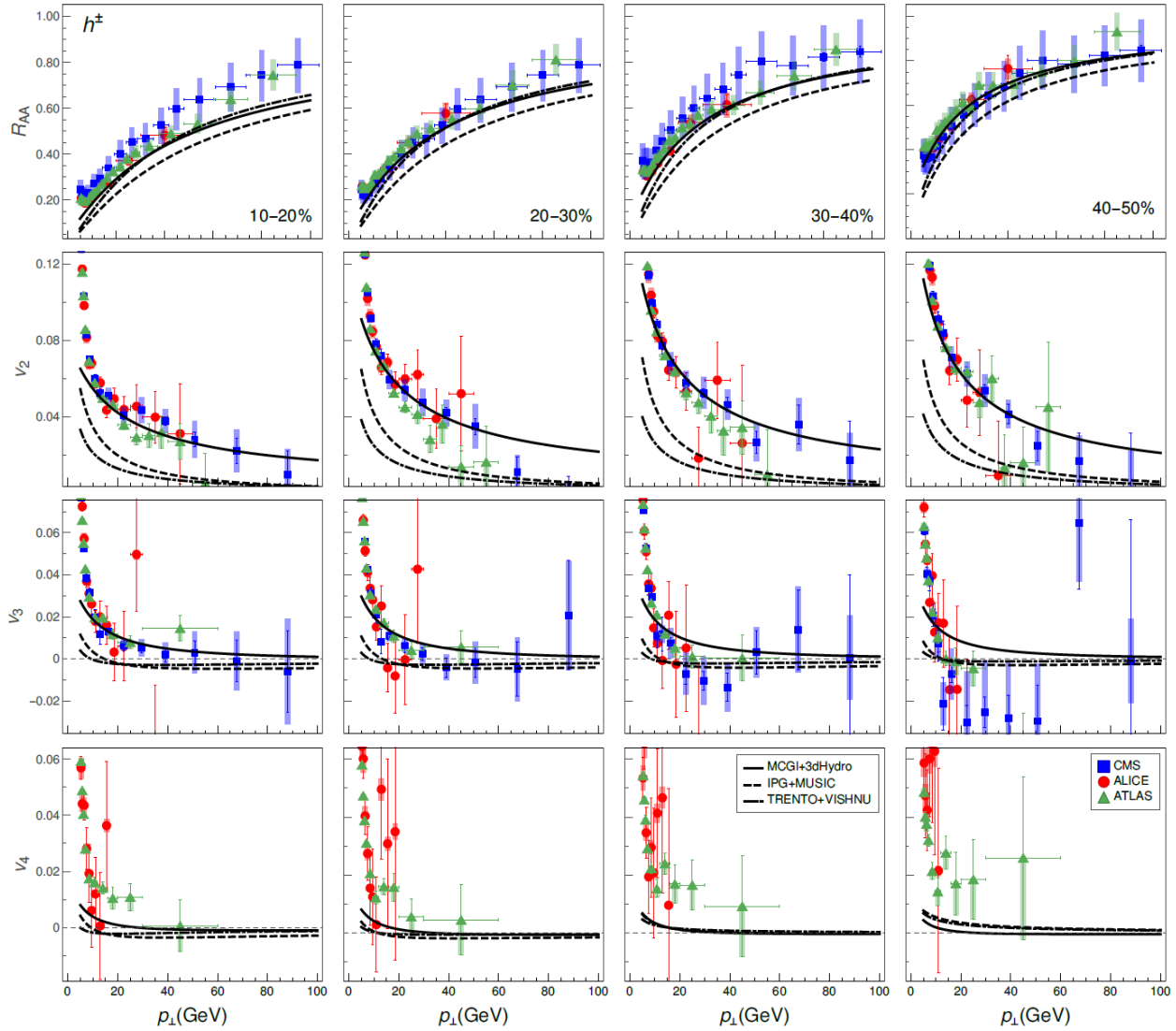

Later thermalization time favored and v_2 ordering as for averaged profiles.

Higher harmonics: qualitatively and quantitatively differentiate between medium evolutions!

More sensitive!

v_4 puzzle!

Good observables for imposing additional constraints on bulk QGP parameters!

MC-Glauber τ_0=1 fm
IP_Glasma τ_{switch}=0.4 fm
T$_R$ENTo τ_0=1.16 fm

D. Zigic, J. Auvinen, I. Salom, P. Huovinen and M. Djordjevic, Phys. Rev. C 106, no.4, 044909 (2022)

ebe DREENA: Heavy flavors

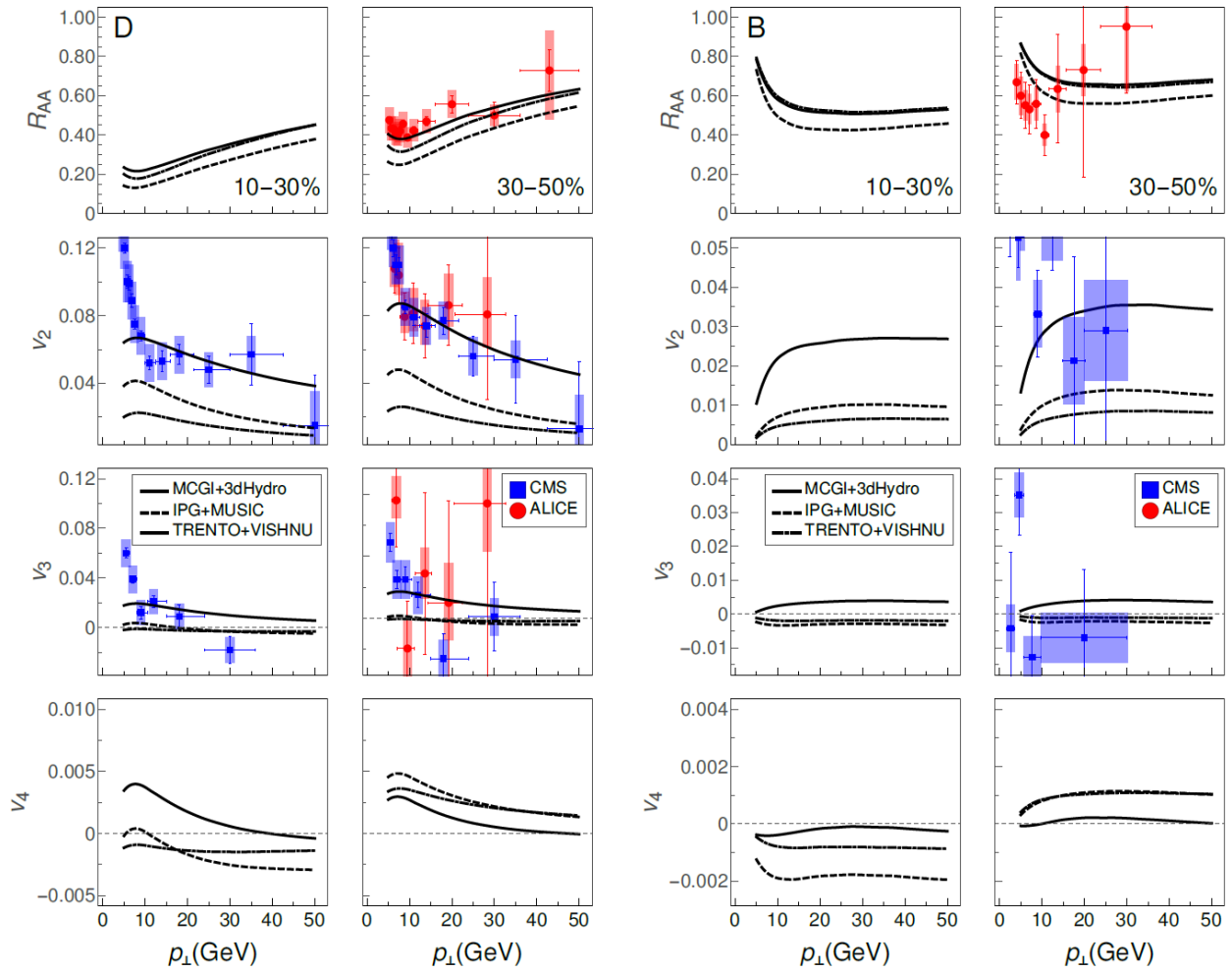

Later thermalization time favored and v_2 ordering as for averaged profiles.

Higher harmonics: qualitatively and quantitatively differentiate between medium evolutions!

More sensitive!

More sensitive than light flavors!

D. Zigic, J. Auvinen, I. Salom, P. Huovinen and M. Djordjevic, Phys. Rev. C 106, no.4, 044909 (2022)

II. DREENA as a high-$p_\perp$ QGP tomography tool for inferring bulk QGP properties?

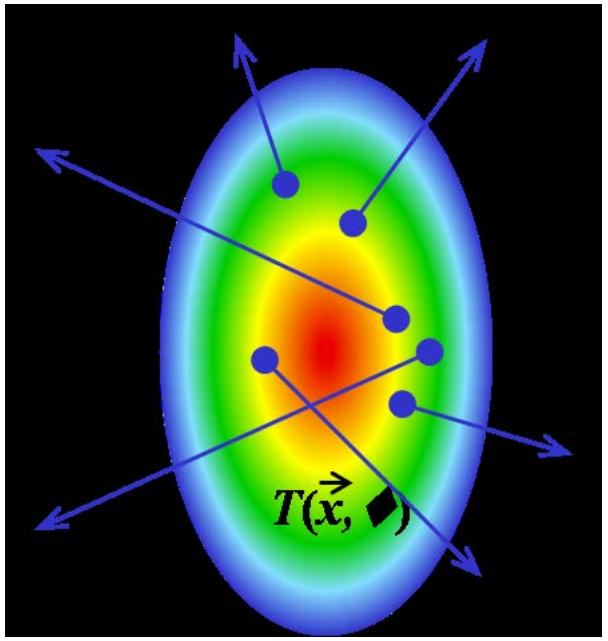

1. Early evolution

S. Stojku, J. Auvinen, M. Djordjevic, P. Huovinen, and M. Djordjevic, Acta Phys. Polon. Supp. 16, 156 (2023); S. Stojku, J. Auvinen, M. Djordjevic, P. Huovinen, and M. Djordjevic, PRC 105, L021901 (2022)

2. QGP anisotropy

S. Stojku, J. Auvinen, L. Zivkovic, P. Huovinen, M. Djordjevic, Phys.Lett.B 835 (2022) 137501

3. η/s(T) parameterization

B. Karmakar, D. Z, I. Salom, J. Auvinen, P. Huovinen, M. Djordjevic and M. Djordjevic, [arXiv:2305.11318 [hep-ph]]

DREENA on GitHub: https://github.com/DusanZigic/DREENA-A

1. Constraining initial time (τ_0) by high-$p_\perp$ QGP tomography

S. Stojku, J. Auvinen, M. Djordjevic, P. Huovinen, and M. Djordjevic, Acta Phys. Polon. Supp. 16, 156 (2023)

τ_0 = initial time – onset of fluid-dynamical expansion

- Low $p_\perp$ sector: Bayesian analysis provides only weak limits τ_0=0.59±0.41 *fm* (NPA 967, 67-73)

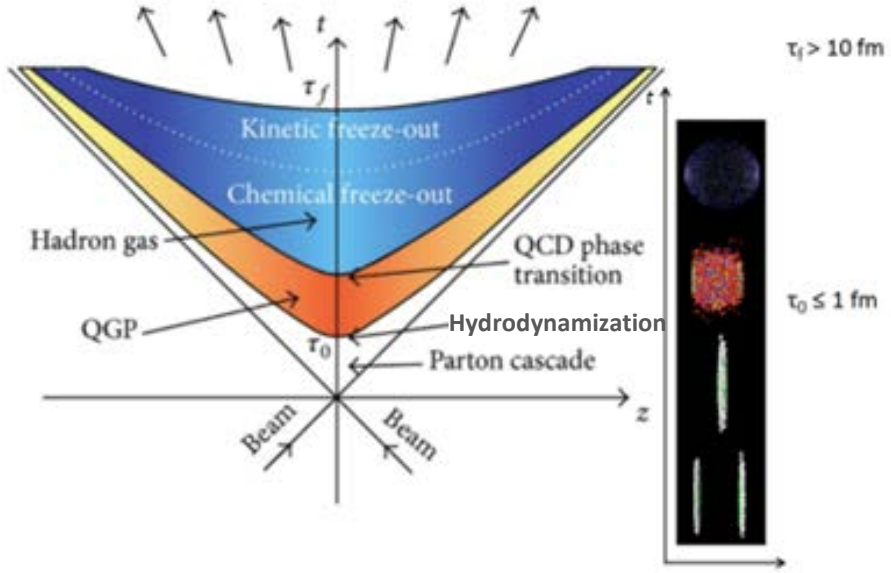

Could high-$p_\perp$ theory and data provide more rigorous constraints?

Within DREENA-A framework upon τ_0:

- High-$p_\perp$ probes: state-of-the-art dynamical energy loss (M. Djordjevic and M. Djordjevic, PLB 734, 286)
  ($\tau_0 = \tau_q$ no interactions before τ_0) τ_q – quenching start time (start of high-p⊥ parton energy loss, i.e., interaction with medium)
- Bulk QGP medium : 3+1D viscous hydrodynamics (E. Molnár, H. Holopainen, P. Huovinen, H. Niemi, PRC 90, 044904 (2014))

D. Zigic, I. Salom, J. Auvinen, P. Huovinen, and M. Djordjevic, Front. In Phys. 10, 957019 (2022)

Sensitivity of high-$p_\perp$ light probes to initial time (τ_0)

Light particles: $h^{\pm}$ Pb+Pb $\sqrt{s_{NN}}$=5.02 TeV

$\tau_0 \in \{0.2, 0.4, 0.6, 0.8, 1.0, 1.2\}\ fm$

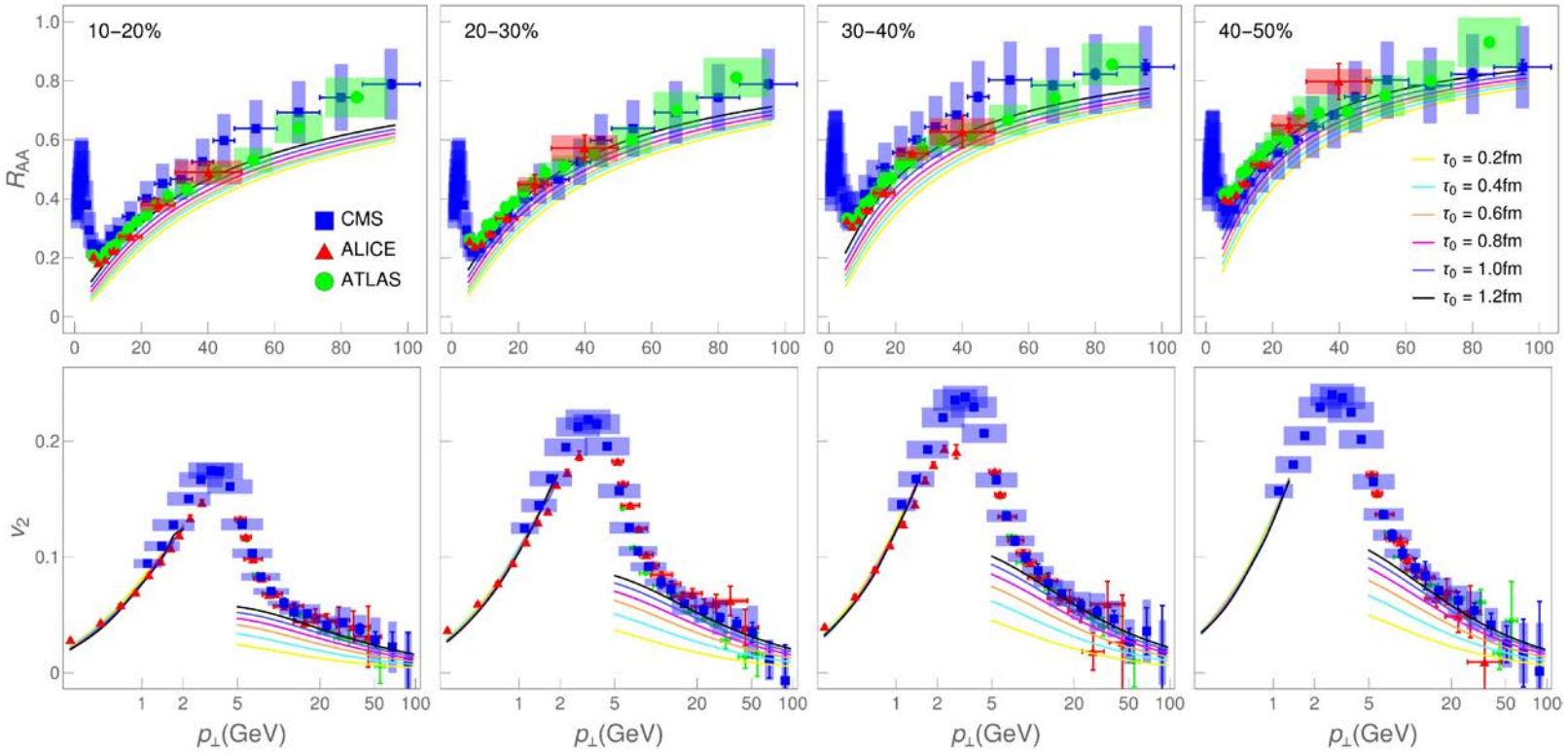

High-$p_\perp$ theory/data can distinguish between different τ_0 .

Delayed onset of fluid dynamics is preferred by both R_{AA} and v_2 (more pronounced in v_2).

Resolution is better at higher centralities (v_2).

CMS JHEP04 (2017) 039; PLB 776 (2018) 195
ALICE JHEP11 (2018) 013; JHEP 07 (2018) 103
ATLAS EPJC 78, 997 (2018)

Optical Glauber, 3+1D hydro PRC 90, 044904

S. Stojku, J. Auvinen, M. Djordjevic, P. Huovinen, and M. Djordjevic, Acta Phys. Polon. Supp. 16, 156 (2023)

Sensitivity of high-$p_\perp$ heavy probes to initial time (τ_0)

Heavy particles: D and B mesons, Pb+Pb $\sqrt{s_{NN}}$=5.02 TeV

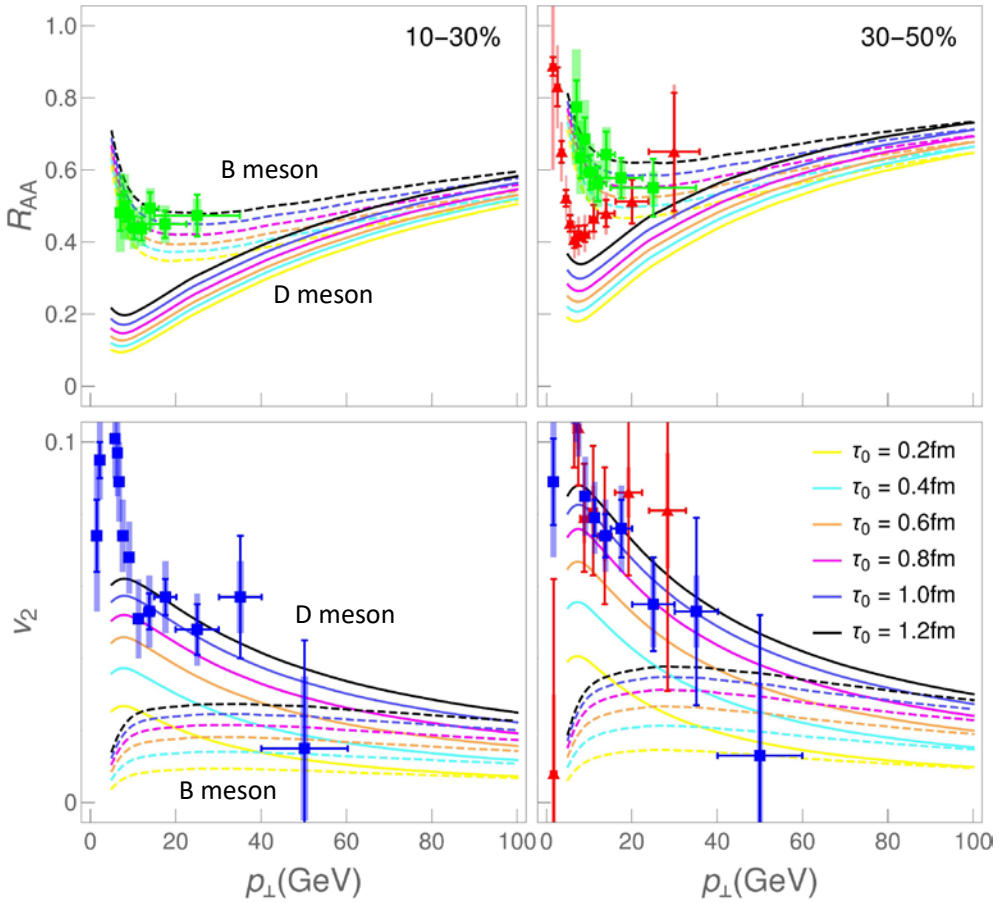

D meson — CMS — PRL 120, 202301 (2018)

D meson — ALICE — JHEP 10, 174 (2018); PRL 120, 102301 (2018)

Non-prompt J/Ψ — CMS — EPJC 78, 509 (2018)

Delayed onset of fluid dynamics is preferred.

High-$p_\perp$ D and B mesons are even more sensitive to τ_0 .

What is the origin of high-$p_\perp$ observables sensitivity to τ_0?

For B mesons true predictions are displayed.

S. Stojku, J. Auvinen, M. Djordjevic, P. Huovinen, and M. Djordjevic, Acta Phys. Polon. Supp. 16, 156 (2023)

Explanation of high-$p_\perp$ observables sensitivity to τ_0

τ_0

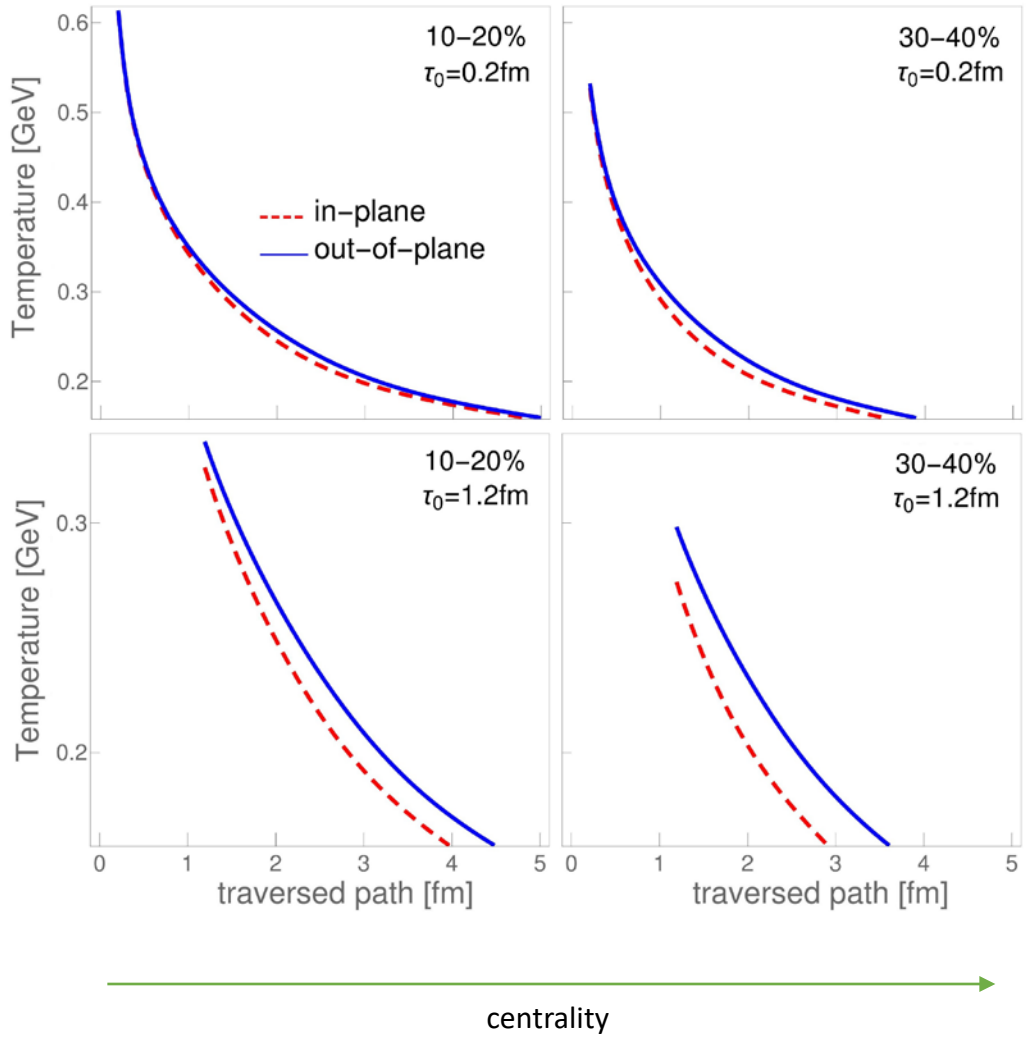

centrality

With increasing τ_0 the difference between T_{out} and T_{in} increases.

$$v_2 \approx \frac{1}{2}\frac{R_{AA}^{in} - R_{AA}^{out}}{R_{AA}^{in} + R_{AA}^{out}}$$

$$R_{AA} \approx 1 - \xi TL$$

D. Zigic, I. Salom, J. Auvinen, M. Djordjevic and M. Djordjevic, JPG 46, 085101 (2019).

Explains v_2 dependence on τ_0.

With increasing τ_0 average T decreases.

$$R_{AA} \approx 1 - \xi TL$$

Explains R_{AA} dependence on τ_0.

S. Stojku, J. Auvinen, M. Djordjevic, P. Huovinen, and M. Djordjevic, Acta Phys. Polon. Supp. 16, 156 (2023)

Various pre-equilibrium evolution scenarios (τ_0)

$h^{\pm}$ Pb+Pb $\sqrt{s_{NN}}$=5.02 TeV

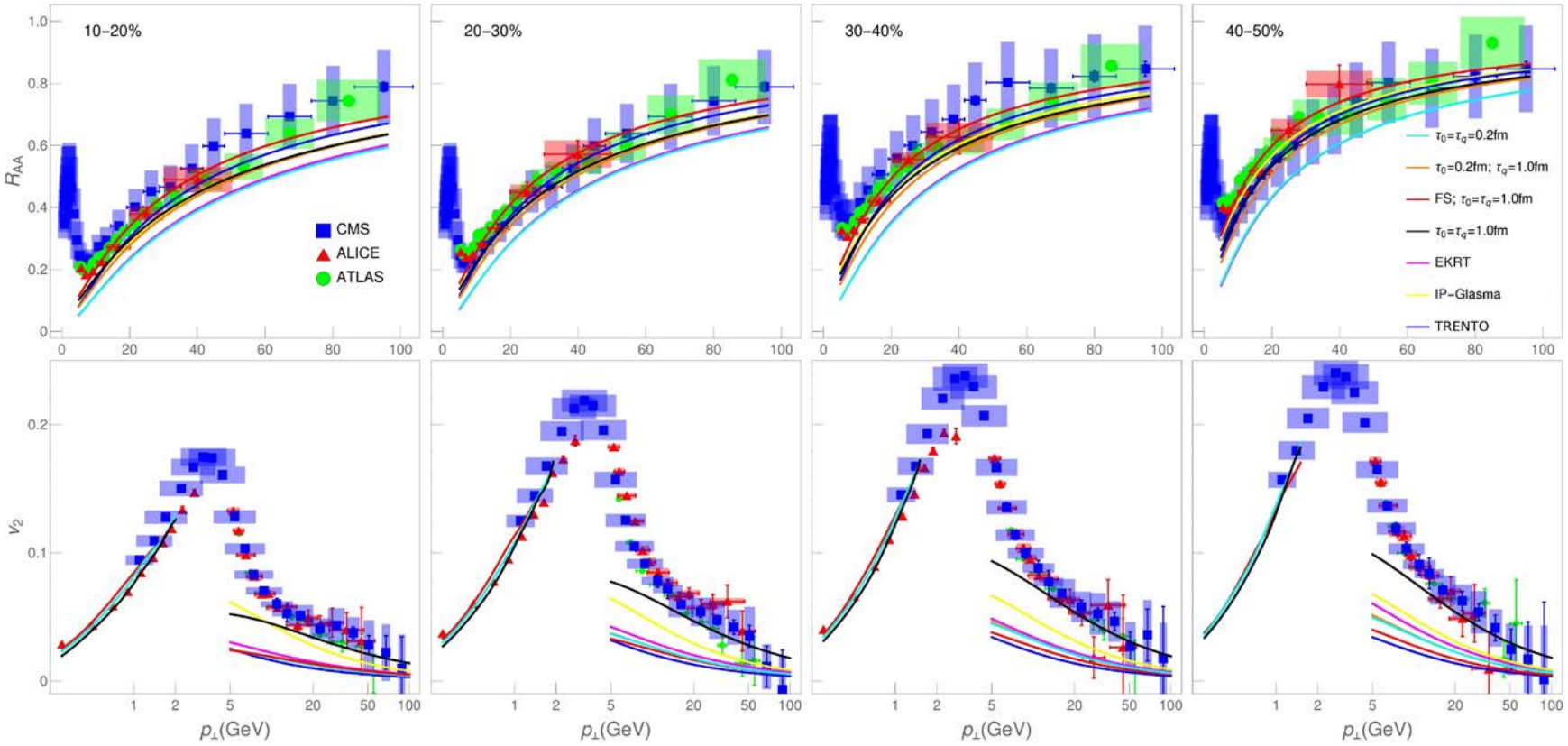

High-$p_\perp$ R_{AA} and v_2 are sensitive to different initializations and early expansion dynamics.

High-$p_\perp$ data prefer later onset of transverse expansion and energy loss!

S. Stojku, J. Auvinen, M. Djordjevic, P. Huovinen, and M. Djordjevic, PRC 105, L021901 (2022)

2. Could high-$p_\perp$ QGP tomography reflect the anisotropy of QGP

- Initial spatial anisotropy – important QGP property
- Still not possible to directly infer the initial anisotropy from experimental measurements
- Experimental observation: high-$p_\perp$ v_2 and $1 - R_{AA}$ directly proportional → $\frac{v_2}{1-R_{AA}}$ is $p_\perp$ independent
- Could fluid dynamical calculation reproduce this proportionality? Connection to anisotropy?

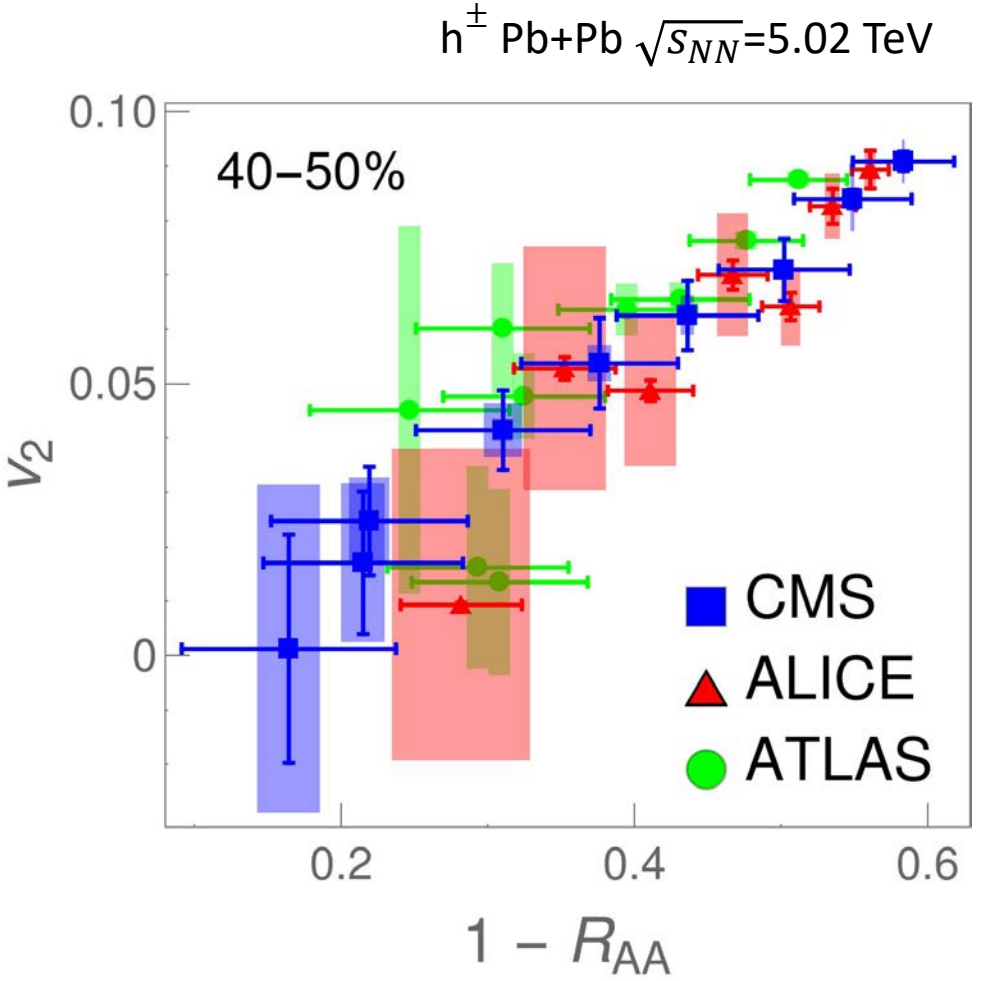

CMS
ALICE
ATLAS

JHEP04 (2017) 039; PLB 776 (2018) 195
JHEP11 (2018) 013; JHEP 07 (2018) 103
ATLAS-CONF-2017-012, EPJC 78, 997 (2018)

S. Stojku, J. Auvinen, L. Zivkovic, P. Huovinen, M. Djordjevic, Phys.Lett.B 835 (2022) 137501

Different evolution scenarios: high-$p_\perp$ observables -intuitive expectations

- DREENA-A framework: different T profiles as the only input

(D. Zigic, I. Salom, J. Auvinen, P. Huovinen and M. Djordjevic, Front. Phys. 10:957019 (2022))

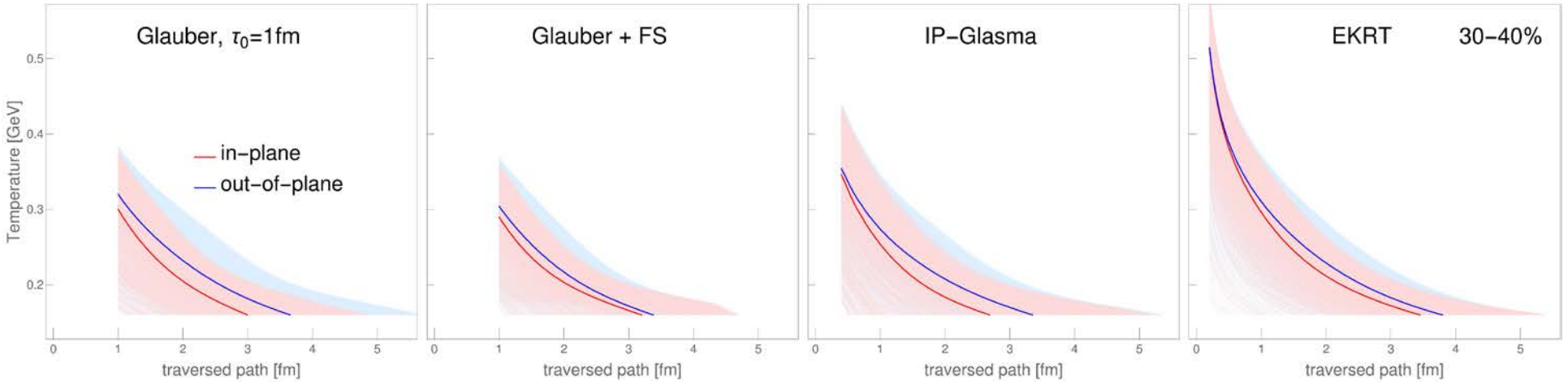

$$R_{AA} \approx 1 - \xi TL \qquad v_2 \approx \Delta T$$

The R_{AA} and v_2 ordering different for different scenarios.

Cannot anticipate $v_2/(1\text{-}R_{AA})$ ordering.

S. Stojku, J. Auvinen, L. Zivkovic, P. Huovinen, M. Djordjevic, Phys.Lett.B 835 (2022) 137501

1. Is saturation in $v_2/(1 - R_{AA})$ at high-$p_\perp$ observed for these different T profiles? M. Djordjevic, S. Stojku, M. Djordjevic, P. Huovinen, Phys. Rev. C **100**, 031901 (2019)
2. If yes, does this saturation carry information about the anisotropy of the system?
3. What kind of anisotropy measure corresponds to the high-$p_\perp$ data?

$v_2/(1-R_{AA})$ DREENA-A predictions for different T profiles

1.

$h^{\pm}$ Pb+Pb $\sqrt{s_{NN}}$=5.02 TeV

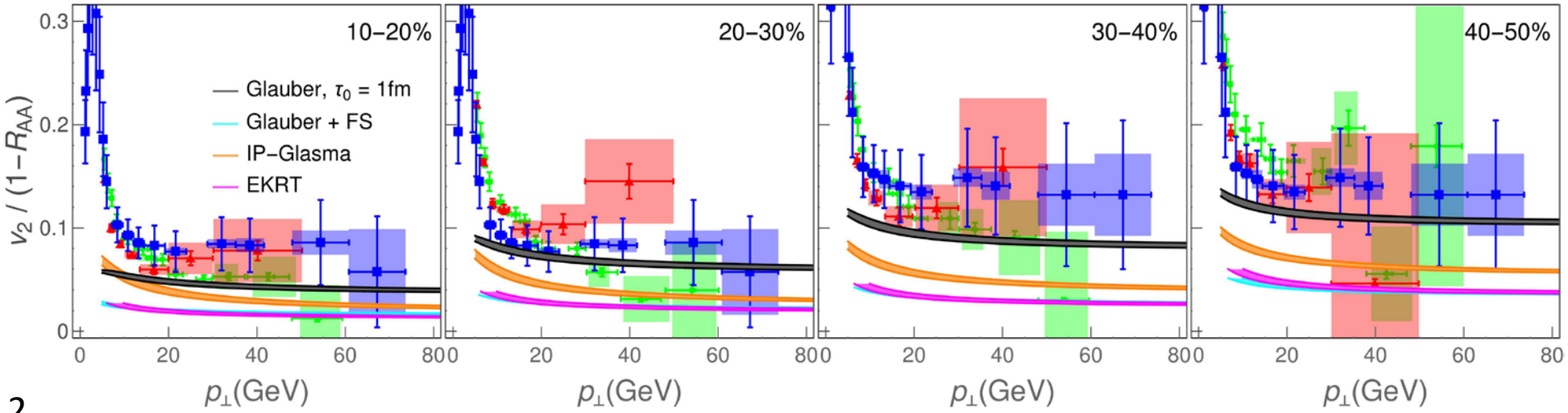

Phenomenon of $v_2/(1-R_{AA})$ saturation is robust to different evolutions!

2.

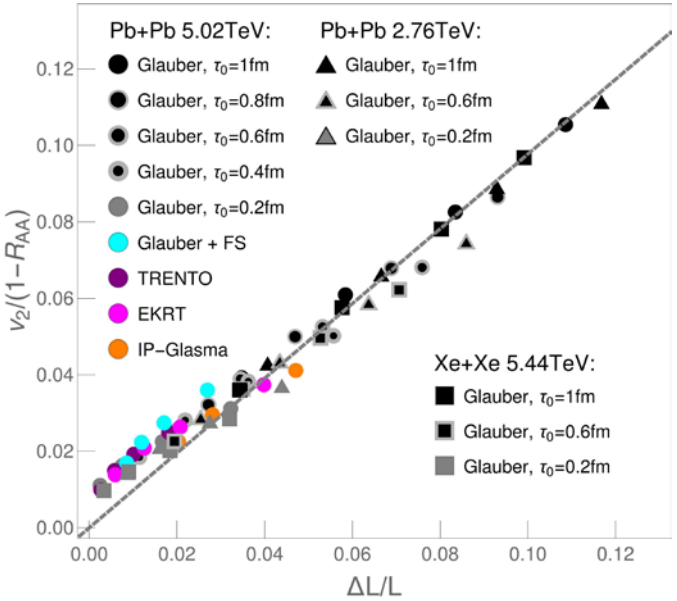

Path-length anisotropy:

$$\frac{\Delta L}{\langle L \rangle} = \frac{\langle L_{out} \rangle - \langle L_{in} \rangle}{\langle L_{out} \rangle + \langle L_{in} \rangle}$$

Surprisingly simple linear dependence, with slope ≈ 1.

Saturation value dominated by system's geometry.

S. Stojku, J. Auvinen, L. Zivkovic, P. Huovinen, M. Djordjevic, Phys.Lett.B 835 (2022) 137501

New observable: Jet-perceived anisotropy

3. We need a more direct measure of anisotropy, with explicit dependence on time evolution

$$jT(\tau,\phi) \equiv \frac{\int \mathrm{d}x\mathrm{d}y\, T^3(x+\tau\cos\phi, y+\tau\sin\phi, \tau)\, n_0(x,y)}{\int \mathrm{d}x\mathrm{d}y\, n_0(x,y)}$$

$$jT_2(\tau) = \frac{\int \mathrm{d}x\mathrm{d}y\, n_0(x,y) \int \mathrm{d}\phi \cos 2\phi\, T^3(x+\tau\cos\phi, y+\tau\sin\phi, \tau)}{\int \mathrm{d}x\mathrm{d}y\, n_0(x,y) \int \mathrm{d}\phi\, T^3(x+\tau\cos\phi, y+\tau\sin\phi, \tau)}$$

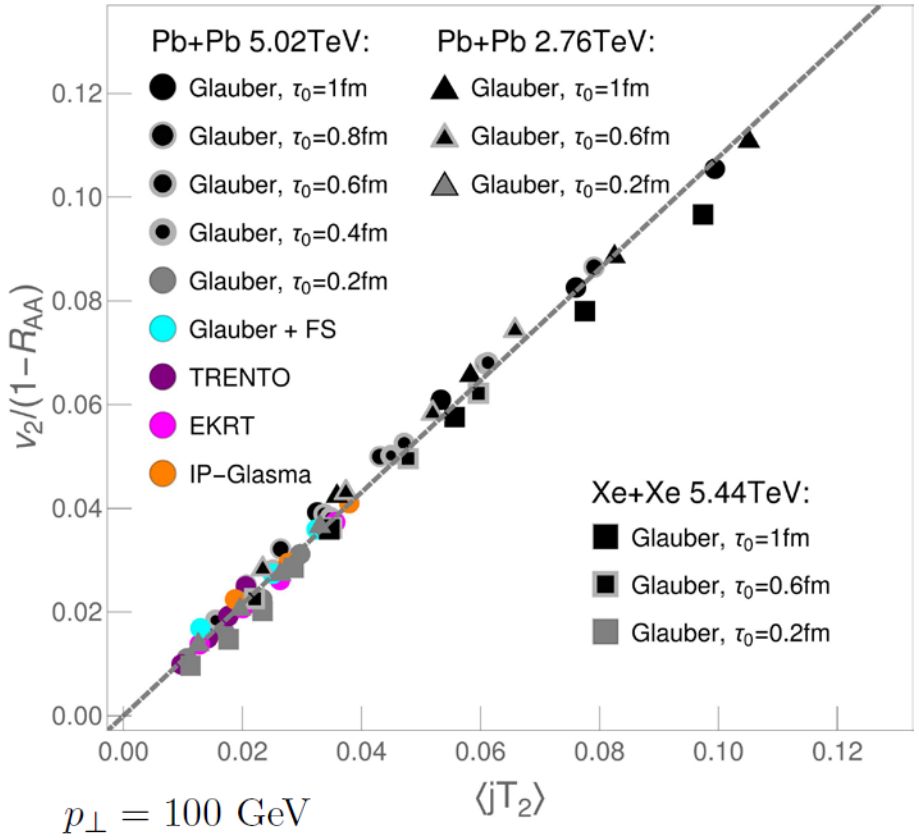

Jet-perceived anisotropy:

$$\langle jT_2 \rangle = \frac{\int_{\tau_0}^{\tau_{\mathrm{cut}}} \mathrm{d}\tau\, jT_2(\tau)}{\tau_{\mathrm{cut}} - \tau_0}$$

τ_{cut} time when the center of the fireball has cooled down to T_c

$v_2/(1-R_{AA})$ displays linear dependence on $\langle jT_2 \rangle$ with slope ≈ 1.

High-$p_\perp$ $v_2/(1-R_{AA})$ carries direct information on a bulk-medium property.

$$v_2/(1-R_{AA}) = \langle jT_2 \rangle$$

$\langle jT_2 \rangle$ can be evaluated from bulk-medium simulations, independently of high-$p_\perp$ data.

$\langle jT_2 \rangle$ new observable, to constrain bulk-medium simulations.

S. Stojku, J. Auvinen, L. Zivkovic, P. Huovinen, M. Djordjevic, Phys.Lett.B 835 (2022) 137501

3.Could high-$p_\perp$ QGP tomography constrain $\eta/s(T)$?

Soft-to-hard medium hypothesis

- QGP is weakly interacting gas? (asymptotic freedom and color screening Physics Today 63, 29)
- $\eta/s \approx \frac{1}{4\pi}$ QGP is perfect fluid? (AdS/CFT: PRL 94, 111601; fluid-dynamical: ARNPS 63, 123)
- At LHC: $T_c<T<4T_c$
- Soft-to-hard QGP hypothesis:
  - Near T_c perfect - fluid (strongly coupled, soft regime)
  - At higher T – gas (weakly coupled, hard regime): η/s may increase with T
- Low-$p_\perp$ sector: η/s is well constrained by Bayesian analysis for $T_c<T<1.5T_c$ but weakly constrained at higher T (NP 15, no.11, 1113-1117; PRC 102, 044911)

⇩

✓ We propose

Complementary approach (high-$p_\perp$ sector): utilize ebe DREENA-A (dynamical energy loss formalism) framework to further constrain $\eta/s(T)$ at high T, and test soft-to-hard hypothesis.

BK, D. Zigic, I. Salom, J. Auvinen, P. Huovinen, M. Djordjevic and M. Djordjevic arXiv:2305.11318

Jet quenching parameter $\frac{\hat{q}}{T^3}$ *vs.* η/s

$\hat{q}$ ≡squared average transverse momentum exchange between high-$\mathbf{p}_\perp$ parton and QGP medium per unit path length

$\frac{\hat{q}}{T^3}$ quantifies the parton coupling strength in QGP: the higher it is the lower η/s should be

In weakly coupled limit: $\eta/s \approx 1.25 \frac{T^3}{\hat{q}}$ PRL 99, 192301; PRD 104, L071501

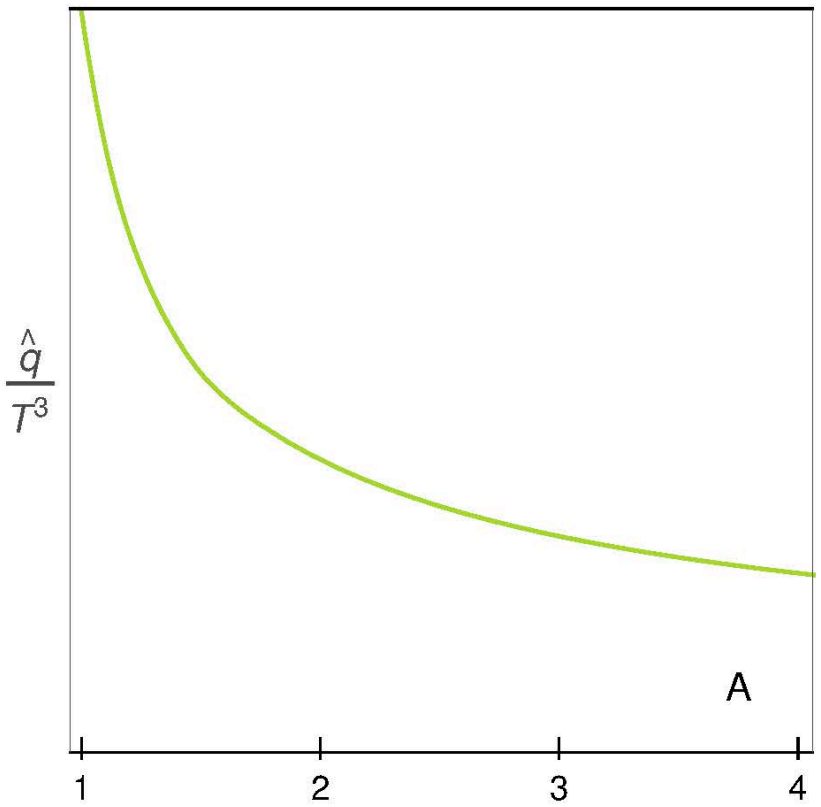

PLB 102, 202302

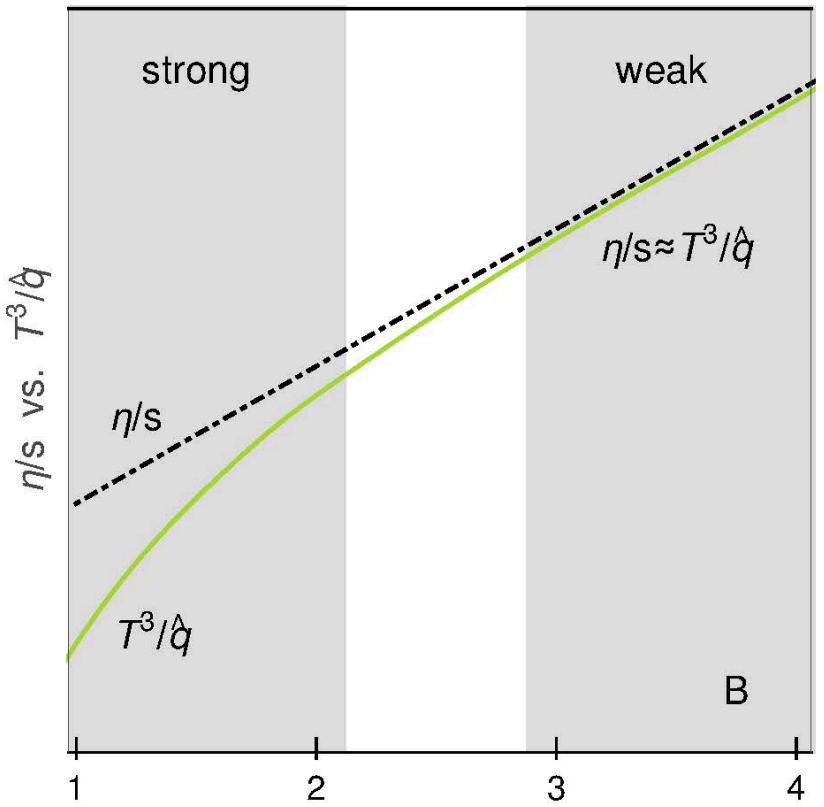

PRL 99, 192301

Dynamical energy loss formalism applicable in weakly coupled regime.

⇩

$\eta/s \approx \frac{\hat{q}}{T^3}$ should hold.

Soft-to-hard boundary?

Theoretical approach: Transport coefficient $\hat{q}$ from dynamical energy loss formalism

$\hat{q}$ ≡squared average transverse momentum exchange between high-$\mathbf{p}_\perp$ parton and QGP medium per unit path length

HTL resummed elastic collision rate:

$$\frac{\mathrm{d}\Gamma_{el}}{\mathrm{d}^2 q} = 4C_A\left(1+\frac{n_f}{6}\right)T^3\frac{\alpha_s^2}{q^2\left(q^2+\mu_E^2\right)}$$

PRC 90, 014909; PRC 74 (2006) 064907

With running coupling, finite magnetic mass:

$$\frac{\mathrm{d}\Gamma_{el}}{\mathrm{d}^2 q} = \frac{C_A}{\pi}T\alpha(ET)\frac{\mu_E^2-\mu_M^2}{(q^2+\mu_E^2)(q^2+\mu_M^2)}$$

PRD 77, 114017; M. Djordjevic and M. Djordjevic, PLB 709, 229

In fluid rest frame:

$$\hat{q} = \int_0^{\sqrt{6ET}} \mathrm{d}^2 q\, q^2 \cdot \frac{\mathrm{d}\Gamma_{el}}{\mathrm{d}^2 q} = C_A T \frac{4\pi}{(11-\frac{2}{3}n_f)} \frac{\left(\mu_E^2 \ln\left[\frac{6ET+\mu_E^2}{\mu E^2}\right] - \mu_M^2 \ln\left[\frac{6ET+\mu_M^2}{\mu_M^2}\right]\right)}{\ln\left(\frac{ET}{\Lambda^2}\right)}$$

$ET \to \infty$

$$\hat{q} \approx C_A\left(\frac{4\pi}{11-\frac{2}{3}n_F}\right)^2 \frac{4\pi\left(1+\frac{n_F}{6}\right)}{W(\xi(T))}\left(1-x_{ME}^2\right)T^3$$

$\hat{q}$ independent on initial parton energy.

Lambert's *W* function $\quad \xi(T) = \frac{1+\frac{n_f}{6}}{11-\frac{2}{3}n_f}\left(\frac{4\pi T}{\Lambda}\right)^2 \quad x_{ME} = \mu_M/\mu_E$

BK, D. Zigic, I. Salom, J. Auvinen, P. Huovinen, M. Djordjevic and M. Djordjevic arXiv:2305.11318

η/s from transport coefficient within dynamical energy loss formalism

BK, D. Zigic, I. Salom, J. Auvinen, P. Huovinen, M. Djordjevic and M. Djordjevic arXiv:2305.11318

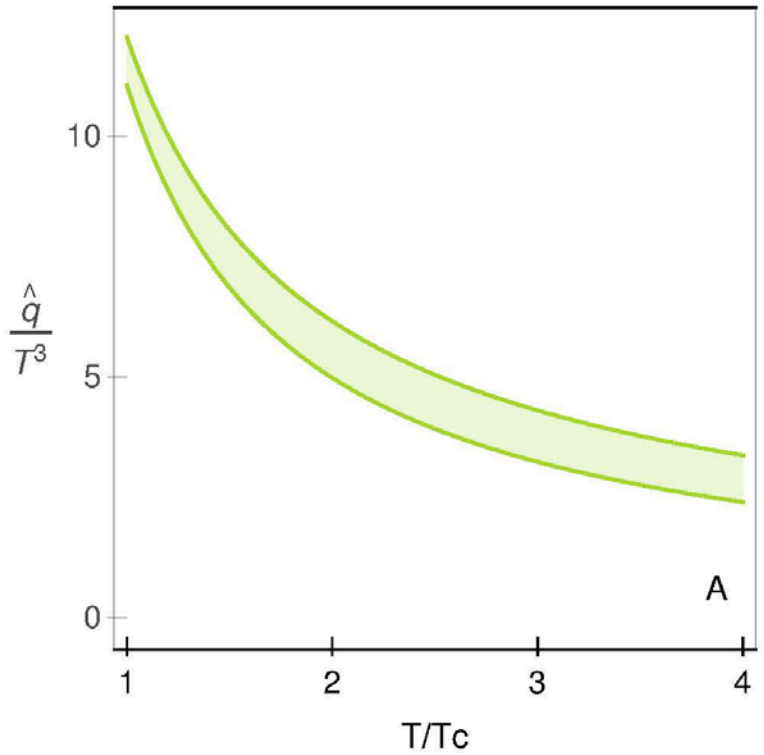

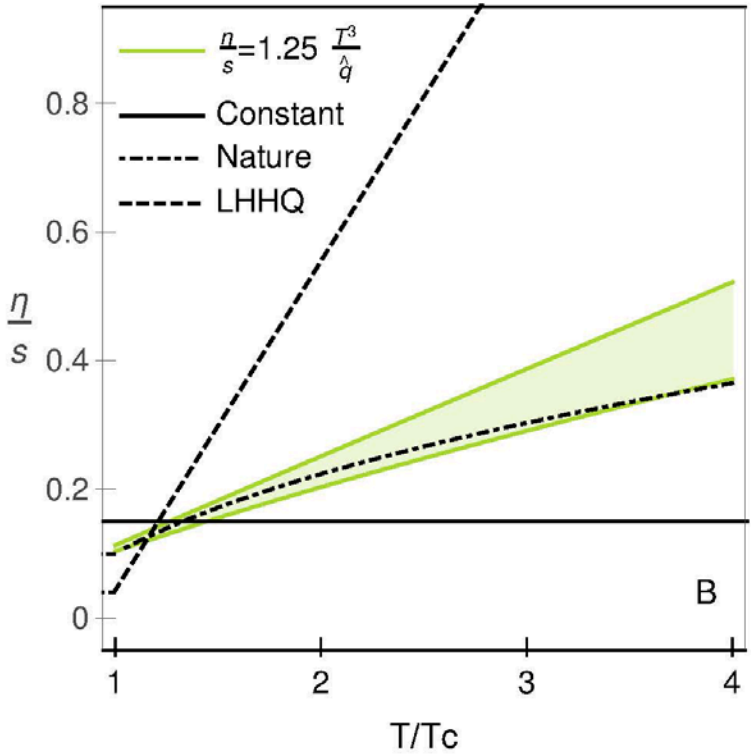

$$(\eta/s)(T) = \begin{cases} (\eta/s)_{\min}, & T < T_c, \\ (\eta/s)_{\min} + (\eta/s)_{\text{slope}}(T - T_c)\left(\frac{T}{T_c}\right)^{(\eta/s)_{\text{crv}}}, & T > T_c, \end{cases}$$

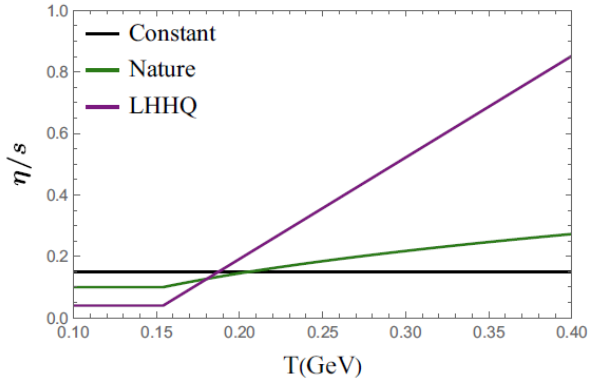

Nature NP 15, no.11, 1113-1117
LHHQ PRL 106, 212302

$\frac{\hat{q}}{T^3}$ exhibits the expected behavior, i.e., large increase near T_c.

Unexpectedly, our high-$p_\perp$ η/s(T) constraint is close to the state-of-the-art Bayesian analysis (NP 15, no.11, 1113-1117).

PRC 90, 014909
PPNP 66, 41-92; PRC 88, 045204

η/s from transport coefficient within dynamical energy loss formalism

BK, D. Zigic, I. Salom, J. Auvinen, P. Huovinen, M. Djordjevic and M. Djordjevic arXiv:2305.11318

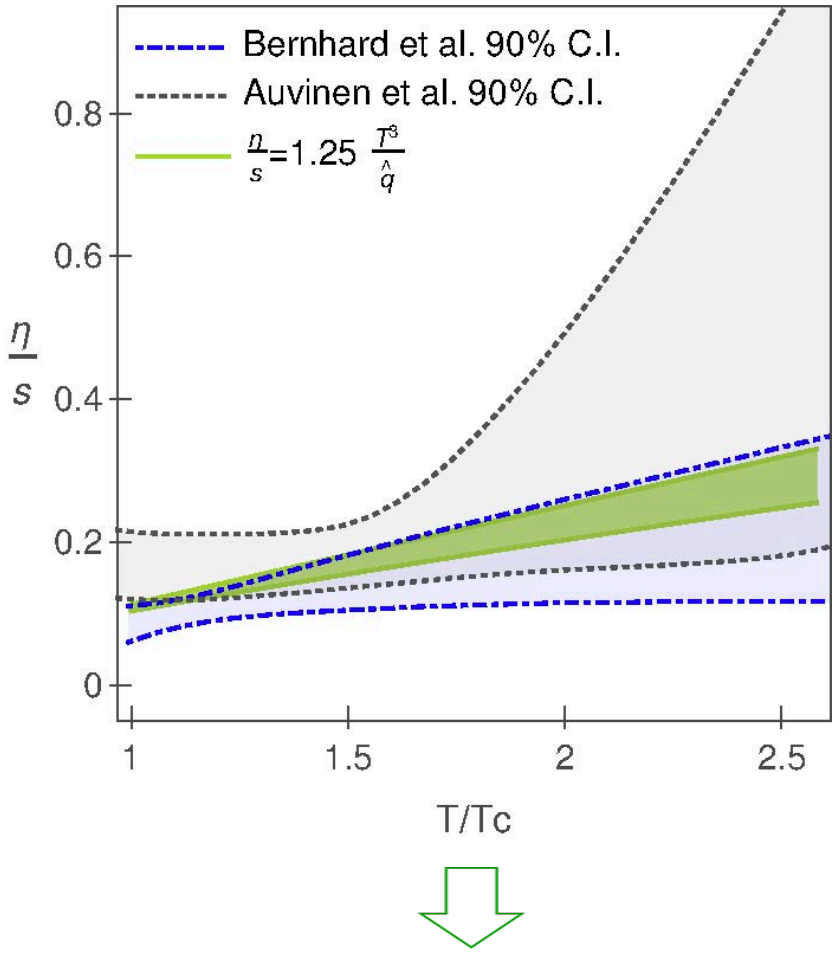

Surprisingly, our η/s(T), extracted from our $\frac{\hat{q}}{T^3}$, agrees well with both state-of-the-art Bayesian analyses (NP 15, no.11, 1113-1117; PRC 102, 044911) in entire T range. Does not drop significantly below inferred values near T_c.

Agreement extends to T_c, i.e., to the regime corresponding to strong coupling!

Hypothesis: quasiparticle description of jet-medium interactions is consistent at the entire T range.

Uncertainty from initial parton energy is much smaller than Bayesian.

No guidance on soft-to-hard boundary.

III. Specific improvement: The effect of including a finite number of scattering centers on high-$p_\perp$ observables

Motivation

- pQCD high-$p_\perp$ radiative energy loss – medium assumptions:
  - Optically thin → One scattering center (SHSA) GLV NPB 594, 371; DGLV NPA 733, 265; HT NPA 696, 788; Prog. PPNP 66,41
  - Optically thick → Infinite number of scattering centers (MSSA, Big Bang) BDMPS-Z NPB 484, 265; NPB 531, 403; JETP Lett. 63, 952; JETP Lett. 65, 615; ASW PRD 69, 114003; AMY JHEP 12, 009
- Realistically, short finite-size droplets of QGP are created at RHIC and LHC (several *fms*, $\lambda \approx 1$ *fm*)

⇩

Relaxing these approximations to the case of a finite number of scattering centers is required!

- Current theoretical attempts to address this highly nontrivial problem are yet inconclusive or incomplete (JHEP 2007, 114; JHEP 2103, 102; JHEP 1907, 057; JHEP 2006, 187; PRD 98, 094010; PLB 795, 502)
- Lacking phenomenological studies (not tested against experimental data)

⇩

These corrections need to be implemented in both analytical calculations (i.e., radiative energy loss model) and numerical framework!

Higher orders in opacity: analytical calculations

In static QGP (D(GLV)):

$$x\frac{dN^{(n)}}{dx\,d^2\mathbf{k}} = \int_0^L dz_1 \cdots \int_{z_{n-1}}^L dz_n \int \prod_{i=1}^{n} \left(d^2\mathbf{q}_i \frac{v^2(\mathbf{q}_i) - \delta^2(\mathbf{q}_i)}{\lambda(z)} \right)$$
$$\times \frac{C_R \alpha_s(Q_k^2)}{\pi^2} \left(-2\,\mathbf{C}_{(1\cdots n)} \cdot \mathbf{B}_n \left[\cos \sum_{k=2}^{n} \omega_{(k\cdots n)} \Delta z_k - \cos \sum_{k=1}^{n} \omega_{(k\cdots n)} \Delta z_k \right] \right)$$

$$\mathbf{C}_{(i_1 i_2 \ldots i_m)} = \frac{(\mathbf{k} - \mathbf{q}_{i_1} - \mathbf{q}_{i_2} - \ldots - \mathbf{q}_{i_m})}{\chi^2 + (\mathbf{k} - \mathbf{q}_{i_1} - \mathbf{q}_{i_2} - \ldots - \mathbf{q}_{i_m})^2}$$

$$\mathbf{B}_i = \mathbf{H} - \mathbf{C}_i$$

$$\mathbf{H} = \frac{\mathbf{k}}{\chi^2 + \mathbf{k}^2}$$

Inverse of formation time:

$$\omega_{(m\ldots n)} = \frac{\chi^2 + (\mathbf{k} - \mathbf{q}_m - \ldots \mathbf{q}_n)^2}{2xE}$$

$$\chi^2 \equiv M^2 x^2 + m_g^2$$

$$\alpha_s(Q^2) = \frac{4\pi}{(11 - 2/3 n_f) \ln(Q^2/\Lambda_{QCD})}$$

$$Q_k^2 = \frac{\mathbf{k}^2 + M^2 x^2 + m_g^2}{x}$$

S. Wicks, arXiv:0804.4704, M. Djordjevic and M. Gyulassy, NPA 733, 265

In dynamical QGP:

M. Djordjevic, PRC 80, 064909; M. Djordjevic and U. Heinz, PRL 101, 022302; M. Djordjevic, PLB 709, 229

Effective potential $$\left[\frac{\mu_E^2}{\pi(\mathbf{q}^2+\mu_E^2)^2}\right]_{\text{stat}} \rightarrow \left[\frac{\mu_E^2 - \mu_M^2}{\pi(\mathbf{q}^2+\mu_E^2)(\mathbf{q}^2+\mu_M^2)}\right]_{\text{dyn}}$$

Mean free path $$\frac{1}{\lambda_{\text{stat}}} = c(n_f)\frac{1}{\lambda_{\text{dyn}}} = 6\frac{1.202}{\pi^2}\frac{1+n_f/4}{1+n_f/6}3\alpha_S T$$

Obtained explicit analytical expressions up to 4th order in opacity within Dynamical energy loss formalism for the first time.

S. Stojku, BI, I. Salom, M. Djordjevic, arXiv:2303.14527, Accepted in PRC

Analytical calculations: examples

1st order in opacity:

$$\left(\frac{dN_g^{(1)}}{dx}\right) = \frac{2C_R}{\pi x}\int\frac{d^2\mathbf{k}}{\pi}\int\frac{d^2\mathbf{q}_1}{\pi}\,\alpha_s(Q_k^2)\frac{L}{\lambda_{dyn}}\frac{\mu_E^2-\mu_M^2}{(\mathbf{q}_1^2+\mu_E^2)(\mathbf{q}_1^2+\mu_M^2)}$$
$$\frac{\chi^2(\mathbf{q}_1\cdot(\mathbf{q}_1-\mathbf{k}))+(\mathbf{q}_1\cdot\mathbf{k})(\mathbf{k}-\mathbf{q}_1)^2}{(\chi^2+\mathbf{k}^2)(\chi^2+(\mathbf{k}-\mathbf{q}_1)^2)^2}\left(1-\frac{\sin(L\omega_{(1)})}{L\omega_{(1)}}\right)$$

2nd order in opacity:

$$\left(\frac{dN_g^{(2)}}{dx}\right)_1 = \frac{2C_R}{\pi x}\int\frac{d^2\mathbf{k}}{\pi}\iint\frac{d^2\mathbf{q}_1}{\pi}\frac{d^2\mathbf{q}_2}{\pi}\,\alpha_s(Q_k^2)\frac{1}{\lambda_{dyn}^2}\frac{\mu_E^2-\mu_M^2}{(\mathbf{q}_1^2+\mu_E^2)(\mathbf{q}_1^2+\mu_M^2)}\frac{\mu_E^2-\mu_M^2}{(\mathbf{q}_2^2+\mu_E^2)(\mathbf{q}_2^2+\mu_M^2)}$$
$$\frac{\chi^2(\mathbf{q}_2\cdot(\mathbf{q}_1+\mathbf{q}_2-\mathbf{k}))+(\mathbf{q}_2\cdot\mathbf{k})(\mathbf{k}-\mathbf{q}_2)^2+(\mathbf{k}\cdot\mathbf{q}_1)(\mathbf{q}_2\cdot(\mathbf{q}_2-2\mathbf{k}))+\mathbf{k}^2(\mathbf{q}_2\cdot\mathbf{q}_1)}{(\chi^2+\mathbf{k}^2)(\chi^2+(\mathbf{k}-\mathbf{q}_2)^2)(\chi^2+(\mathbf{k}-\mathbf{q}_1-\mathbf{q}_2)^2)}$$
$$\frac{1}{\omega_{(2)}}\left(\frac{\omega_{(2)}\cos\left(L(\omega_{(2)}+\omega_{(12)})\right)}{(\omega_{(2)}+\omega_{(12)})\,\omega_{(12)}}+L\sin(L\omega_{(2)})-\frac{(\omega_{(2)}-\omega_{(12)})\cos(L\omega_{(2)})}{\omega_{(2)}\omega_{(12)}}-\frac{\omega_{(12)}}{\omega_{(2)}(\omega_{(2)}+\omega_{(12)})}\right)$$

3rd order in opacity:

$$\left(\frac{dN_g^{(3)}}{dx}\right)_1 = \frac{2C_R}{\pi x}\int\frac{d^2\mathbf{k}}{\pi}\iiint\frac{d^2\mathbf{q}_1}{\pi}\frac{d^2\mathbf{q}_2}{\pi}\frac{d^2\mathbf{q}_3}{\pi}$$
$$\alpha_s(Q_k^2)\frac{1}{\lambda_{dyn}^3}\frac{\mu_E^2-\mu_M^2}{(\mathbf{q}_1^2+\mu_E^2)(\mathbf{q}_1^2+\mu_M^2)}\frac{\mu_E^2-\mu_M^2}{(\mathbf{q}_2^2+\mu_E^2)(\mathbf{q}_2^2+\mu_M^2)}\frac{\mu_E^2-\mu_M^2}{(\mathbf{q}_3^2+\mu_E^2)(\mathbf{q}_3^2+\mu_M^2)}$$
$$\frac{\chi^2(\mathbf{q}_3\cdot(\mathbf{q}_1+\mathbf{q}_2+\mathbf{q}_3-\mathbf{k}))+(\mathbf{q}_3\cdot\mathbf{k})(\mathbf{k}-\mathbf{q}_3)^2+(\mathbf{k}\cdot(\mathbf{q}_1+\mathbf{q}_2))(\mathbf{q}_3\cdot(\mathbf{q}_3-2\mathbf{k}))+\mathbf{k}^2(\mathbf{q}_3\cdot(\mathbf{q}_1+\mathbf{q}_2))}{(\chi^2+\mathbf{k}^2)(\chi^2+(\mathbf{k}-\mathbf{q}_3)^2)(\chi^2+(\mathbf{k}-\mathbf{q}_1-\mathbf{q}_2-\mathbf{q}_3)^2)}$$
$$\left(\frac{\omega_{(3)}\omega_{(123)}+2\omega_{(23)}\omega_{(123)}-\omega_{(23)}^2-\omega_{(3)}\omega_{(23)}}{\omega_{(23)}^2(\omega_{(3)}+\omega_{(23)})^2\omega_{(123)}}\sin\left(L(\omega_{(3)}+\omega_{(23)})\right)-\frac{\omega_{(123)}\sin\left(L\omega_{(3)}\right)}{\omega_{(3)}\omega_{(23)}^2\left(\omega_{(23)}+\omega_{(123)}\right)}\right.$$
$$\left.+\frac{\sin\left(L\left(\omega_{(3)}+\omega_{(23)}+\omega_{(123)}\right)\right)}{\omega_{(123)}\left(\omega_{(23)}+\omega_{(123)}\right)\left(\omega_{(3)}+\omega_{(23)}+\omega_{(123)}\right)}-\frac{L\cos\left(L\left(\omega_{(3)}+\omega_{(23)}\right)\right)}{\omega_{(23)}\left(\omega_{(3)}+\omega_{(23)}\right)}\right),$$

Highly oscillatory, and difficult to converge!

4th order in opacity:

$$\left(\frac{dN_g^{(4)}}{dx}\right)_1 = \frac{2C_R}{\pi x}\int\frac{d^2\mathbf{k}}{\pi}\iiint\frac{d^2\mathbf{q}_1}{\pi}\frac{d^2\mathbf{q}_2}{\pi}\frac{d^2\mathbf{q}_3}{\pi}\frac{d^2\mathbf{q}_4}{\pi}$$
$$\alpha_s(Q_k^2)\frac{1}{\lambda_{dyn}^4}\frac{\mu_E^2-\mu_M^2}{(\mathbf{q}_1^2+\mu_E^2)(\mathbf{q}_1^2+\mu_M^2)}\frac{\mu_E^2-\mu_M^2}{(\mathbf{q}_2^2+\mu_E^2)(\mathbf{q}_2^2+\mu_M^2)}\frac{\mu_E^2-\mu_M^2}{(\mathbf{q}_3^2+\mu_E^2)(\mathbf{q}_3^2+\mu_M^2)}\frac{\mu_E^2-\mu_M^2}{(\mathbf{q}_4^2+\mu_E^2)(\mathbf{q}_4^2+\mu_M^2)}$$
$$\frac{\chi^2(\mathbf{q}_4\cdot(\mathbf{q}_1+\mathbf{q}_2+\mathbf{q}_3+\mathbf{q}_4-\mathbf{k}))+(\mathbf{q}_4\cdot\mathbf{k})(\mathbf{k}-\mathbf{q}_4)^2+(\mathbf{k}\cdot(\mathbf{q}_1+\mathbf{q}_2+\mathbf{q}_3))(\mathbf{q}_4\cdot(\mathbf{q}_4-2\mathbf{k}))+\mathbf{k}^2(\mathbf{q}_4\cdot(\mathbf{q}_1+\mathbf{q}_2+\mathbf{q}_3))}{(\chi^2+\mathbf{k}^2)(\chi^2+(\mathbf{k}-\mathbf{q}_4)^2)(\chi^2+(\mathbf{k}-\mathbf{q}_1-\mathbf{q}_2-\mathbf{q}_3-\mathbf{q}_4)^2)}$$
$$\left(-\frac{L\sin\left(L\left(\omega_{(4)}+\omega_{(34)}+\omega_{(234)}\right)\right)}{\omega_{(234)}\left(\omega_{(34)}+\omega_{(234)}\right)\left(\omega_{(4)}+\omega_{(34)}+\omega_{(234)}\right)}\right.$$
$$-\frac{\cos\left(L\left(\omega_{(4)}+\omega_{(34)}+\omega_{(234)}+\omega_{(1234)}\right)\right)}{\omega_{(1234)}\left(\omega_{(234)}+\omega_{(1234)}\right)\left(\omega_{(34)}+\omega_{(234)}+\omega_{(1234)}\right)\left(\omega_{(4)}+\omega_{(34)}+\omega_{(234)}+\omega_{(1234)}\right)}$$
$$+\frac{F_{41}}{\omega_{(234)}^2\left(\omega_{(34)}+\omega_{(234)}\right)^2\left(\omega_{(4)}+\omega_{(34)}+\omega_{(234)}\right)^2\omega_{(1234)}}\cos\left(L(\omega_{(4)}+\omega_{(34)}+\omega_{(234)})\right)$$
$$+\frac{\omega_{(1234)}\cos\left(L\left(\omega_{(4)}+\omega_{(34)}\right)\right)}{\omega_{(34)}\left(\omega_{(4)}+\omega_{(34)}\right)\omega_{(234)}^2\left(\omega_{(234)}+\omega_{(1234)}\right)}-\frac{\omega_{(1234)}\cos\left(L\omega_{(4)}\right)}{\omega_{(4)}\omega_{(34)}\left(\omega_{(34)}+\omega_{(234)}\right)^2\left(\omega_{(34)}+\omega_{(234)}+\omega_{(1234)}\right)}$$
$$\left.+\frac{\omega_{(1234)}}{\omega_{(4)}\left(\omega_{(4)}+\omega_{(34)}\right)\left(\omega_{(4)}+\omega_{(34)}+\omega_{(234)}\right)^2\left(\omega_{(4)}+\omega_{(34)}+\omega_{(234)}+\omega_{(1234)}\right)}\right),$$

$$F_{41}=(\omega_{(34)}+\omega_{(234)})\left[(\omega_{(4)}+\omega_{(34)})(\omega_{(234)}-\omega_{(1234)})+\omega_{(234)}^2-3\omega_{(234)}\omega_{(1234)}\right]-\omega_{(4)}\omega_{(234)}\omega_{(1234)}$$

S. Stojku, BI, I. Salom, M. Djordjevic, arXiv:2303.14527 Accepted in PRC

Higher orders in opacity: Numerical calculations

S. Stojku, BI, I. Salom, M. Djordjevic, arXiv:2303.14527
Accepted in PRC

Representative contribution:

$$\left(\frac{dN_g^{(3)}}{dx}\right)_1 = \frac{2C_R}{\pi x}\int\frac{d^2\mathbf{k}}{\pi}\iiint\frac{d^2\mathbf{q}_1}{\pi}\frac{d^2\mathbf{q}_2}{\pi}\frac{d^2\mathbf{q}_3}{\pi}$$
$$\alpha_s(Q_k^2)\frac{1}{\lambda_{dyn}^3}\frac{\mu_E^2-\mu_M^2}{(\mathbf{q}_1^2+\mu_E^2)(\mathbf{q}_1^2+\mu_M^2)}\frac{\mu_E^2-\mu_M^2}{(\mathbf{q}_2^2+\mu_E^2)(\mathbf{q}_2^2+\mu_M^2)}\frac{\mu_E^2-\mu_M^2}{(\mathbf{q}_3^2+\mu_E^2)(\mathbf{q}_3^2+\mu_M^2)}$$
$$\frac{\chi^2(\mathbf{q}_3\cdot(\mathbf{q}_1+\mathbf{q}_2+\mathbf{q}_3-\mathbf{k}))+(\mathbf{q}_3\cdot\mathbf{k})(\mathbf{k}-\mathbf{q}_3)^2+(\mathbf{k}\cdot(\mathbf{q}_1+\mathbf{q}_2))(\mathbf{q}_3\cdot(\mathbf{q}_3-2\mathbf{k}))+\mathbf{k}^2(\mathbf{q}_3\cdot(\mathbf{q}_1+\mathbf{q}_2))}{(\chi^2+\mathbf{k}^2)(\chi^2+(\mathbf{k}-\mathbf{q}_3)^2)(\chi^2+(\mathbf{k}-\mathbf{q}_1-\mathbf{q}_2-\mathbf{q}_3)^2)}$$
$$\left(\frac{\omega_{(3)}\omega_{(123)}+2\omega_{(23)}\omega_{(123)}-\omega_{(23)}^2-\omega_{(3)}\omega_{(23)}}{\omega_{(23)}^2(\omega_{(3)}+\omega_{(23)})^2\omega_{(123)}}\sin\left(L(\omega_{(3)}+\omega_{(23)})\right)-\frac{\omega_{(123)}\sin\left(L\omega_{(3)}\right)}{\omega_{(3)}\omega_{(23)}^2\left(\omega_{(23)}+\omega_{(123)}\right)}\right.$$
$$\left.+\frac{\sin\left(L\left(\omega_{(3)}+\omega_{(23)}+\omega_{(123)}\right)\right)}{\omega_{(123)}\left(\omega_{(23)}+\omega_{(123)}\right)\left(\omega_{(3)}+\omega_{(23)}+\omega_{(123)}\right)}-\frac{L\cos\left(L\left(\omega_{(3)}+\omega_{(23)}\right)\right)}{\omega_{(23)}\left(\omega_{(3)}+\omega_{(23)}\right)}\right)$$

Highly oscillatory, and difficult to converge!

Up to 3rd order: required 70 000 CPUh to converge.

Numerical integration w.r.t. **k** and **q** → $\frac{dN^g}{dx}$ up to 3rd order in opacity

Implemented into generalized DREENA-C (Dynamical Radiative and Elastic ENergy loss Approach, C-constant T medium) framework to generate predictions for high-$p_\perp$ R_{AA} and v_2.

Optimal framework for this analysis.

Effect of higher orders in opacity on $\frac{dN^g}{dx}$

x - fraction of initial parton's energy carried away by radiated gluon

S. Stojku, BI, I. Salom, M. Djordjevic, arXiv:2303.14527 Accepted in PRC

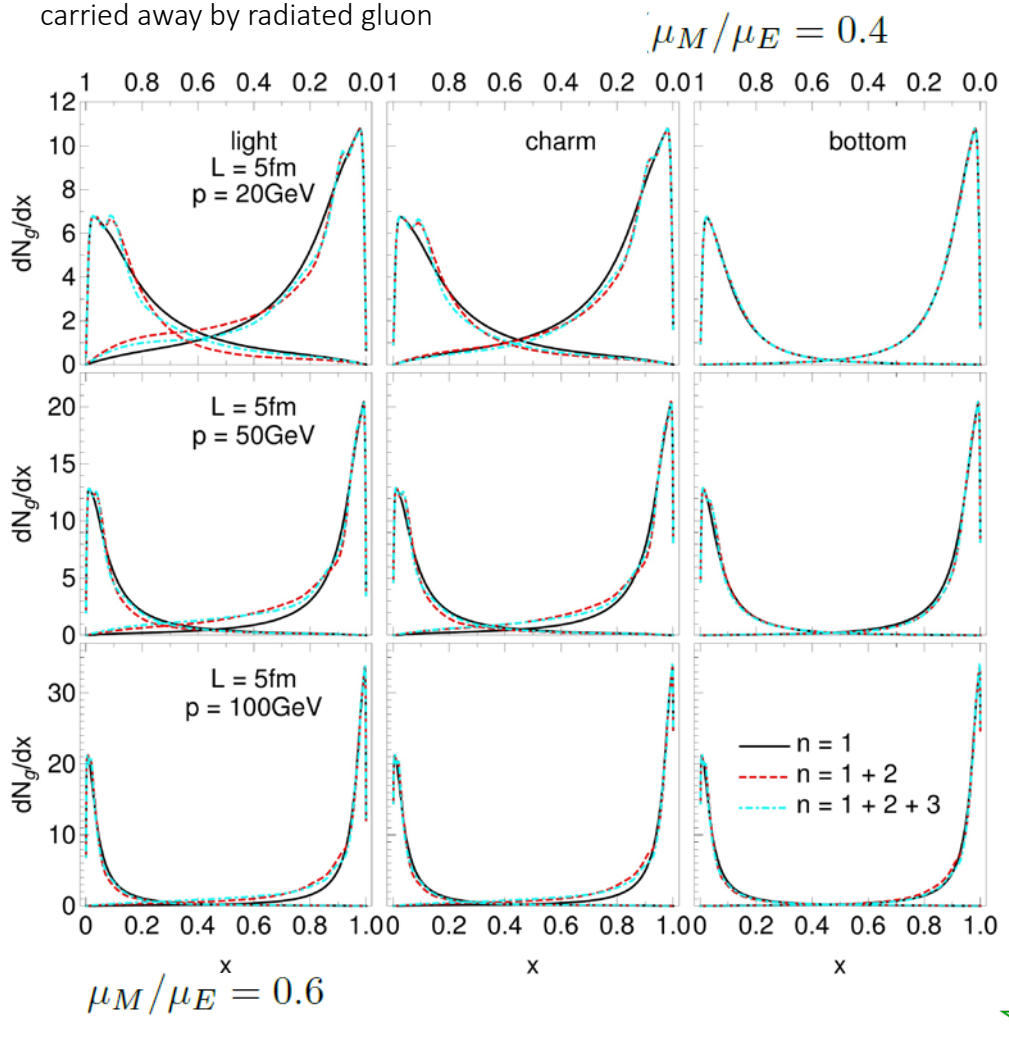

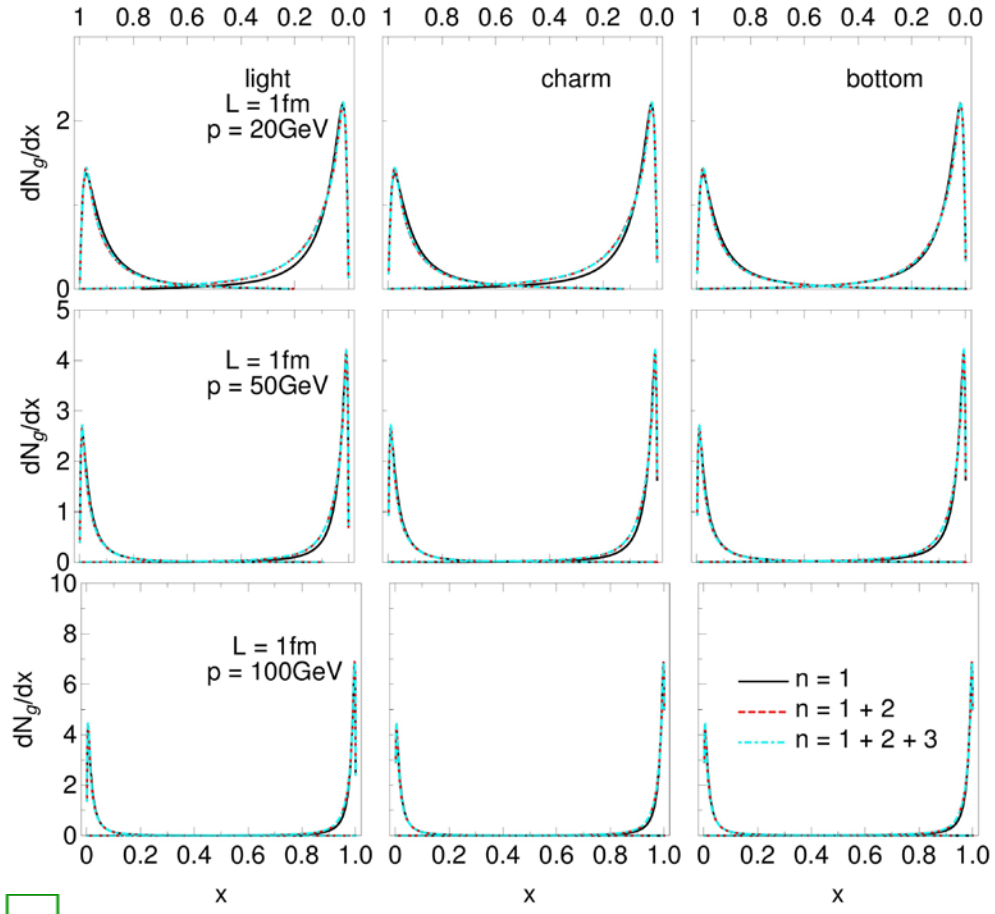

Bottom quark practically unaffected.

Light and charm quarks moderately affected.

What is the effect on observables?

Diminishes with the increase of high-$p_\perp$ partons energy and mass, as well as with the decrease of QCD medium size.

PRD 81 091501; PRD 69, 014506

Effect of higher orders in opacity on radiative R_{AA} and v_2

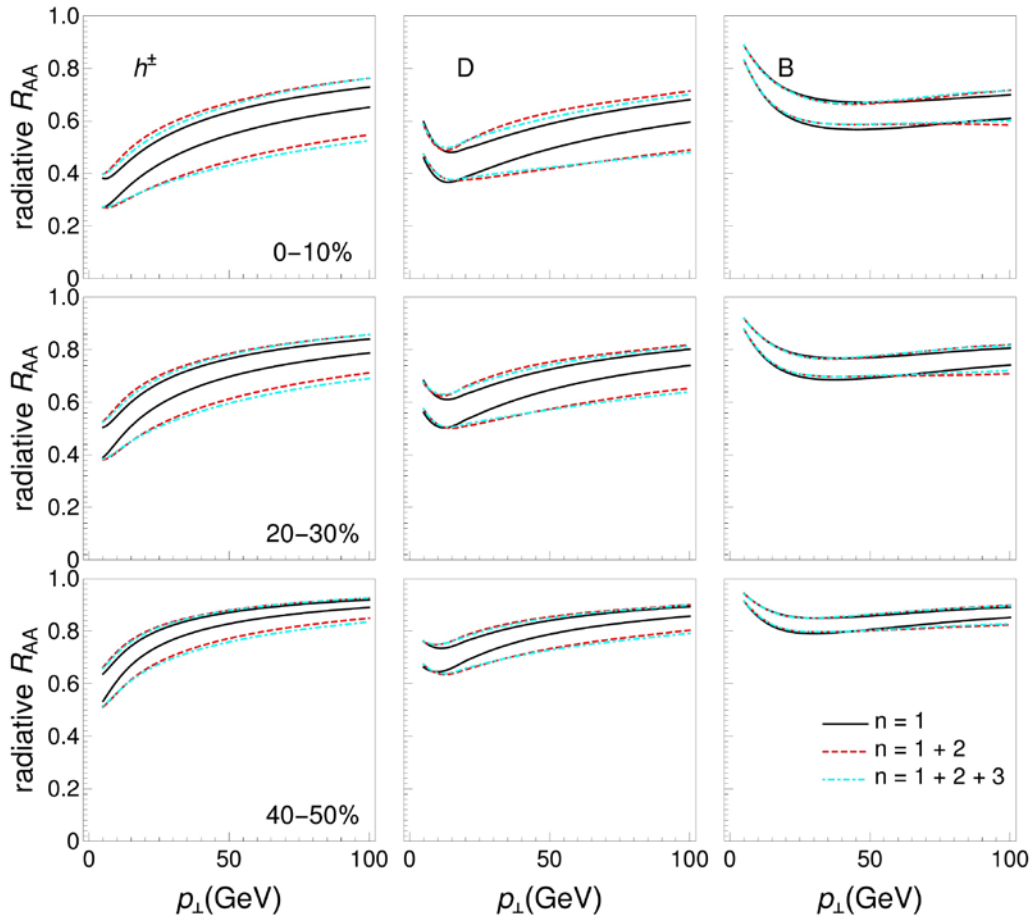

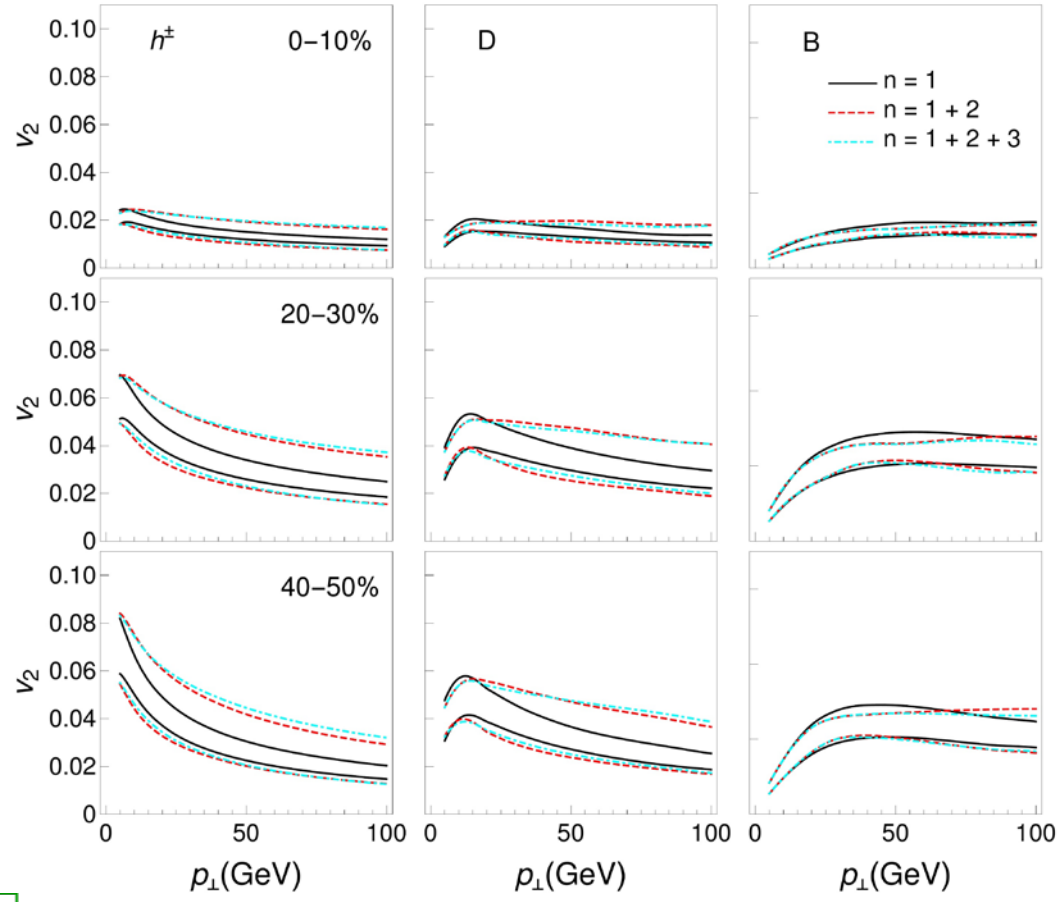

3rd overlaps with 2nd order.

2nd order sufficient!

M. Djordjevic and M. Gyulassy, NPA 733, 265; C. Andres et al., JHEP 07, 114

Qualitatively and quantitatively similar effect on R_{AA} and v_2: Decreases for more peripheral collisions. Effect on B meson insignificant (short formation time; approaches incoherent limit), whereas increases with decreasing mass.

Effect of higher orders in opacity on radiative R_{AA} (I)

(dependence on magnetic mass)

S. Stojku, BI, I. Salom, M. Djordjevic, arXiv:2303.14527 Accepted in PRC

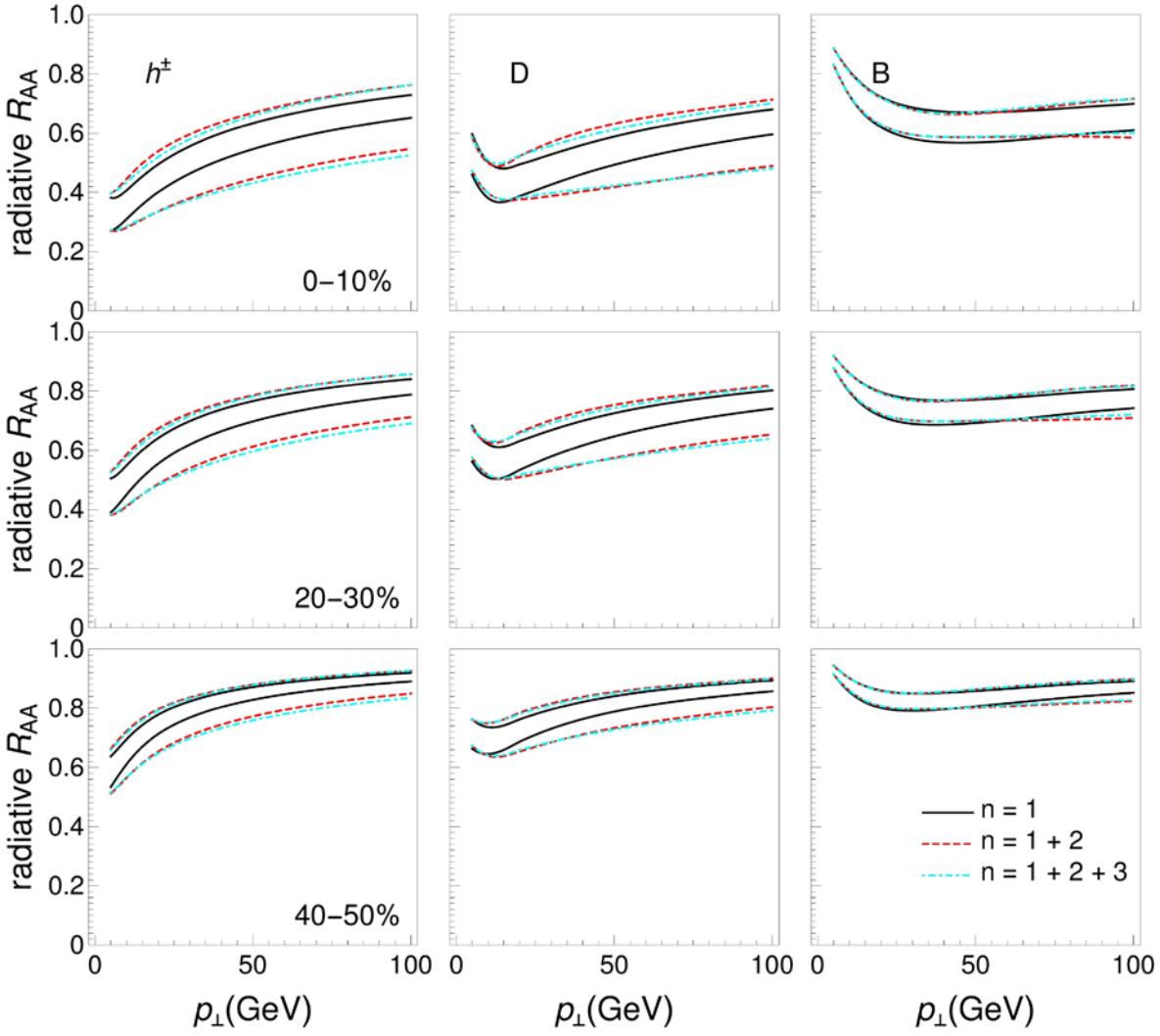

Surprisingly, the effect is opposite in sign for limiting values of $\frac{\mu_M}{\mu_E}$

For $\frac{\mu_M}{\mu_E} = 0.6$: negligible and decreases energy loss (increases R_{AA})

For $\frac{\mu_M}{\mu_E} = 0.4$: noticeable and increases energy loss (decreases R_{AA})

What is the origin of such behavior?

PRD 81, 091501; PRD 69, 014506

Effective potential in dynamical QCD medium: theoretical analysis

S. Stojku, BI, I. Salom, M. Djordjevic, arXiv:2303.14527
Accepted in PRC

$$v(\mathbf{q}) = v_L(\mathbf{q}) - v_T(\mathbf{q})$$

M. Djordjevic, PLB 709, 229

$$v_L(\mathbf{q}) = \frac{1}{\pi}\left(\frac{1}{(\mathbf{q}^2+\mu_{pl}^2)} - \frac{1}{(\mathbf{q}^2+\mu_E^2)}\right), \quad v_T(\mathbf{q}) = \frac{1}{\pi}\left(\frac{1}{(\mathbf{q}^2+\mu_{pl}^2)} - \frac{1}{(\mathbf{q}^2+\mu_M^2)}\right)$$

$$\mu_{pl} = \mu_E/\sqrt{3}$$

$\mu_{pl} < \mu_E$

Longitudinal (electric) contribution to effective potential is always positive.

Radiative energy loss > 0 ($R_{AA} < 1$).

Transverse (magnetic) contribution to effective potential changes sign.

$\mu_M/\mu_E = 0.6$

$\mu_M/\mu_E = 0.4$

If $\mu_M > \mu_{pl}$ decreases radiative energy loss (increases R_{AA})
If $\mu_M < \mu_{pl}$ increases radiative energy loss (decreases R_{AA})

Consistent with previous slide and provides possible explanation of R_{AA} behavior.

Effect of higher orders in opacity on electric contribution to R_{AA} in dynamical QCD medium:

Electric effective potential is well-defined within dynamical QCD medium, as μ_E is set from lattice QCD, consistently with perturbative calculations.

A. Peshier, arXiv:0601119

$$v(\mathbf{q}) = v_L(\mathbf{q})$$

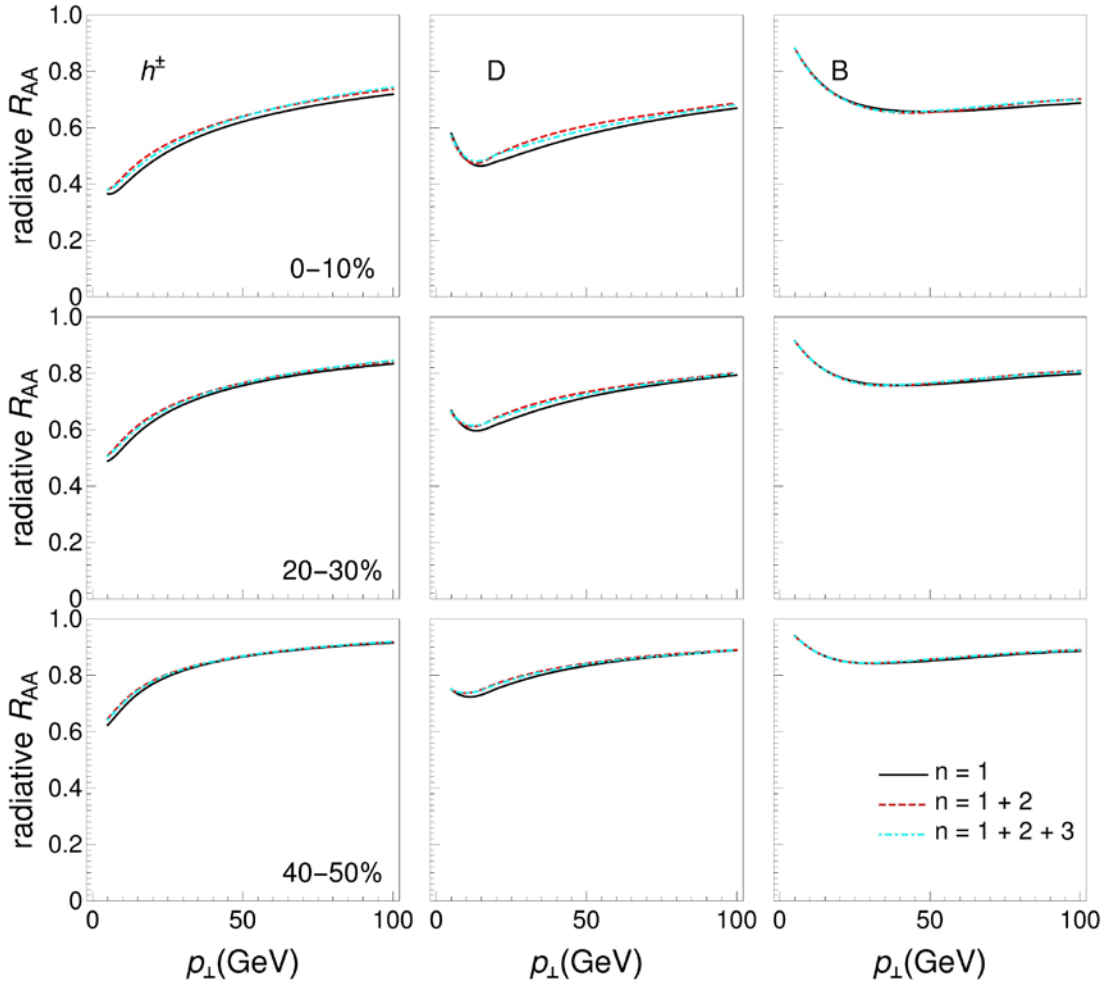

Unexpectedly, electric contribution to radiative energy loss in a dynamical QCD medium is insignificantly affected.

Higher orders in opacity dominantly influence magnetic contribution to radiative energy loss.

Sign and magnitude of the effect is controlled by μ_M value.

S. Stojku, BI, I. Salom, M. Djordjevic, arXiv:2303.14527
Accepted in PRC

Effect of higher orders in opacity on radiative RAA (II)

The upper set of curves: $\mu_M/\mu_E = 0.6$

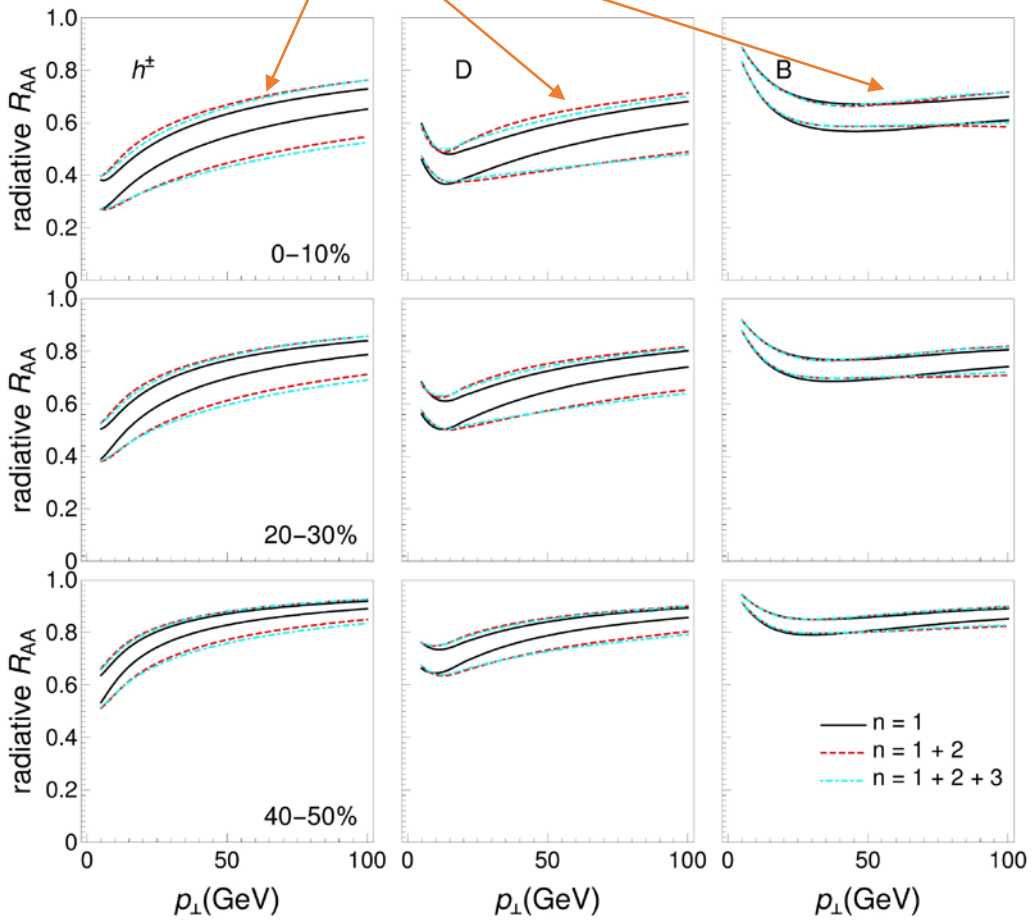

$\mu_{pl}/\mu_E = 1/\sqrt{3}$

For $\frac{\mu_M}{\mu_E} = 0.4$ (μ_M substantialy smaller than μ_{pl}):
Effect significant and decreases R_{AA}

For $\frac{\mu_M}{\mu_E} = 0.6$ (μ_M close to, but a bit larger than μ_{pl}):
Effect negligible and slightly increases R_{AA}

In agreement with our analytical arguments.

2+1 flavor lQCD:

$0.58 < \mu_M/\mu_E < 0.64$

S. Borsanyi et al., JHEP 1504, 138

The effect of higher orders in opacity on R_{AA} is negligible ($\lesssim 5\%$) in a dynamical medium!

Effect of higher orders in opacity in evolving medium: a preview

Quite a demanding task, out of the scope of this talk

We mimic medium evolution by assuming different medium T

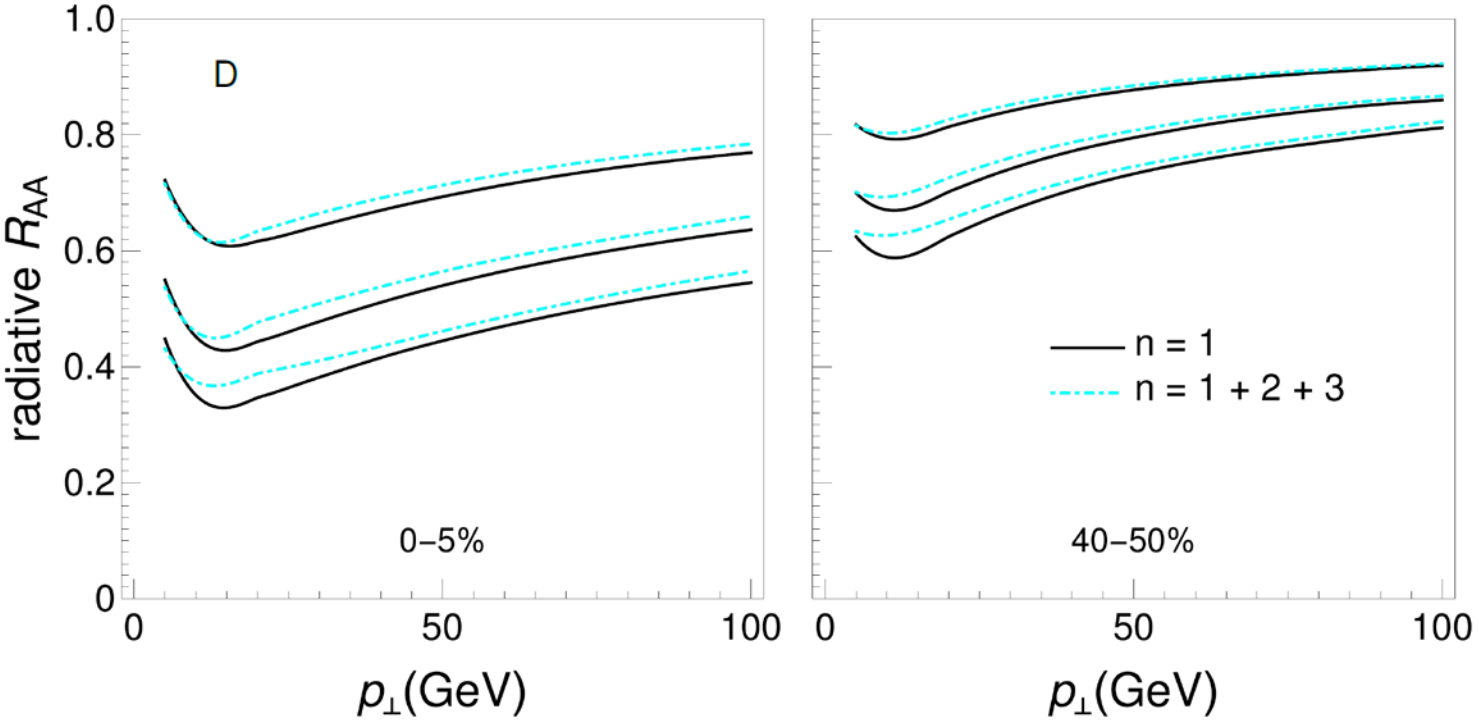

Uppermost curves: T=200 MeV
Middle curves: T=400 MeV
Lowest curves: T=600 MeV

$\mu_M/\mu_E = 0.6$

S. Stojku, BI, I. Salom, M. Djordjevic, arXiv:2303.14527
Accepted in PRC

The effect is nearly the same and small regardless of the medium T.

We expect the conclusions to remain the same for evolving medium.

The higher orders in opacity should be negligible in evolving medium.

Conclusions

- ✓ We presented DREENA framework, which can accommodate arbitrary T profile within state-of-the-art dynamical loss formalism (as the only input)
- ✓ Traditionally, high-$p_\perp$ probes used to explore parton-QGP medium interactions
- ✓ Our approach: Utilize high-$p_\perp$ probes to constrain global QGP properties
- ✓ We obtained that high-$p_\perp$:
  - ✓ R_{AA}, v_2, v_3, v_4 can differentiate between diverse (early) evolutions
  - ✓ R_{AA}, v_2 prefer a later onset of transverse medium expansion and energy loss (1 *fm*)
  - ✓ $v_2/(1-R_{AA})$ presents a reliable and robust observable for straightforward extraction of spatial anisotropy of QGP: New observable – Jet-perceived anisotropy
  - ✓ $\eta/s(T)$ from dynamical energy loss formalism shows surprisingly good agreement all the way to T_c with constraints extracted from Bayesian analyses. Provides much smaller uncertainties at high temperature
- ✓ QGP tomography: constraining bulk QGP properties jointly from low- and high-$p_\perp$ physics
- ✓ 1st order in opacity approximation is adequate for a finite size medium created at the RHIC and LHC
  - ✓ The same conclusions should remain valid when an evolving medium is introduced.

Thank you for your attention!

BACK UP

High- p_T observables

Nuclear modification factor R_{AA} (suppression)

$$R^{tr}_{AA}(p_f, H_Q) = \frac{E_f d^3\sigma_q(H_Q)}{dp_f^3} \Big/ \frac{E_f d^3\sigma_u(H_Q)}{dp_f^3}$$

$$\frac{E_f d^3\sigma_q(H_Q)}{dp_f^3} = \frac{E_i d^3\sigma(Q)}{dp_i^3} \otimes P(E_i \to E_f) \otimes D(Q \to H_Q)$$

$$\frac{E_f d^3\sigma_u(H_Q)}{dp_f^3} = \frac{E_i d^3\sigma(Q)}{dp_i^3} \otimes D(Q \to H_Q)\,.$$

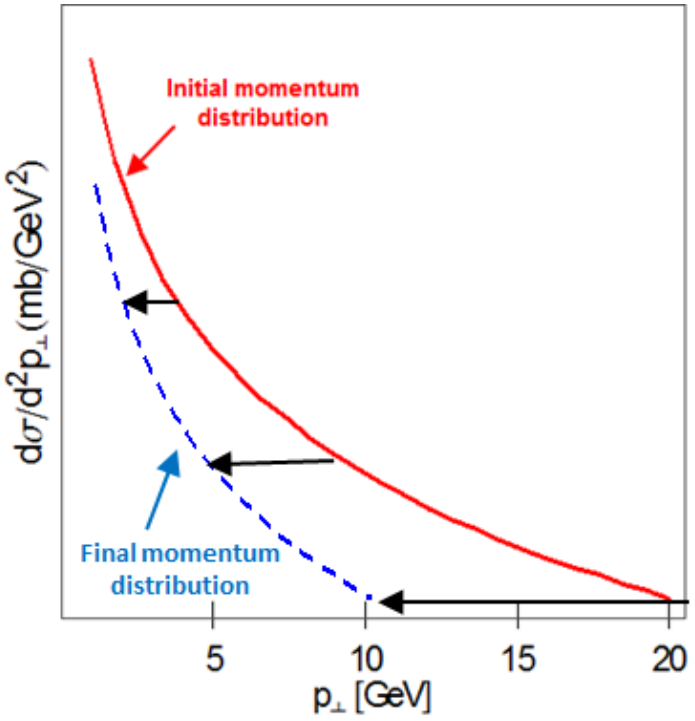

Anisotropic flow (e.g., elliptic v_2)

$$\frac{\mathrm{d}N}{\mathrm{d}\varphi} \propto 1 + 2\sum_{n=1}^{+\infty} v_n \cos\left[n(\varphi - \Psi_n)\right]$$

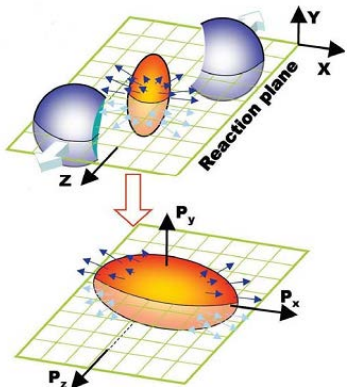

Radiative energy loss

Radiative energy loss comes from the processes in which there are more outgoing than incoming particles:

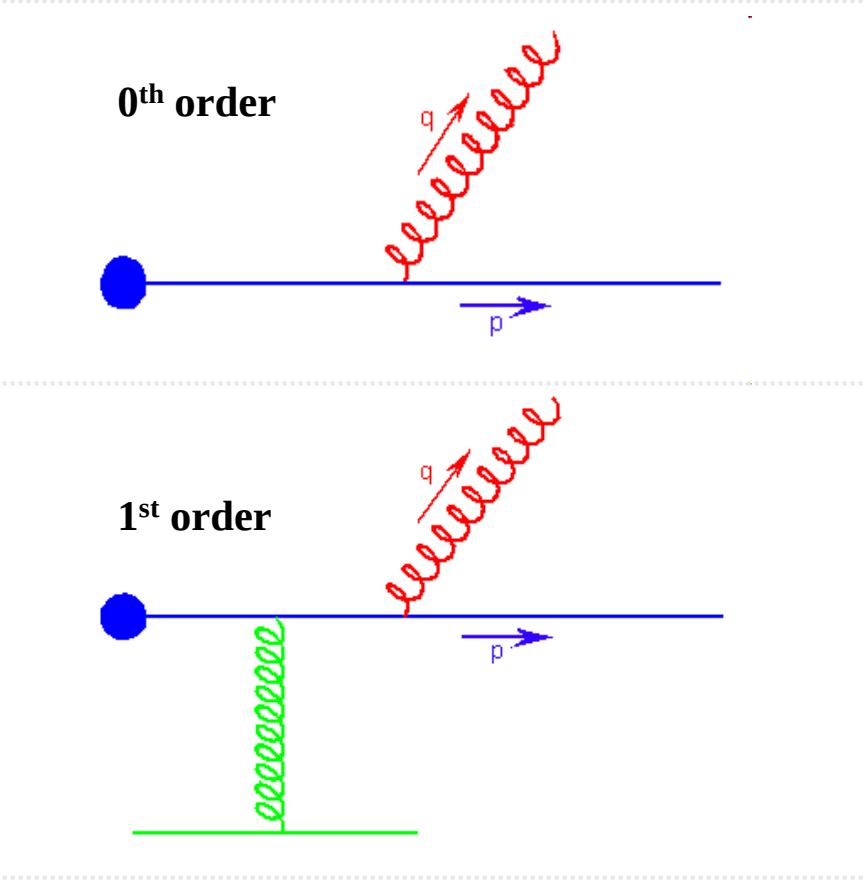

Collisional energy loss

Collisional (elastic) energy loss comes from the processes which have the same number of incoming and outgoing particles:

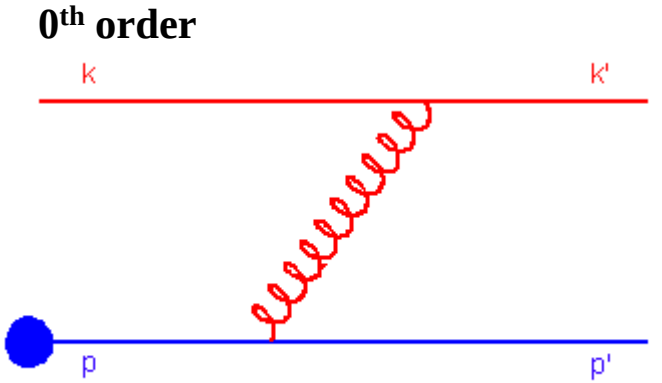

Radiative energy loss in dynamical medium

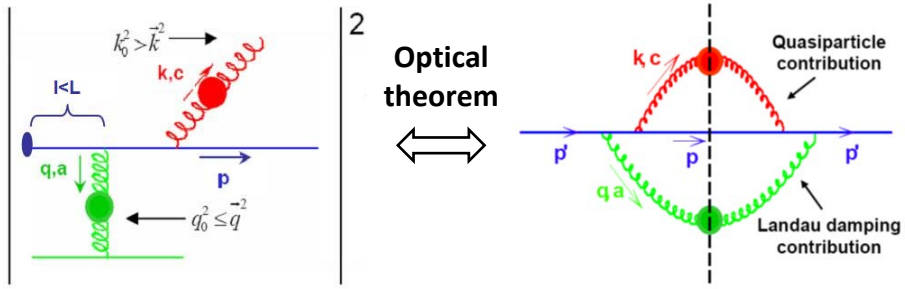

✓ We assume:

- Dynamical medium of a finite size L, consisting of thermally distributed massless partons
- 1st order in opacity (two Hard-Thermal Loop approach)

M. Djordjevic, PRC 80,064909 (2009) (highlighted in APS physics),

M. Djordjevic and U. Heinz, PRL 101,022302 (2008).

- Radiated gluon: transversely polarized with effective mass given by $\boldsymbol{m_g = \mu_E/\sqrt{2}}$

M.Djordjevic and M. Gyulassy, PRC 68, 034914 (2003).

- Exchanged gluon cut 1-HTL propagator retains both transverse (magnetic) and longitudinal (electric) parts.

Radiative energy loss in dynamical medium

In finite size dynamical QGP medium produced quark can be both on- and off-shell.

Beside central cut, left and right cuts are allowed.

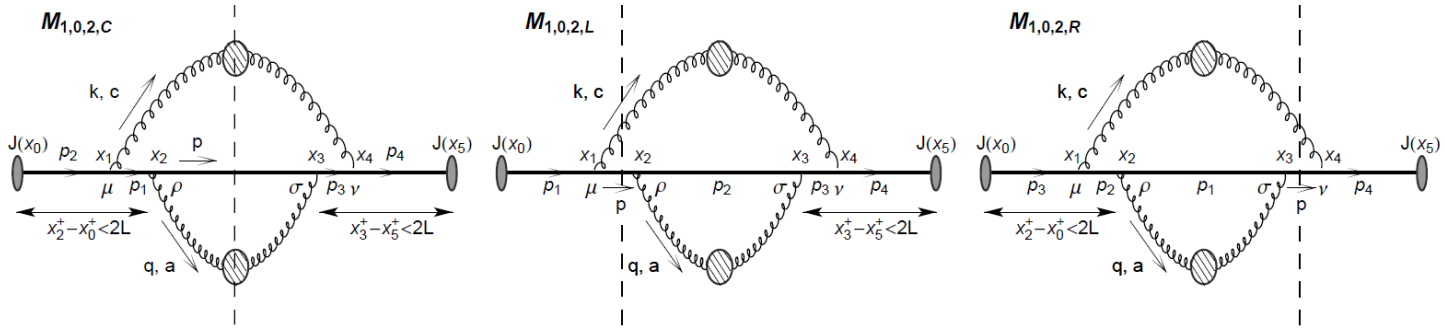

All 24 relevant diagrams are calculated. Each of them is infrared divergent, due to the absence of magnetic screening.

The divergence is naturally regulated when all the diagrams are taken into account.

$$\frac{\Delta E_{dyn}}{E}=\frac{C_R\alpha_s}{\pi}\frac{L}{\lambda_{dyn}}\int dx\int\frac{d^2\mathbf{q}_1}{\pi}\frac{\mu_E^2}{\mathbf{q}_1^2(\mathbf{q}_1^2+\mu_E^2)}\int d\mathbf{k}^2\frac{2}{(\mathbf{k}-\mathbf{q}_1)^2+\chi}\left(1-\frac{\sin\left(\frac{(\mathbf{k}-\mathbf{q}_1)^2+\chi}{2xE}L\right)}{\frac{(\mathbf{k}-\mathbf{q}_1)^2+\chi}{2xE}L}\right)\left(\frac{(\mathbf{k}-\mathbf{q}_1)^2}{(\mathbf{k}-\mathbf{q}_1)^2+\chi}-\frac{\mathbf{k}\cdot(\mathbf{k}-\mathbf{q}_1)}{\mathbf{k}^2+\chi}\right)$$

M. Djordjevic, PRC 80, 064909 (2009) (highlighted in APS physics).

1-HTL gluon propagator:

$$iD^{\mu\nu}(l) = \frac{P^{\mu\nu}(l)}{l^2 - \Pi_T(l)} + \frac{Q^{\mu\nu}(l)}{l^2 - \Pi_L(l)}$$

Cut 1-HTL gluon propagator:

$$D^{>}_{\mu\nu}(l) = -(1+f(l_0))\Big(P_{\mu\nu}(l)\rho_T(l) + Q_{\mu\nu}(l)\rho_L(l)\Big)\,,$$

$$\rho_{L,T}(l) = \underbrace{2\pi\,\delta(l^2 - \Pi_{T,L}(l))}_{\text{Radiated gluon}} \underbrace{- 2\,\mathrm{Im}\left(\frac{1}{l^2 - \Pi_{T,L}(l)}\right)\theta(1 - \frac{l_0^2}{\vec{l}^2})}_{\text{Exchanged gluon}}$$

For radiated gluon, cut 1-HTL gluon propagator can be simplified to

(M.D. and M. Gyulassy, PRC 68, 034914 (2003).

$$D^{>}_{\mu\nu}(k) \approx -2\pi\,\frac{P_{\mu\nu}(k)}{2\omega}\,\delta(k_0 - \omega) \qquad \omega \approx \sqrt{\vec{k}^2 + m_g^2}\,;\; m_g \approx \mu/\sqrt{2}$$

For exchanged gluon, cut 1-HTL gluon propagator cannot be simplified, since both transverse (magnetic) and longitudinal (electric) contributions will prove to be important.

$$D^{>}_{\mu\nu}(q) = \theta(1 - \frac{q_0^2}{\vec{q}^2})\,(1 + f(q_0))\,2\,\mathrm{Im}\left(\frac{P_{\mu\nu}(q)}{q^2 - \Pi_T(q)} + \frac{Q_{\mu\nu}(q)}{q^2 - \Pi_L(q)}\right)$$

Collisional energy loss in a finite size QCD medium

Consider a medium of size L in thermal equilibrium at temperature T.

The main order collisional energy loss is determined from:

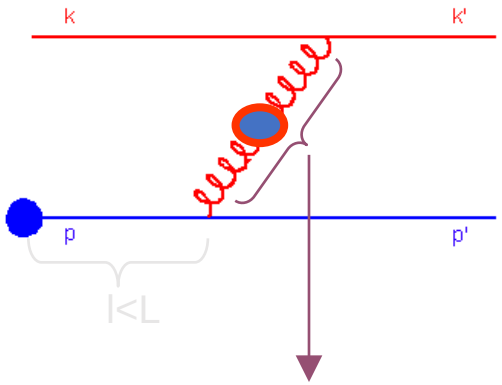

The effective gluon propagator:

$$D^{\mu\nu}(\omega,\vec{\mathbf{q}}) = -P^{\mu\nu}\Delta_T(\omega,\vec{\mathbf{q}}) - Q^{\mu\nu}\Delta_L(\omega,\vec{\mathbf{q}})$$

M. D., Phys.Rev.C74:064907,2006

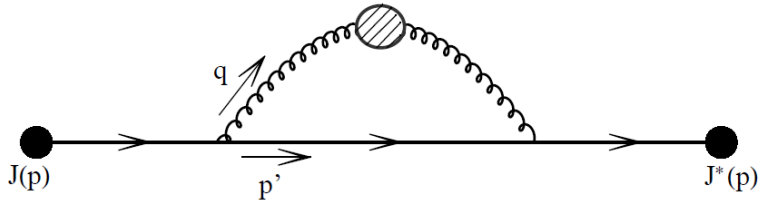

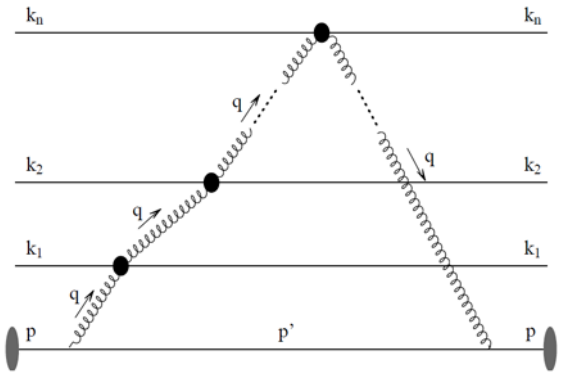

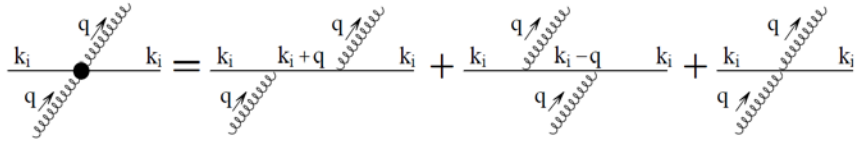

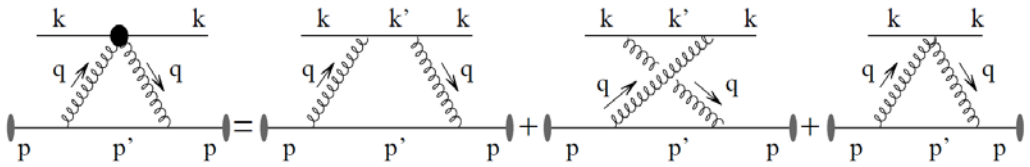

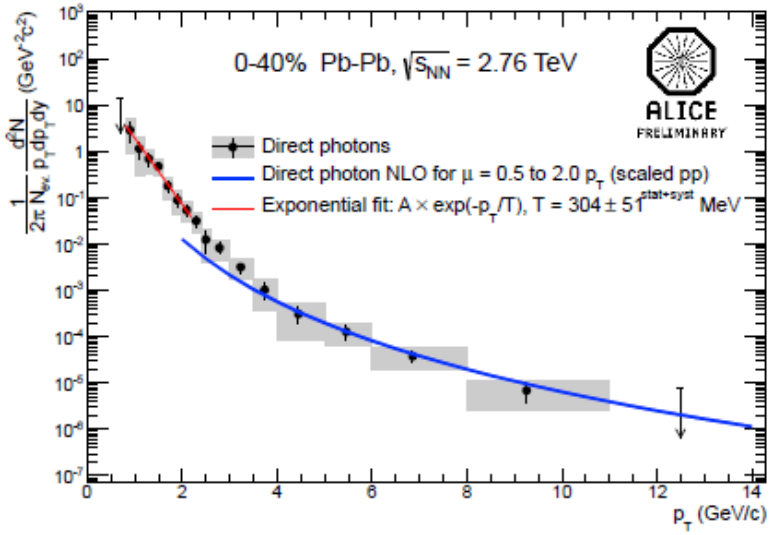

ALICE: NPA 904-905 573c

(T_{eff}) of 304 MeV for 0-40% centrality 2.76 TeV Pb+Pb

$$T^3 \sim \frac{\frac{dN_g}{dy}}{V} \rightarrow T = c\left(\frac{\frac{dN_g}{dy}}{N_{part}}\right)^{1/3}$$

$$V \sim N_{part} \qquad \frac{\frac{dN_g}{dy}}{N_{part}} \sim \frac{\frac{dN_{ch}}{dy}}{N_{part}/2}$$

measured

For each centrality region.

M. Gyulassy, P. Levai and I. Vitev, NPB 594 371
M. Djordjevic, M. Djordjevic and B. Blagojevic, PLB 737, 298

Analytical calculations: examples

$$\left(\frac{dN_g}{dx}\right) = \left(\frac{dN_g^{(1)}}{dx}\right) + \left(\frac{dN_g^{(2)}}{dx}\right)_1 - \left(\frac{dN_g^{(2)}}{dx}\right)_2 + \left(\frac{dN_g^{(3)}}{dx}\right)_1 - \left(\frac{dN_g^{(3)}}{dx}\right)_2 - \left(\frac{dN_g^{(3)}}{dx}\right)_3 + \left(\frac{dN_g^{(3)}}{dx}\right)_4 + \left(\frac{dN_g^{(4)}}{dx}\right)_1 - \left(\frac{dN_g^{(4)}}{dx}\right)_2 - \left(\frac{dN_g^{(4)}}{dx}\right)_3 + \left(\frac{dN_g^{(4)}}{dx}\right)_4 - \left(\frac{dN_g^{(4)}}{dx}\right)_5 + \left(\frac{dN_g^{(4)}}{dx}\right)_6 + \left(\frac{dN_g^{(4)}}{dx}\right)_7 - \left(\frac{dN_g^{(4)}}{dx}\right)_8$$

1st order in opacity:

$$\left(\frac{dN_g^{(1)}}{dx}\right) = \frac{4C_R}{\pi x}\int_0^L dz_1 \int \frac{d^2\mathbf{k}}{\pi}\int \frac{d^2\mathbf{q}_1}{\pi}\,\alpha_s(Q_k^2)\frac{1}{\lambda_{dyn}}\frac{\mu_E^2-\mu_M^2}{(\mathbf{q}_1^2+\mu_E^2)(\mathbf{q}_1^2+\mu_M^2)} \frac{\chi^2(\mathbf{q}_1\cdot(\mathbf{q}_1-\mathbf{k}))+(\mathbf{q}_1\cdot\mathbf{k})(\mathbf{k}-\mathbf{q}_1)^2}{(\chi^2+\mathbf{k}^2)(\chi^2+(\mathbf{k}-\mathbf{q}_1)^2)^2}\sin^2\left(\frac{\chi^2+(\mathbf{k}^2-\mathbf{q}_1)^2}{4xE}z_1\right)$$

2nd order in opacity:

$$\left(\frac{dN_g^{(2)}}{dx}\right)_1 = \frac{4C_R}{\pi x}\int_0^L\int_{z_1}^L dz_1 dz_2 \int \frac{d^2\mathbf{k}}{\pi}\iint \frac{d^2\mathbf{q}_1}{\pi}\frac{d^2\mathbf{q}_2}{\pi} \alpha_s(Q_k^2)\frac{1}{\lambda_{dyn}^2}\frac{\mu_E^2-\mu_M^2}{(\mathbf{q}_1^2+\mu_E^2)(\mathbf{q}_1^2+\mu_M^2)}\frac{\mu_E^2-\mu_M^2}{(\mathbf{q}_2^2+\mu_E^2)(\mathbf{q}_2^2+\mu_M^2)} \frac{\chi^2(\mathbf{q}_2\cdot(\mathbf{q}_1+\mathbf{q}_2-\mathbf{k}))+(\mathbf{q}_2\cdot\mathbf{k})(\mathbf{k}-\mathbf{q}_2)^2+(\mathbf{k}\cdot\mathbf{q}_1)(\mathbf{q}_2\cdot(\mathbf{q}_2-2\mathbf{k}))+\mathbf{k}^2(\mathbf{q}_2\cdot\mathbf{q}_1)}{(\chi^2+\mathbf{k}^2)(\chi^2+(\mathbf{k}-\mathbf{q}_2)^2)(\chi^2+(\mathbf{k}-\mathbf{q}_1-\mathbf{q}_2)^2)} \sin\left(\frac{\chi^2+(\mathbf{k}-\mathbf{q}_1-\mathbf{q}_2)^2}{4xE}z_1\right)\sin\left(\frac{\chi^2+(\mathbf{k}-\mathbf{q}_1-\mathbf{q}_2)^2}{4xE}z_1+\frac{\chi^2+(\mathbf{k}-\mathbf{q}_2)^2}{2xE}z_2\right)$$

$$\left(\frac{dN_g^{(2)}}{dx}\right)_2 = \frac{2C_R}{\pi x}\int\frac{d^2\mathbf{k}}{\pi}\int\frac{d^2\mathbf{q}_2}{\pi}\,\alpha_s(Q_k^2)\frac{1}{\lambda_{dyn}^2}\frac{\mu_E^2-\mu_M^2}{(\mathbf{q}_2^2+\mu_E^2)(\mathbf{q}_2^2+\mu_M^2)} \frac{\chi^2(\mathbf{q}_2\cdot(\mathbf{q}_2-\mathbf{k}))+(\mathbf{q}_2\cdot\mathbf{k})(\mathbf{k}-\mathbf{q}_2)^2}{(\chi^2+\mathbf{k}^2)(\chi^2+(\mathbf{k}-\mathbf{q}_2)^2)^2}\frac{\sin(L\omega_{(2)})\,(L\omega_{(2)}-\sin(L\omega_{(2)}))}{\omega_{(2)}^2}$$

3rd order in opacity:

$$\left(\frac{dN_g^{(3)}}{dx}\right)_1 = \frac{4C_R}{\pi x}\int_0^L\int_{z_1}^L\int_{z_2}^L dz_1dz_2dz_3\int\frac{d^2\mathbf{k}}{\pi}\iiint\frac{d^2\mathbf{q}_1}{\pi}\frac{d^2\mathbf{q}_2}{\pi}\frac{d^2\mathbf{q}_3}{\pi} \alpha_s(Q_k^2)\frac{1}{\lambda_{dyn}^3}\frac{\mu_E^2-\mu_M^2}{(\mathbf{q}_1^2+\mu_E^2)(\mathbf{q}_1^2+\mu_M^2)}\frac{\mu_E^2-\mu_M^2}{(\mathbf{q}_2^2+\mu_E^2)(\mathbf{q}_2^2+\mu_M^2)}\frac{\mu_E^2-\mu_M^2}{(\mathbf{q}_3^2+\mu_E^2)(\mathbf{q}_3^2+\mu_M^2)} \frac{\chi^2(\mathbf{q}_3\cdot(\mathbf{q}_1+\mathbf{q}_2+\mathbf{q}_3-\mathbf{k}))+(\mathbf{q}_3\cdot\mathbf{k})(\mathbf{k}-\mathbf{q}_3)^2+(\mathbf{k}\cdot(\mathbf{q}_1+\mathbf{q}_2))(\mathbf{q}_3\cdot(\mathbf{q}_3-2\mathbf{k}))+\mathbf{k}^2(\mathbf{q}_3\cdot(\mathbf{q}_1+\mathbf{q}_2))}{(\chi^2+\mathbf{k}^2)(\chi^2+(\mathbf{k}-\mathbf{q}_3)^2)(\chi^2+(\mathbf{k}-\mathbf{q}_1-\mathbf{q}_2-\mathbf{q}_3)^2)} \sin\left(\frac{\chi^2+(\mathbf{k}-\mathbf{q}_1-\mathbf{q}_2-\mathbf{q}_3)^2}{4xE}z_1\right) \sin\left(\frac{\chi^2+(\mathbf{k}-\mathbf{q}_1-\mathbf{q}_2-\mathbf{q}_3)^2}{4xE}z_1+\frac{\chi^2+(\mathbf{k}-\mathbf{q}_2-\mathbf{q}_3)^2}{2xE}z_2+\frac{\chi^2+(\mathbf{k}-\mathbf{q}_3)^2}{2xE}z_3\right)$$

$$\left(\frac{dN_g^{(3)}}{dx}\right)_2 = \frac{C_R}{\pi x}\int\frac{d^2\mathbf{k}}{\pi}\iint\frac{d^2\mathbf{q}_1}{\pi}\frac{d^2\mathbf{q}_3}{\pi}\alpha_s(Q_k^2)\frac{1}{\lambda_{dyn}^3}\frac{\mu_E^2-\mu_M^2}{(\mathbf{q}_1^2+\mu_E^2)(\mathbf{q}_1^2+\mu_M^2)}\frac{\mu_E^2-\mu_M^2}{(\mathbf{q}_3^2+\mu_E^2)(\mathbf{q}_3^2+\mu_M^2)} \frac{\chi^2(\mathbf{q}_3\cdot(\mathbf{q}_1+\mathbf{q}_3-\mathbf{k}))+(\mathbf{q}_3\cdot\mathbf{k})(\mathbf{k}-\mathbf{q}_3)^2+(\mathbf{k}\cdot\mathbf{q}_1)(\mathbf{q}_3\cdot(\mathbf{q}_3-2\mathbf{k}))+\mathbf{k}^2(\mathbf{q}_3\cdot\mathbf{q}_1)}{(\chi^2+\mathbf{k}^2)(\chi^2+(\mathbf{k}-\mathbf{q}_3)^2)(\chi^2+(\mathbf{k}-\mathbf{q}_1-\mathbf{q}_3)^2)} \left(\frac{\left(\frac{3\omega_{(13)}}{2}-\omega_{(3)}\right)\sin(2L\omega_{(3)})}{\omega_{(3)}^3\omega_{(13)}}-\frac{2\omega_{(13)}\sin(L\omega_{(3)})}{\omega_{(3)}^3(\omega_{(3)}+\omega_{(13)})}+\frac{\sin\left(2L\left(\omega_{(3)}+\frac{\omega_{(13)}}{2}\right)\right)}{\left(\omega_{(3)}+\frac{\omega_{(13)}}{2}\right)\omega_{(13)}(\omega_{(3)}+\omega_{(13)})}-\frac{L\cos(2L\omega_{(3)})}{\omega_{(3)}^2}\right)$$

Analytical calculations: examples

3rd order in opacity:

$$\left(\frac{dN_g^{(3)}}{dx}\right)_3 = \frac{2C_R}{\pi x}\int\frac{d^2\mathbf{k}}{\pi}\iint\frac{d^2\mathbf{q}_2}{\pi}\frac{d^2\mathbf{q}_3}{\pi}\alpha_s(Q_k^2)\frac{1}{\lambda_{dyn}^3}\frac{\mu_E^2-\mu_M^2}{(\mathbf{q}_2^2+\mu_E^2)(\mathbf{q}_2^2+\mu_M^2)}\frac{\mu_E^2-\mu_M^2}{(\mathbf{q}_3^2+\mu_E^2)(\mathbf{q}_3^2+\mu_M^2)}$$
$$\frac{\chi^2(\mathbf{q}_3\cdot(\mathbf{q}_2+\mathbf{q}_3-\mathbf{k}))+(\mathbf{q}_3\cdot\mathbf{k})(\mathbf{k}-\mathbf{q}_3)^2+(\mathbf{k}\cdot\mathbf{q}_2)(\mathbf{q}_3\cdot(\mathbf{q}_3-2\mathbf{k}))+\mathbf{k}^2(\mathbf{q}_3\cdot\mathbf{q}_2)}{(\chi^2+\mathbf{k}^2)(\chi^2+(\mathbf{k}-\mathbf{q}_3)^2)(\chi^2+(\mathbf{k}-\mathbf{q}_2-\mathbf{q}_3)^2)}$$
$$\left(\frac{\sin\left(2L\left(\frac{\omega_{(3)}}{2}+\omega_{(23)}\right)\right)}{4\omega_{(23)}^2\left(\frac{\omega_{(3)}}{2}+\omega_{(23)}\right)}-\frac{\sin\left(L\omega_{(3)}\right)}{2\omega_{(23)}^2\omega_{(3)}}+\frac{\frac{\sin\left(L\left(\omega_{(3)}+\omega_{(23)}\right)\right)}{\omega_{(3)}+\omega_{(23)}}-L\cos\left(L\left(\omega_{(3)}+\omega_{(23)}\right)\right)}{\omega_{(23)}\left(\omega_{(3)}+\omega_{(23)}\right)}\right),$$

$$\left(\frac{dN_g^{(3)}}{dx}\right)_4 = \frac{C_R}{\pi x}\int\frac{d^2\mathbf{k}}{\pi}\int\frac{d^2\mathbf{q}_3}{\pi}\alpha_s(Q_k^2)\frac{1}{\lambda_{dyn}^3}\frac{\mu_E^2-\mu_M^2}{(\mathbf{q}_3^2+\mu_E^2)(\mathbf{q}_3^2+\mu_M^2)}\frac{\chi^2(\mathbf{q}_3\cdot(\mathbf{q}_3-\mathbf{k}))+(\mathbf{q}_3\cdot\mathbf{k})(\mathbf{k}-\mathbf{q}_3)^2}{(\chi^2+\mathbf{k}^2)(\chi^2+(\mathbf{k}-\mathbf{q}_3)^2)^2}$$
$$\frac{1}{\omega_{(3)}^2}\left(-\frac{\sin\left(L\omega_{(3)}\right)}{\omega_{(3)}}+\frac{\sin\left(2L\omega_{(3)}\right)}{2\omega_{(3)}}+\frac{\sin\left(3L\omega_{(3)}\right)}{3\omega_{(3)}}-L\cos\left(2L\omega_{(3)}\right)\right),$$

4th order in opacity:

$$\left(\frac{dN_g^{(4)}}{dx}\right)_1 = \frac{4C_R}{\pi x}\int_0^L\int_{z_1}^L\int_{z_2}^L\int_{z_3}^L dz_1dz_2dz_3dz_4\int\frac{d^2\mathbf{k}}{\pi}\iiint\frac{d^2\mathbf{q}_1}{\pi}\frac{d^2\mathbf{q}_2}{\pi}\frac{d^2\mathbf{q}_3}{\pi}\frac{d^2\mathbf{q}_4}{\pi}$$
$$\alpha_s(Q_k^2)\frac{1}{\lambda_{dyn}^4}\frac{\mu_E^2-\mu_M^2}{(\mathbf{q}_1^2+\mu_E^2)(\mathbf{q}_1^2+\mu_M^2)}\frac{\mu_E^2-\mu_M^2}{(\mathbf{q}_2^2+\mu_E^2)(\mathbf{q}_2^2+\mu_M^2)}\frac{\mu_E^2-\mu_M^2}{(\mathbf{q}_3^2+\mu_E^2)(\mathbf{q}_3^2+\mu_M^2)}\frac{\mu_E^2-\mu_M^2}{(\mathbf{q}_4^2+\mu_E^2)(\mathbf{q}_4^2+\mu_M^2)}$$
$$\frac{\chi^2(\mathbf{q}_4\cdot(\mathbf{q}_1+\mathbf{q}_2+\mathbf{q}_3+\mathbf{q}_4-\mathbf{k}))+(\mathbf{q}_4\cdot\mathbf{k})(\mathbf{k}-\mathbf{q}_4)^2+(\mathbf{k}\cdot(\mathbf{q}_1+\mathbf{q}_2+\mathbf{q}_3))(\mathbf{q}_4\cdot(\mathbf{q}_4-2\mathbf{k}))+\mathbf{k}^2(\mathbf{q}_4\cdot(\mathbf{q}_1+\mathbf{q}_2+\mathbf{q}_3))}{(\chi^2+\mathbf{k}^2)(\chi^2+(\mathbf{k}-\mathbf{q}_4)^2)(\chi^2+(\mathbf{k}-\mathbf{q}_1-\mathbf{q}_2-\mathbf{q}_3-\mathbf{q}_4)^2)}$$
$$\sin\left(\frac{\chi^2+(\mathbf{k}-\mathbf{q}_1-\mathbf{q}_2-\mathbf{q}_3-\mathbf{q}_4)^2}{4xE}z_1+\frac{\chi^2+(\mathbf{k}-\mathbf{q}_2-\mathbf{q}_3-\mathbf{q}_4)^2}{2xE}z_2+\frac{\chi^2+(\mathbf{k}-\mathbf{q}_3-\mathbf{q}_4)^2}{2xE}z_3+\frac{\chi^2+(\mathbf{k}-\mathbf{q}_4)^2}{2xE}z_4\right)$$
$$\sin\left(\frac{\chi^2+(\mathbf{k}-\mathbf{q}_1-\mathbf{q}_2-\mathbf{q}_3-\mathbf{q}_4)^2}{4xE}z_1\right),$$

4th order in opacity:

$$\left(\frac{dN_g^{(4)}}{dx}\right)_2 = \frac{C_R}{\pi x}\int\frac{d^2\mathbf{k}}{\pi}\iiint\frac{d^2\mathbf{q}_1}{\pi}\frac{d^2\mathbf{q}_2}{\pi}\frac{d^2\mathbf{q}_4}{\pi}$$
$$\alpha_s(Q_k^2)\frac{1}{\lambda_{dyn}^4}\frac{\mu_E^2-\mu_M^2}{(\mathbf{q}_1^2+\mu_E^2)(\mathbf{q}_1^2+\mu_M^2)}\frac{\mu_E^2-\mu_M^2}{(\mathbf{q}_2^2+\mu_E^2)(\mathbf{q}_2^2+\mu_M^2)}\frac{\mu_E^2-\mu_M^2}{(\mathbf{q}_4^2+\mu_E^2)(\mathbf{q}_4^2+\mu_M^2)}$$
$$\frac{\chi^2(\mathbf{q}_4\cdot(\mathbf{q}_1+\mathbf{q}_2+\mathbf{q}_4-\mathbf{k}))+(\mathbf{q}_4\cdot\mathbf{k})(\mathbf{k}-\mathbf{q}_4)^2+(\mathbf{k}\cdot(\mathbf{q}_1+\mathbf{q}_2))(\mathbf{q}_4\cdot(\mathbf{q}_4-2\mathbf{k}))+\mathbf{k}^2(\mathbf{q}_4\cdot(\mathbf{q}_1+\mathbf{q}_2))}{(\chi^2+\mathbf{k}^2)(\chi^2+(\mathbf{k}-\mathbf{q}_4)^2)(\chi^2+(\mathbf{k}-\mathbf{q}_1-\mathbf{q}_2-\mathbf{q}_4)^2)}$$
$$\left(\frac{2\left(\omega_{(24)}\left(2\omega_{(4)}^2+3\omega_{(24)}\omega_{(4)}+\omega_{(24)}^2\right)-\left(2\omega_{(4)}^2+6\omega_{(24)}\omega_{(4)}+3\omega_{(24)}^2\right)\omega_{(124)}\right)\cos\left(L\left(2\omega_{(4)}+\omega_{(24)}\right)\right)}{\omega_{(24)}^2\left(\omega_{(4)}+\omega_{(24)}\right)^2\left(2\omega_{(4)}+\omega_{(24)}\right)^2\omega_{(124)}}\right.$$
$$-\frac{2\cos\left(L\left(2\omega_{(4)}+\omega_{(24)}+\omega_{(124)}\right)\right)}{\omega_{(124)}\left(\omega_{(24)}+\omega_{(124)}\right)\left(\omega_{(4)}+\omega_{(24)}+\omega_{(124)}\right)\left(2\omega_{(4)}+\omega_{(24)}+\omega_{(124)}\right)}+\frac{\omega_{(124)}\cos\left(2L\omega_{(4)}\right)}{\omega_{(4)}^2\omega_{(24)}^2\left(\omega_{(24)}+\omega_{(124)}\right)}$$
$$-\frac{2L\sin\left(L\left(2\omega_{(4)}+\omega_{(24)}\right)\right)}{\omega_{(24)}\left(\omega_{(4)}+\omega_{(24)}\right)\left(2\omega_{(4)}+\omega_{(24)}\right)}-\frac{2\omega_{(124)}\cos\left(L\omega_{(4)}\right)}{\omega_{(4)}^2\left(\omega_{(4)}+\omega_{(24)}\right)^2\left(\omega_{(4)}+\omega_{(24)}+\omega_{(124)}\right)}$$
$$\left.+\frac{\omega_{(124)}}{\omega_{(4)}^2\left(2\omega_{(4)}+\omega_{(24)}\right)^2\left(2\omega_{(4)}+\omega_{(24)}+\omega_{(124)}\right)}\right),$$

$$\left(\frac{dN_g^{(4)}}{dx}\right)_3 = \frac{C_R}{2\pi x}\int\frac{d^2\mathbf{k}}{\pi}\iiint\frac{d^2\mathbf{q}_1}{\pi}\frac{d^2\mathbf{q}_3}{\pi}\frac{d^2\mathbf{q}_4}{\pi}$$
$$\alpha_s(Q_k^2)\frac{1}{\lambda_{dyn}^4}\frac{\mu_E^2-\mu_M^2}{(\mathbf{q}_1^2+\mu_E^2)(\mathbf{q}_1^2+\mu_M^2)}\frac{\mu_E^2-\mu_M^2}{(\mathbf{q}_3^2+\mu_E^2)(\mathbf{q}_3^2+\mu_M^2)}\frac{\mu_E^2-\mu_M^2}{(\mathbf{q}_4^2+\mu_E^2)(\mathbf{q}_4^2+\mu_M^2)}$$
$$\frac{\chi^2(\mathbf{q}_4\cdot(\mathbf{q}_1+\mathbf{q}_3+\mathbf{q}_4-\mathbf{k}))+(\mathbf{q}_4\cdot\mathbf{k})(\mathbf{k}-\mathbf{q}_4)^2+(\mathbf{k}\cdot(\mathbf{q}_1+\mathbf{q}_3))(\mathbf{q}_4\cdot(\mathbf{q}_4-2\mathbf{k}))+\mathbf{k}^2(\mathbf{q}_4\cdot(\mathbf{q}_1+\mathbf{q}_3))}{(\chi^2+\mathbf{k}^2)(\chi^2+(\mathbf{k}-\mathbf{q}_4)^2)(\chi^2+(\mathbf{k}-\mathbf{q}_1-\mathbf{q}_3-\mathbf{q}_4)^2)}$$
$$\left(-\frac{2L\sin\left(L\left(\omega_{(4)}+2\omega_{(34)}\right)\right)}{\omega_{(34)}^2\left(\omega_{(4)}+2\omega_{(34)}\right)}-\frac{4\cos\left(L\left(\omega_{(4)}+2\omega_{(34)}+\omega_{(134)}\right)\right)}{\omega_{(134)}\left(\omega_{(34)}+\omega_{(134)}\right)\left(2\omega_{(34)}+\omega_{(134)}\right)\left(\omega_{(4)}+2\omega_{(34)}+\omega_{(134)}\right)}\right.$$
$$+\frac{\left(2\omega_{(34)}\left(\omega_{(4)}+2\omega_{(34)}\right)-\left(3\omega_{(4)}+8\omega_{(34)}\right)\omega_{(134)}\right)\cos\left(L\left(\omega_{(4)}+2\omega_{(34)}\right)\right)}{\omega_{(34)}^3\left(\omega_{(4)}+2\omega_{(34)}\right)^2\omega_{(134)}}-\frac{\omega_{(134)}\cos\left(L\omega_{(4)}\right)}{\omega_{(4)}\omega_{(34)}^3\left(2\omega_{(34)}+\omega_{(134)}\right)}$$
$$\left.+\frac{4\omega_{(134)}}{\left(\omega_{(4)}+\omega_{(34)}\right)}\left(\frac{\cos\left(L\left(\omega_{(4)}+\omega_{(34)}\right)\right)}{\omega_{(34)}^3\left(\omega_{(34)}+\omega_{(134)}\right)}+\frac{1}{\omega_{(4)}\left(\omega_{(4)}+2\omega_{(34)}\right)^2\left(\omega_{(4)}+2\omega_{(34)}+\omega_{(134)}\right)}\right)\right),$$

Analytical calculations: examples

4th order in opacity:

$$\left(\frac{dN_g^{(4)}}{dx}\right)_4 = \frac{C_R}{3\pi x}\int\frac{d^2\mathbf{k}}{\pi}\iint\frac{d^2\mathbf{q}_1}{\pi}\frac{d^2\mathbf{q}_4}{\pi}\alpha_s(Q_k^2)\frac{1}{\lambda_{dyn}^4}\frac{\mu_E^2-\mu_M^2}{(\mathbf{q}_1^2+\mu_E^2)(\mathbf{q}_1^2+\mu_M^2)}\frac{\mu_E^2-\mu_M^2}{(\mathbf{q}_4^2+\mu_E^2)(\mathbf{q}_4^2+\mu_M^2)}$$
$$\frac{\chi^2(\mathbf{q}_4\cdot(\mathbf{q}_1+\mathbf{q}_4-\mathbf{k}))+(\mathbf{q}_4\cdot\mathbf{k})(\mathbf{k}-\mathbf{q}_4)^2+(\mathbf{k}\cdot\mathbf{q}_1)(\mathbf{q}_4\cdot(\mathbf{q}_4-2\mathbf{k}))+\mathbf{k}^2(\mathbf{q}_4\cdot\mathbf{q}_1)}{(\chi^2+\mathbf{k}^2)(\chi^2+(\mathbf{k}-\mathbf{q}_4)^2)(\chi^2+(\mathbf{k}-\mathbf{q}_1-\mathbf{q}_4)^2)}$$
$$\frac{1}{\omega_{(4)}^3}\Bigg(-\frac{6\omega_{(4)}^3\cos\left(L\left(3\omega_{(4)}+\omega_{(14)}\right)\right)}{\omega_{(14)}\left(\omega_{(4)}+\omega_{(14)}\right)\left(2\omega_{(4)}+\omega_{(14)}\right)\left(3\omega_{(4)}+\omega_{(14)}\right)}+\left(\frac{1}{\omega_{(14)}}-\frac{11}{6\omega_{(4)}}\right)\cos(3L\omega_{(4)})$$
$$-L\sin\left(3L\omega_{(4)}\right)-\frac{3\omega_{(14)}\cos\left(L\omega_{(4)}\right)}{4\omega_{(4)}^2+2\omega_{(14)}\omega_{(4)}}+\frac{3\omega_{(14)}\cos\left(2L\omega_{(4)}\right)}{\left(\omega_{(4)}+\omega_{(14)}\right)\omega_{(4)}}+\frac{\omega_{(14)}}{9\omega_{(4)}^2+3\omega_{(14)}\omega_{(4)}}\Bigg),$$

$$\left(\frac{dN_g^{(4)}}{dx}\right)_5 = \frac{C_R}{\pi x}\int\frac{d^2\mathbf{k}}{\pi}\iiint\frac{d^2\mathbf{q}_2}{\pi}\frac{d^2\mathbf{q}_3}{\pi}\frac{d^2\mathbf{q}_4}{\pi}$$
$$\alpha_s(Q_k^2)\frac{1}{\lambda_{dyn}^4}\frac{\mu_E^2-\mu_M^2}{(\mathbf{q}_2^2+\mu_E^2)(\mathbf{q}_2^2+\mu_M^2)}\frac{\mu_E^2-\mu_M^2}{(\mathbf{q}_3^2+\mu_E^2)(\mathbf{q}_3^2+\mu_M^2)}\frac{\mu_E^2-\mu_M^2}{(\mathbf{q}_4^2+\mu_E^2)(\mathbf{q}_4^2+\mu_M^2)}$$
$$\frac{\chi^2(\mathbf{q}_4\cdot(\mathbf{q}_2+\mathbf{q}_3+\mathbf{q}_4-\mathbf{k}))+(\mathbf{q}_4\cdot\mathbf{k})(\mathbf{k}-\mathbf{q}_4)^2+(\mathbf{k}\cdot(\mathbf{q}_2+\mathbf{q}_3))(\mathbf{q}_4\cdot(\mathbf{q}_4-2\mathbf{k}))+\mathbf{k}^2(\mathbf{q}_4\cdot(\mathbf{q}_2+\mathbf{q}_3))}{(\chi^2+\mathbf{k}^2)(\chi^2+(\mathbf{k}-\mathbf{q}_4)^2)(\chi^2+(\mathbf{k}-\mathbf{q}_2-\mathbf{q}_3-\mathbf{q}_4)^2)}$$
$$\frac{1}{\omega_{(234)}^2}\Bigg(\frac{2\omega_{(234)}^3}{\omega_{(4)}\left(\omega_{(4)}+\omega_{(34)}\right)\left(\omega_{(4)}+\omega_{(34)}+\omega_{(234)}\right)^2\left(\omega_{(4)}+\omega_{(34)}+2\omega_{(234)}\right)}+\frac{\cos\left(L\left(\omega_{(4)}+\omega_{(34)}\right)\right)}{\omega_{(34)}\left(\omega_{(4)}+\omega_{(34)}\right)}$$
$$-\frac{2\omega_{(234)}^3\cos\left(L\omega_{(4)}\right)}{\omega_{(4)}\omega_{(34)}\left(\omega_{(34)}+\omega_{(234)}\right)^2\left(\omega_{(34)}+2\omega_{(234)}\right)}-\frac{2L\omega_{(234)}\sin(L(\omega_{(4)}+\omega_{(34)}+\omega_{(234)}))}{\left(\omega_{(34)}+\omega_{(234)}\right)\left(\omega_{(4)}+\omega_{(34)}+\omega_{(234)}\right)}$$
$$-\frac{\cos\left(L\left(\omega_{(4)}+\omega_{(34)}+2\omega_{(234)}\right)\right)}{\left(\omega_{(34)}+2\omega_{(234)}\right)\left(\omega_{(4)}+\omega_{(34)}+2\omega_{(234)}\right)}-\frac{2\omega_{(234)}(\omega_{(4)}+2\omega_{(34)}+2\omega_{(234)})\cos(L(\omega_{(4)}+\omega_{(34)}+\omega_{(234)}))}{\left(\omega_{(34)}+\omega_{(234)}\right)^2\left(\omega_{(4)}+\omega_{(34)}+\omega_{(234)}\right)^2}\Bigg)$$

$$\left(\frac{dN_g^{(4)}}{dx}\right)_6 = \frac{C_R}{\pi x}\int\frac{d^2\mathbf{k}}{\pi}\iint\frac{d^2\mathbf{q}_2}{\pi}\frac{d^2\mathbf{q}_4}{\pi}\alpha_s(Q_k^2)\frac{1}{\lambda_{dyn}^4}\frac{\mu_E^2-\mu_M^2}{(\mathbf{q}_2^2+\mu_E^2)(\mathbf{q}_2^2+\mu_M^2)}\frac{\mu_E^2-\mu_M^2}{(\mathbf{q}_4^2+\mu_E^2)(\mathbf{q}_4^2+\mu_M^2)}$$
$$\frac{\chi^2(\mathbf{q}_4\cdot(\mathbf{q}_2+\mathbf{q}_4-\mathbf{k}))+(\mathbf{q}_4\cdot\mathbf{k})(\mathbf{k}-\mathbf{q}_4)^2+(\mathbf{k}\cdot\mathbf{q}_2)(\mathbf{q}_4\cdot(\mathbf{q}_4-2\mathbf{k}))+\mathbf{k}^2(\mathbf{q}_4\cdot\mathbf{q}_2)}{(\chi^2+\mathbf{k}^2)(\chi^2+(\mathbf{k}-\mathbf{q}_4)^2)(\chi^2+(\mathbf{k}-\mathbf{q}_2-\mathbf{q}_4)^2)}$$
$$\Bigg(\frac{\omega_{(24)}}{8\omega_{(4)}^2\left(\omega_{(4)}+\frac{\omega_{(24)}}{2}\right)^2\left(\omega_{(4)}+\omega_{(24)}\right)}-\frac{L\sin\left(L\left(2\omega_{(4)}+\omega_{(24)}\right)\right)+\frac{\left(\frac{3\omega_{(4)}}{2}+\omega_{(24)}\right)\cos\left(2L\left(\omega_{(4)}+\frac{\omega_{(24)}}{2}\right)\right)}{\left(\omega_{(4)}+\frac{\omega_{(24)}}{2}\right)\left(\omega_{(4)}+\omega_{(24)}\right)}}{\left(\omega_{(4)}+\frac{\omega_{(24)}}{2}\right)\left(\omega_{(4)}+\omega_{(24)}\right)\omega_{(24)}}$$
$$+\frac{\left(\frac{\cos\left(2L\omega_{(4)}\right)}{2\omega_{(4)}}-\frac{\omega_{(4)}\cos\left(2L\left(\omega_{(4)}+\omega_{(24)}\right)\right)}{4\left(\frac{\omega_{(4)}}{2}+\omega_{(24)}\right)\left(\omega_{(4)}+\omega_{(24)}\right)}\right)}{\omega_{(4)}\omega_{(24)}^2}-\frac{\omega_{(24)}\cos\left(L\omega_{(4)}\right)}{\omega_{(4)}^2\left(\frac{\omega_{(4)}}{2}+\omega_{(24)}\right)\left(\omega_{(4)}+\omega_{(24)}\right)^2}\Bigg),$$

$$\left(\frac{dN_g^{(4)}}{dx}\right)_7 = \frac{C_R}{2\pi x}\int\frac{d^2\mathbf{k}}{\pi}\iint\frac{d^2\mathbf{q}_3}{\pi}\frac{d^2\mathbf{q}_4}{\pi}\alpha_s(Q_k^2)\frac{1}{\lambda_{dyn}^4}\frac{\mu_E^2-\mu_M^2}{(\mathbf{q}_3^2+\mu_E^2)(\mathbf{q}_3^2+\mu_M^2)}\frac{\mu_E^2-\mu_M^2}{(\mathbf{q}_4^2+\mu_E^2)(\mathbf{q}_4^2+\mu_M^2)}$$
$$\frac{\chi^2(\mathbf{q}_4\cdot(\mathbf{q}_3+\mathbf{q}_4-\mathbf{k}))+(\mathbf{q}_4\cdot\mathbf{k})(\mathbf{k}-\mathbf{q}_4)^2+(\mathbf{k}\cdot\mathbf{q}_3)(\mathbf{q}_4\cdot(\mathbf{q}_4-2\mathbf{k}))+\mathbf{k}^2(\mathbf{q}_4\cdot\mathbf{q}_3)}{(\chi^2+\mathbf{k}^2)(\chi^2+(\mathbf{k}-\mathbf{q}_4)^2)(\chi^2+(\mathbf{k}-\mathbf{q}_3-\mathbf{q}_4)^2)}$$
$$\frac{1}{\omega_{(34)}^2\left(\frac{\omega_{(4)}}{2}+\omega_{(34)}\right)}\Bigg(\frac{2\omega_{(34)}^3}{\omega_{(4)}\left(\omega_{(4)}+\omega_{(34)}\right)\left(\omega_{(4)}+2\omega_{(34)}\right)\left(\omega_{(4)}+3\omega_{(34)}\right)}-\frac{\left(\frac{\omega_{(4)}}{2}+2\omega_{(34)}\right)\cos\left(L\left(\omega_{(4)}+2\omega_{(34)}\right)\right)}{\left(\omega_{(4)}+2\omega_{(34)}\right)\omega_{(34)}}$$
$$-L\sin\left(L\left(\omega_{(4)}+2\omega_{(34)}\right)\right)-\frac{\left(\frac{\omega_{(4)}}{2}+\omega_{(34)}\right)\left(\frac{\cos\left(L\omega_{(4)}\right)}{\omega_{(4)}}-\frac{6\cos\left(L\left(\omega_{(4)}+\omega_{(34)}\right)\right)}{\omega_{(4)}+\omega_{(34)}}+\frac{2\cos\left(L\left(\omega_{(4)}+3\omega_{(34)}\right)\right)}{\omega_{(4)}+3\omega_{(34)}}\right)}{3\omega_{(34)}}\Bigg),$$

$$\left(\frac{dN_g^{(4)}}{dx}\right)_8 = \frac{C_R}{3\pi x}\int\frac{d^2\mathbf{k}}{\pi}\int\frac{d^2\mathbf{q}_4}{\pi}\alpha_s(Q_k^2)\frac{1}{\lambda_{dyn}^4}\frac{\mu_E^2-\mu_M^2}{(\mathbf{q}_4^2+\mu_E^2)(\mathbf{q}_4^2+\mu_M^2)}\frac{\chi^2\mathbf{q}_4\cdot(\mathbf{q}_4-\mathbf{k})+(\mathbf{q}_4\cdot\mathbf{k})(\mathbf{k}-\mathbf{q}_4)^2}{(\chi^2+\mathbf{k}^2)(\chi^2+(\mathbf{k}-\mathbf{q}_4)^2)^2}$$
$$\frac{1}{\omega_{(4)}^3}\left(\frac{1}{12\omega_{(4)}}-L\sin\left(3L\omega_{(4)}\right)-\frac{\cos\left(L\omega_{(4)}\right)}{2\omega_{(4)}}+\frac{3\cos\left(2L\omega_{(4)}\right)}{2\omega_{(4)}}-\frac{5\cos\left(3L\omega_{(4)}\right)}{6\omega_{(4)}}-\frac{\cos\left(4L\omega_{(4)}\right)}{4\omega_{(4)}}\right)$$

Effect of higher orders in opacity on radiative R_{AA} in *static* QCD medium (DGLV)

Static QCD medium approximation → only electric contribution

Static effective potential: $\frac{\mu_E^2}{\pi(\mathbf{q}^2+\mu_E^2)^2}$ Static mfp: $\lambda_{\rm stat}$

S. Stojku, BI, I. Salom, M. Djordjevic, arXiv:2303.14527

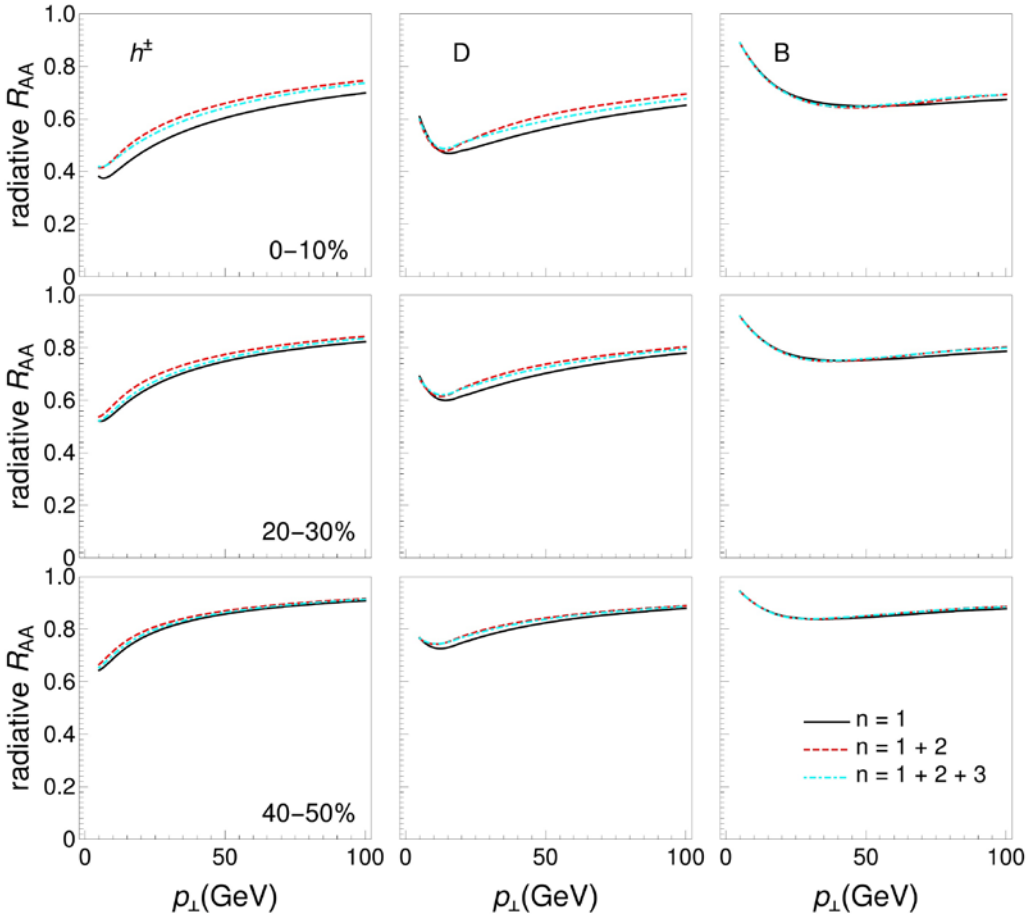

The effect is slightly larger than in the dynamical case, but yet small (≲6%).

For optically thin *static* medium models the effect of higher order in opacity on high-$p_\perp$ observables is still insignificant.

1st order in opacity is an adequate approximation for optically thin *static* medium.

Averaged (smooth) evolution models

- Optical Glauber:
  - Optical Glauber initialization (τ_0=1 fm, no initial transverse flow)
  - 3+1D viscous fluid code (E. Molnar, H. Holopainen, P. Huovinen and H. Niemi, PRC 90, 044904), η/s=0.12, no bulk viscosity (for RHIC η/s=0.16)
  - EoS parametrisation s95p-PCE-v1 (P. Huovinen and P. Petreczky, NPA 837, 26-53)
- EKRT:
  - EKRT initialization (K. J. Eskola, K. Kajantie, P. V. Ruuskanen and K. Tuominen, NPB 570, 379; PRC 87, 044904; PLB 731, 126) τ_0=0.2 fm
  - 3+1D viscous fluid code with boost-invariant expansion (E. Molnar, H. Holopainen, P. Huovinen and H. Niemi, PRC 90, 044904)
  - Bayesian analysis η/s(T) (min 0.18), no bulk viscosity
  - EoS parametrization $s83s_{18}$ (J. Auvinen, K. J. Eskola, P. Huovinen, H. Niemi, R. Paatelainen and P. Petreczky, PRC 102, 044911)
- T_RENTo:
  - T_RENTo initialization (J. S. Moreland, J. E. Bernhard and S. A. Bass, PRC 92, 011901), with free streaming until τ_0=1.16 fm
  - VISH2+1 code (H. Song and U. W. Heinz, PRC 77, 064901; arXiv:1804.06469; NP 15, no.11, 1113-1117)
  - Bayesian analysis η/s(T) (min 0.081), ζ/s(T) (max 0.052)
  - EoS lattice (A. Bazavov et al. [HotQCD], PRD 90, 094503)

DREENA-A

$$\frac{E_f d^3\sigma_q(H_Q)}{dp_f^3} = \frac{E_i d^3\sigma(Q)}{dp_i^3} \otimes P(E_i \to E_f) \otimes D(Q \to H_Q)$$

$$\frac{E_f d^3\sigma_u(H_Q)}{dp_f^3} = \frac{E_i d^3\sigma(Q)}{dp_i^3} \otimes D(Q \to H_Q)\,.$$

$$T(\mathrm{x}_0, \mathrm{x}_0, \phi, \tau) = T_{profile}(\mathrm{x}_0 + \tau\cos\phi, \mathrm{y}_0 + \tau\sin\phi, \tau)$$

$$\frac{d^2N_{\rm rad}}{dxd\tau} = \int \frac{d^2k}{\pi}\frac{d^2q}{\pi}\frac{2\,C_R C_2(G)\,T}{x}\frac{\mu_E(T)^2-\mu_M(T)^2}{(\boldsymbol{q}^2+\mu_M(T)^2)(\boldsymbol{q}^2+\mu_E(T)^2)}\frac{\alpha_S(E\,T)\,\alpha_S(\frac{\boldsymbol{k}^2+\chi(T)}{x})}{\pi}$$
$$\times\frac{(\boldsymbol{k}+\boldsymbol{q})}{(\boldsymbol{k}+\boldsymbol{q})^2+\chi(T)}\left(1-\cos\left(\frac{(\boldsymbol{k}+\boldsymbol{q})^2+\chi(T)}{xE^+}\,\tau\right)\right)\left(\frac{(\boldsymbol{k}+\boldsymbol{q})}{(\boldsymbol{k}+\boldsymbol{q})^2+\chi(T)}-\frac{\boldsymbol{k}}{\boldsymbol{k}^2+\chi(T)}\right)$$

$$\frac{dE_{col}}{d\tau} = \frac{2C_R}{\pi\,v^2}\alpha_S(E\,T)\,\alpha_S(\mu_E^2(T))\times$$
$$\int_0^\infty n_{eq}(|\vec{\mathbf{k}}|,T)d|\vec{\mathbf{k}}|\left(\int_0^{|\vec{\mathbf{k}}|/(1+v)}d|\vec{\mathbf{q}}|\int_{-v|\vec{\mathbf{q}}|}^{v|\vec{\mathbf{q}}|}\omega d\omega + \int_{|\vec{\mathbf{k}}|/(1+v)}^{|\vec{\mathbf{q}}|_{max}}d|\vec{\mathbf{q}}|\int_{|\vec{\mathbf{q}}|-2|\vec{\mathbf{k}}|}^{v|\vec{\mathbf{q}}|}\omega d\omega\right)\times$$
$$\left(|\Delta_L(q,T)|^2\frac{(2|\vec{\mathbf{k}}|+\omega)^2-|\vec{\mathbf{q}}|^2}{2}+|\Delta_T(q,T)|^2\frac{(|\vec{\mathbf{q}}|^2-\omega^2)((2|\vec{\mathbf{k}}|+\omega)^2+|\vec{\mathbf{q}}|^2)}{4|\vec{\mathbf{q}}|^4}(v^2|\vec{\mathbf{q}}|^2-\omega^2)\right)$$

$$\overline{N}_{tr}(E) = \int_{tr}\left(\int\frac{d^2N_{\rm rad}}{dxd\tau}dx\right)d\tau, \qquad \overline{N}'_{tr}(E,x) = \int_{tr}\frac{d^2N_{\rm rad}}{dxd\tau}d\tau$$

$$\overline{E}^{tr}_{\rm col}(E) = \int_{tr}\frac{dE_{col}}{d\tau}d\tau$$

$$P^{tr}_{rad}(E_i\to E_f) = \frac{\delta(E_i-E_f)}{e^{\overline{N}_{tr}(E_i)}}+\frac{\overline{N}'_{tr}(E_i,1-\frac{E_f}{E_i})}{e^{\overline{N}_{tr}(E_i)}}+$$
$$+\sum_{n=2}^{\infty}\frac{e^{-\overline{N}_{tr}(E_i)}}{n!}\int dx_1\cdots dx_n\overline{N}'_{tr}(E_i,x_1)\cdots\overline{N}'_{tr}(E_i,x_{n-1})\overline{N}'_{tr}(E_i,1-\frac{E_f}{E_i}-x_1-\cdots-x_{n-1})$$

$$P^{tr}_{\rm col}(E_i,E_f) = \frac{1}{\sqrt{2\pi}\sigma^{tr}_{\rm col}(E_i)}\exp\left(-\frac{(E_i-E_f-\overline{E}^{tr}_{\rm col}(E_i))^2}{2\,\sigma^{tr}_{\rm col}(E_i)^2}\right)$$

$$\sigma^{tr}_{\rm col}(E) = \sqrt{2\overline{T^{tr}}\,\overline{E}^{tr}_{\rm col}(E)}$$

$$R^{tr}_{AA}(p_f,H_Q) = \frac{E_f d^3\sigma_q(H_Q)}{dp_f^3}\Big/\frac{E_f d^3\sigma_u(H_Q)}{dp_f^3}$$

$$R_{AA}(p_\perp) = \frac{1}{2\pi}\int_0^{2\pi}R_{AA}(p_\perp,\phi)d\phi,$$

$$v_2(p_\perp) = \frac{\frac{1}{2\pi}\int_0^{2\pi}\cos(2\phi)R_{AA}(p_\perp,\phi)d\phi}{R_{AA}(p_\perp)}$$

Constraining initial time (τ_0) by high-$p_\perp$ QGP tomography: Low-$p_\perp$ setup

$\tau_0 \in \{0.2, 0.4, 0.6, 0.8, 1.0, 1.2\}\ fm$

$h^{\pm}$ Pb+Pb $\sqrt{s_{NN}}$=5.02 TeV

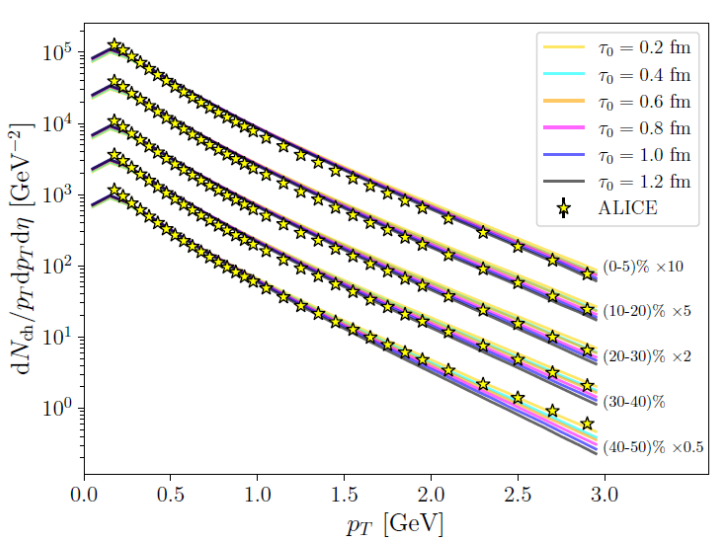

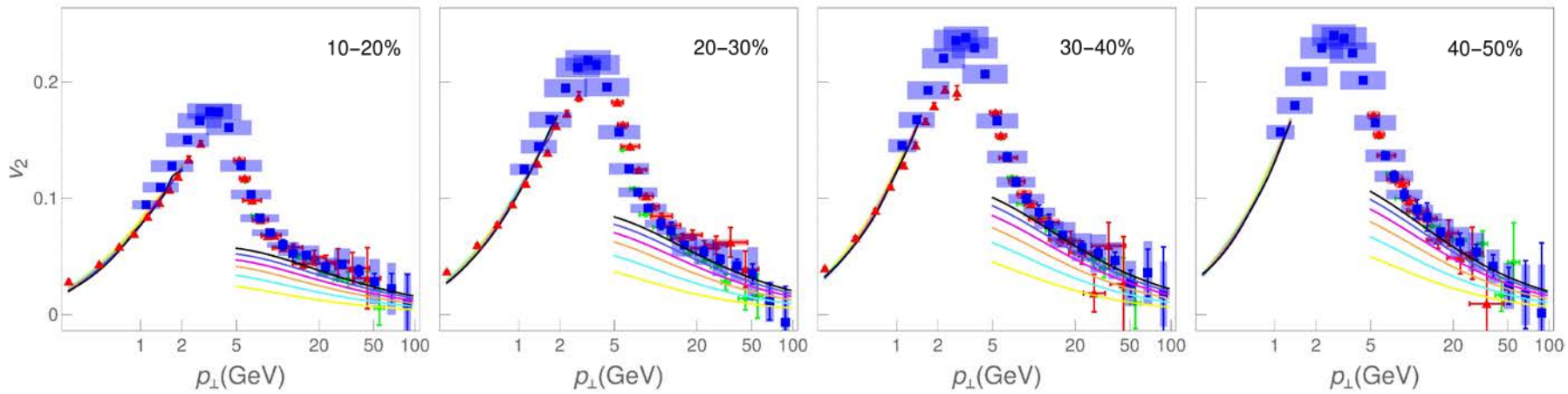

CMS PLB 776 (2018) 195
ALICE JHEP 07 (2018) 103

Good agreement with low-$p_\perp$ data.

What about high-$p_\perp$ sector?

S. Stojku, J. Auvinen, M. Djordjevic, P. Huovinen, and M. Djordjevic, Acta Phys. Polon. Supp. 16, 156 (2023)

Averaged evolution models for anisotropy

- Optical Glauber:
  - Optical Glauber initialization (τ_0=1 fm)
  - 3+1D viscous fluid code (E. Molnar, H. Holopainen, P. Huovinen and H. Niemi, PRC 90, 044904), η/s=0.12, no bulk viscosity (for RHIC η/s=0.16)
  - EoS parametrisation s95p-PCE-v1 (P. Huovinen and P. Petreczky, NPA 837, 26-53)
- Glauber+Free Streaming:
  - Glauber initialization (free streaming from 0.2 to 1 fm)
  - 3+1D viscous fluid code (E. Molnar, H. Holopainen, P. Huovinen and H. Niemi, PRC 90, 044904), η/s=0.16, no bulk viscosity
  - EoS parametrisation *s*95*p*-PCE175
- EKRT:
  - EKRT initialization (K. J. Eskola, K. Kajantie, P. V. Ruuskanen and K. Tuominen, NPB 570, 379; PRC 87, 044904; PLB 731, 126) τ_0=0.2 fm
  - 3+1D viscous fluid code with boost-invariant expansion (E. Molnar, H. Holopainen, P. Huovinen and H. Niemi, PRC 90, 044904)
  - Bayesian analysis η/s(T) (min 0.18), no bulk viscosity
  - EoS parametrization $s83s_{18}$ (J. Auvinen, K. J. Eskola, P. Huovinen, H. Niemi, R. Paatelainen and P. Petreczky, PRC 102, 044911)
- IP-Glasma:
  - IP-Glasma (B. Schenke, P. Tribedy and R. Venugopalan, PRL 108, 252301; PRC 86, 034908; B. Schenke, C. Shen and P. Tribedy, PRC 102, 044905) τ_{switch}=0.4
  - MUSIC code with boost-invariant expansion (B. Schenke, S. Jeon and C. Gale, PRC 82, 014903; PRL 106, 042301; PRC 85, 024901), η/s=0.12, ζ/s(T) (max 0.13)
  - EoS HotQCD lattice (J. S. Moreland and R. A. Soltz, PRC 93, 044913)
- T_RENTo:
  - T_RENTo initialization (J. S. Moreland, J. E. Bernhard and S. A. Bass, PRC 92, 011901), with free streaming until τ_0=1.16 fm
  - VISH2+1 code (H. Song and U. W. Heinz, PRC 77, 064901; arXiv:1804.06469; NP 15, no.11, 1113-1117)
  - Bayesian analysis η/s(T) (min 0.081), ζ/s(T) (max 0.052)
  - EoS lattice (A. Bazavov et al. [HotQCD], PRD 90, 094503)

New observable: High-$p_\perp$ data constraining QGP evolution simulations

$$v_2/(1-R_{AA}) = \langle jT_2 \rangle$$

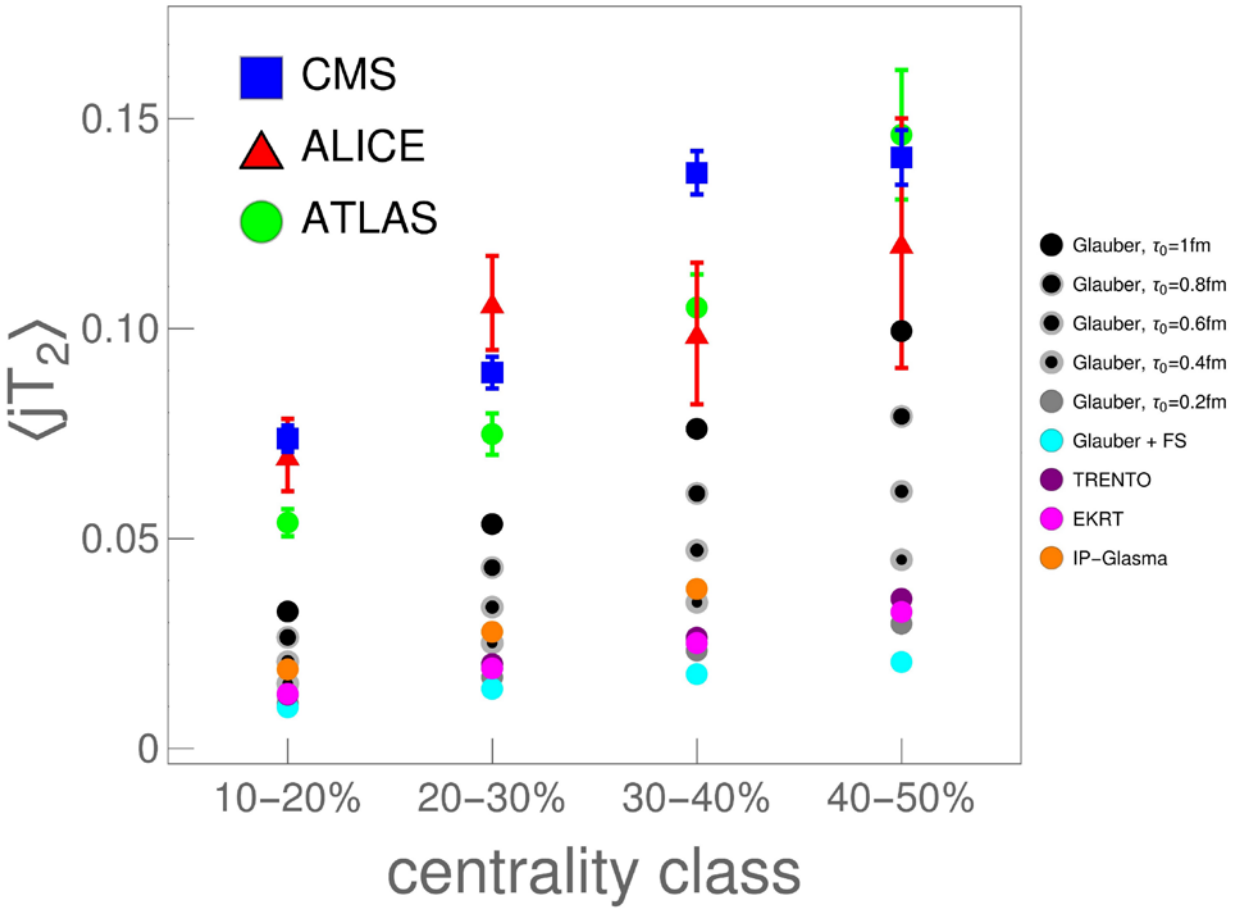

High-$p_\perp$ data from 3 experiments agree (large error-bars)

On the other hand, $\langle jT_2 \rangle$ can be evaluated from bulk-medium simulations (considered scenarios underestimate data).

$\langle jT_2 \rangle$ is an important constraint on bulk-medium simulations.

Event-by-event evolution models

- MC Glauber:
  - Monte-Carlo Glauber initialization (τ_0=1 fm, no initial transverse flow)
  - 3+1D viscous fluid code (E. Molnar, H. Holopainen, P. Huovinen and H. Niemi, PRC 90, 044904), η/s=0.03, no bulk viscosity
  - EoS parametrisation s95p-PCE-v1 (P. Huovinen and P. Petreczky, NPA 837, 26-53)
- T_RENTo:
  - T_RENTo initialization, with free streaming until τ_0=1.16 fm
  - VISH2+1 code (H. Song and U. W. Heinz, PRC 77, 064901; arXiv:1804.06469; NP 15, no.11, 1113-1117)
  - Bayesian analysis η/s(T) (min 0.081), ζ/s(T) (max 0.052)
  - EoS lattice (A. Bazavov et al. [HotQCD], PRD 90, 094503)
- IP-Glasma:
  - IP-Glasma (B. Schenke, P. Tribedy and R. Venugopalan, PRL 108, 252301; PRC 86, 034908; B. Schenke, C. Shen and P. Tribedy, PRC 102, 044905) τ_{switch}=0.4
  - MUSIC code with boost-invariant expansion (B. Schenke, S. Jeon and C. Gale, PRC 82, 014903; PRL 106, 042301; PRC 85, 024901), η/s=0.12, ζ/s(T) (max 0.13)
  - EoS HotQCD lattice (J. S. Moreland and R. A. Soltz, PRC 93, 044913)

$$n_{BC}(x,y) = \frac{1}{2\pi\sigma_{BC}^2} \sum_{i=1}^{N_{BC}} \exp\left(-\frac{(x-x_i)^2 + (y-y_i)^2}{2\sigma_{BC}^2}\right)$$

$$\epsilon(x,y) = C_0(n_{BC} + c_1 n_{BC}^2 + c_2 n_{BC}^3)$$

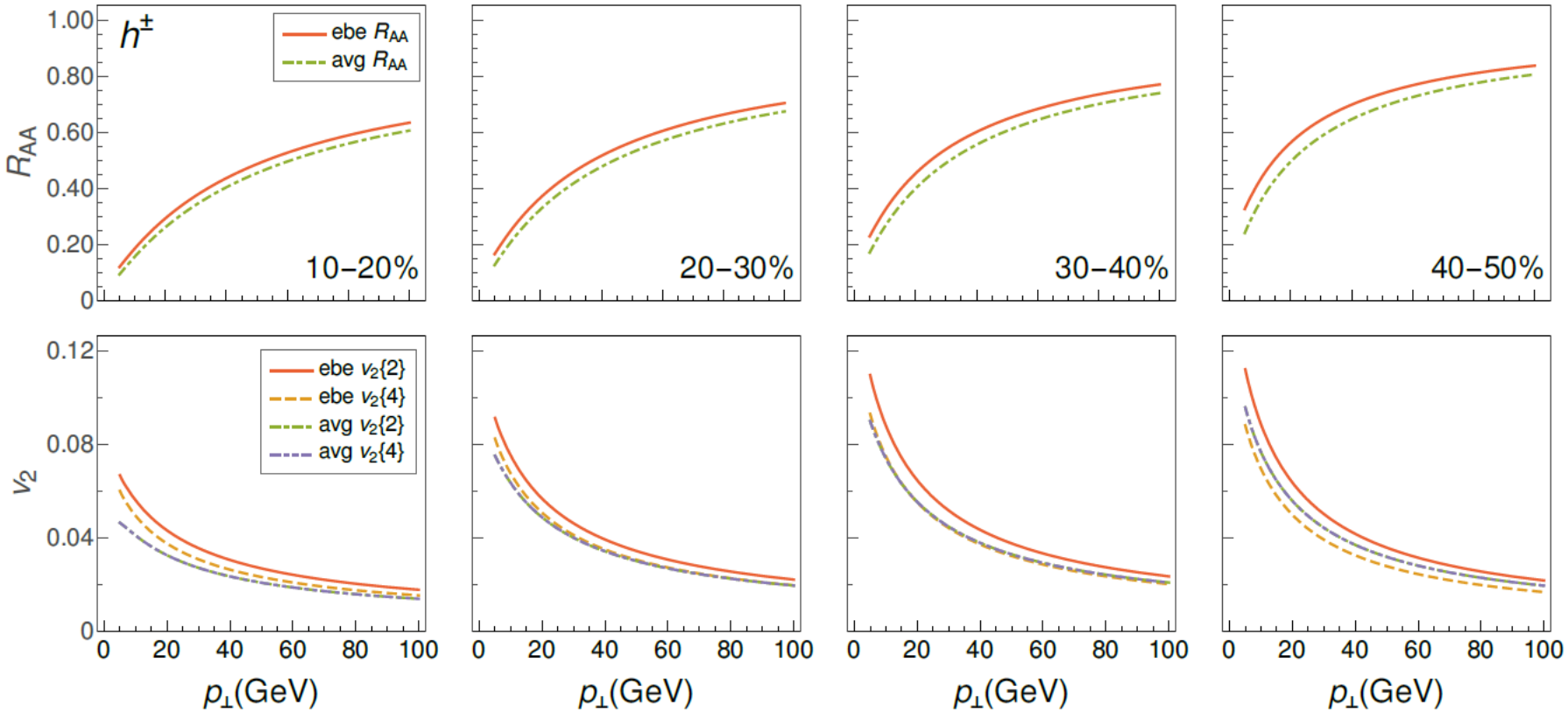
$h^{\pm}$
ebe R_{AA}
avg R_{AA}
R_{AA}
1.00
0.80
0.60
0.40
0.20
0
10–20%
20–30%
30–40%
40–50%
ebe $v_2\{2\}$
ebe $v_2\{4\}$
avg $v_2\{2\}$
avg $v_2\{4\}$
v_2
0.12
0.08
0.04
0
0
20
40
60
80
100
$p_\perp$(GeV)

1. Early evolution of QGP constrained by high-$p_\perp$ QGP tomography

S. Stojku, J. Auvinen, M. Djordjevic, P. Huovinen, and M. Djordjevic, Acta Phys. Polon. Supp. 16, 156 (2023)

1. Early-time dynamics and hydrodynamization are still open questions (D. Zigic, B. Ilic, M. Djordjevic and M. Djordjevic, Phys. Rev. C 101, 064909 (2020), hydro attractors: PRL 115, 072501; NPA 1005, 122000, effective kinetic theory: PRL 122, 122302, PRC 99, 034910)

2. No adequate methods for high-$p_\perp$ parton energy loss in out-of-equilibrium QGP medium

- Standard approach: comparison of relativistic hydrodynamics to low-$p_\perp$ data – weakly sensitive to early evolution parameters
- Our approach: Utilizing high-$p_\perp$ theory and data (R_{AA} and v_2) to constrain τ_0 and τ_q

τ_0 – initial time of fluid-dynamical expansion

τ_q – quenching start time (start of high-$p_\perp$ parton energy loss, i.e., interaction with medium)

D. Zigic, I. Salom, J. Auvinen, P. Huovinen, and M. Djordjevic, Front. In Phys. 10, 957019 (2022)

DREENA-B

$$L(x,y,\phi) = \frac{\int_0^\infty \mathrm{d}\lambda\, \lambda\, \rho(x+\lambda\cos(\phi), y+\lambda\sin(\phi))}{\int_0^\infty \mathrm{d}\lambda\, \rho(x+\lambda\cos(\phi), y+\lambda\sin(\phi))}$$

$$\langle L_{in}\rangle = \frac{1}{\Delta\phi}\int_{-\Delta\phi/2}^{\Delta\phi/2} \mathrm{d}\phi\, \langle L(\phi)\rangle$$

$$\langle L_{out}\rangle = \frac{1}{\Delta\phi}\int_{\pi/2-\Delta\phi/2}^{\pi/2+\Delta\phi/2} \mathrm{d}\phi\, \langle L(\phi)\rangle$$

$$\frac{\Delta L}{\langle L\rangle} = \frac{\langle L_{out}\rangle - \langle L_{in}\rangle}{\langle L_{out}\rangle + \langle L_{in}\rangle}$$

$$\frac{v_2}{1-R_{\mathrm{AA}}} \approx 0.57\ \Delta L/\langle L\rangle$$

$$\epsilon_{2L} = \frac{\langle L_{out}\rangle^2 - \langle L_{in}\rangle^2}{\langle L_{out}\rangle^2 + \langle L_{in}\rangle^2} = \frac{2\varsigma}{1+\varsigma^2}$$

$$\varsigma = \frac{\langle L_{out}\rangle - \langle L_{in}\rangle}{\langle L_{out}\rangle + \langle L_{in}\rangle}$$

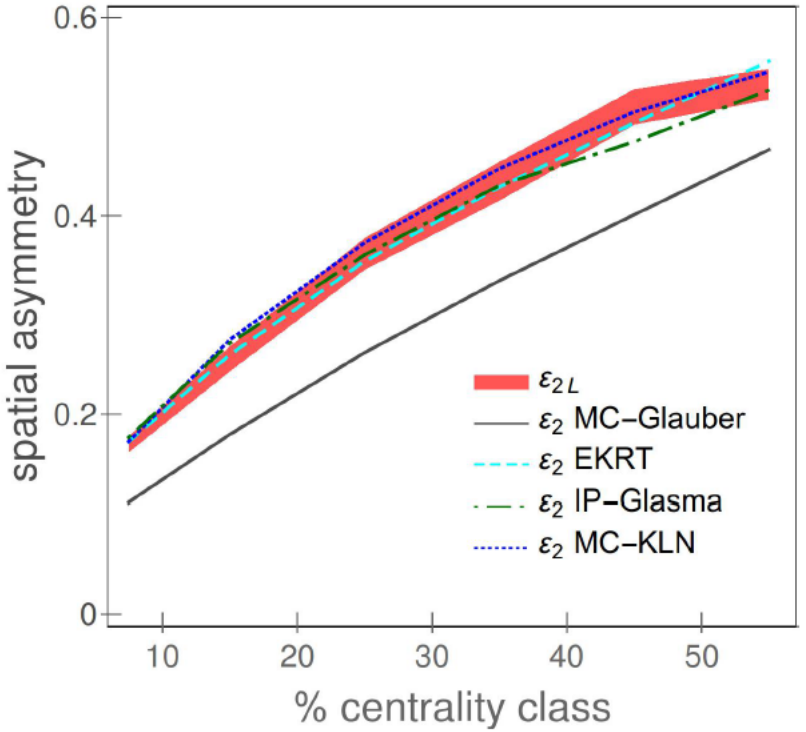

$$\epsilon_2 = \frac{\langle y^2 - x^2\rangle}{\langle y^2 + x^2\rangle} = \frac{\int \mathrm{d}x\,\mathrm{d}y\,(y^2-x^2)\,\rho(x,y)}{\int \mathrm{d}x\,\mathrm{d}y\,(y^2+x^2)\,\rho(x,y)}$$

Phys.Rev.C 100 (2019) 3, 031901

$$\langle T_x(t)\rangle = \frac{1}{N}\sum_{i=1}^{N} T(x_i+t, y_i, t)$$

$$\langle T_y(t)\rangle = \frac{1}{N}\sum_{i=1}^{N} T(x_i, y_i+t, t)$$

$$\alpha_s(Q^2) = \frac{4\pi}{(11 - 2/3 n_f)\ln(Q^2/\Lambda_{QCD})}$$

$$Q_k^2 = \frac{\mathbf{k}^2 + M^2 x^2 + m_g^2}{x}$$

$$Q_v^2 = ET$$

$$\frac{\mu_E^2}{\Lambda_{QCD}^2} \ln\left(\frac{\mu_E^2}{\Lambda_{QCD}^2}\right) = \frac{1 + n_f/6}{11 - 2/3\, n_f} \left(\frac{4\pi T}{\Lambda_{QCD}}\right)^2$$

$$\alpha_s^2 \to \alpha_s(ET)\alpha_s\left(\mu_E^2\right)$$

PRD 77, 114017

$$\mu_E^2 = \left(1 + \frac{n_f}{6}\right) 4\pi\alpha\left(\mu_E^2\right) T^2$$

arXiv:hep-ph/0601119 [hep-ph]]

$$\alpha(t) = \frac{4\pi}{(11 - \frac{2}{3}n_f)} \frac{1}{\ln\left(\frac{t}{\Lambda^2}\right)}$$

$$\left[\frac{\mu_E^2}{\pi(\mathbf{q}^2+\mu_E^2)^2}\right]_{\text{stat}} \to \left[\frac{\mu_E^2 - \mu_M^2}{\pi(\mathbf{q}^2+\mu_E^2)(\mathbf{q}^2+\mu_M^2)}\right]_{\text{dyn}}$$

M. Djordjevic and M. Djordjevic, PLB 709, 229

$$(\eta/s)(T) = \begin{cases} (\eta/s)_{\rm min}, & T < T_c, \\ (\eta/s)_{\rm min} + (\eta/s)_{\rm slope}(T - T_c)\left(\dfrac{T}{T_c}\right)^{(\eta/s)_{\rm crv}}, & T > T_c, \end{cases}$$

(i) constant η/s (0.15 for Pb+Pb collision at LHC and 0.12 for Au+Au collision at RHIC)

(ii) $(\eta/s)_{\rm min} = 0.1$, $(\eta/s)_{\rm slope} = 1.11$, $(\eta/s)_{\rm crv} = -0.48$, Nature NP 15, no.11, 1113-1117

(iii) $(\eta/s)_{\rm min} = 0.04$, $(\eta/s)_{\rm slope} = 3.30$, $(\eta/s)_{\rm crv} = 0$. LHHQ PRL 106, 212302

T_c=154 MeV PRD 90, 094503

Phenomenological approach to η/s(T) constraining from high-$p_\perp$ data

- Modeling the bulk medium:
  - Initial state: ebe TRENTO (no pre-equilibrium evolution τ_0=1fm)
  - T evolution: VISHNew 2+1D, boost invariant (PRC 77, 064901; PRC 78, 024902)
  - EoS: high T lattice QCD-based of HotQCD collaboration below 151 MeV hadron resonance gas (PRD 90, 094503)
  - Hadronic stage: UrQMD hadron cascade (PPNP 41, 255-369; JPG 25, 1859-1896)

$$(\zeta/s)(T) = \frac{(\zeta/s)_{\max}}{1+\left(\frac{T-T_0}{(\zeta/s)_{\text{width}}}\right)^2}$$

$$(\eta/s)(T) = \begin{cases} (\eta/s)_{\min}, & T < T_c, \\ (\eta/s)_{\min} + (\eta/s)_{\text{slope}}(T-T_c)\left(\frac{T}{T_c}\right)^{(\eta/s)_{\text{crv}}}, & T > T_c, \end{cases}$$

Three different scenarios:

(i) constant η/s (0.15 for Pb+Pb collision at LHC and 0.12 for Au+Au collision at RHIC)

(ii) $(\eta/s)_{\min} = 0.1$, $(\eta/s)_{\text{slope}} = 1.11$, $(\eta/s)_{\text{crv}} = -0.48$, Nature NP 15, no.11, 1113-1117

(iii) $(\eta/s)_{\min} = 0.04$, $(\eta/s)_{\text{slope}} = 3.30$, $(\eta/s)_{\text{crv}} = 0.$ LHHQ PRL 106, 212302

- Modeling high-$p_\perp$ parton-medium interactions: ebe DREENA (PRC 106, 044909)

Phenomenological approach to η/s(T) constraining from high-$p_\perp$ data

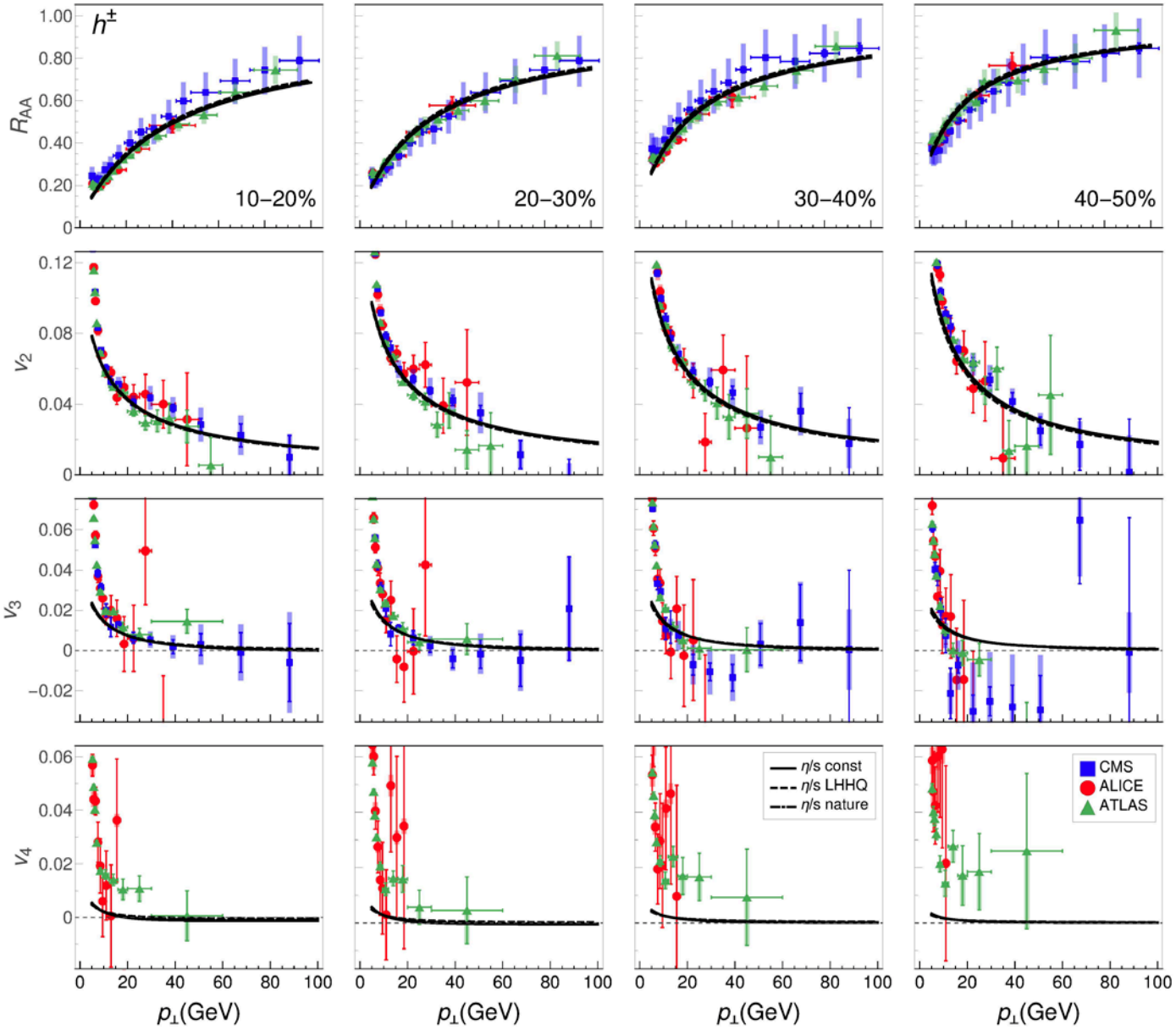

In all 3 scenarios, all high-$p_\perp$ observables are practically indistinguishable.

High-$p_\perp$ observables are insensitive to η/s(T) parameterization (at high T) and cannot constrain it.

Phenomenological approach to η/s(T) constraining from high-$p_\perp$ data